ANALYSIS OF A NOVEL COMBINED THERMAL POWER AND COOLING CYCLE USING AMMONIA-WATER MIXTURE AS A WORKING FLUID

By

FENG XU

A DISSERTATION PRESENTED TO THE GRADUATE SCHOOL
OF THE UNIVERSITY OF FLORIDA IN PARTIAL FULFILLMENT
OF THE REQUIREMENTS FOR THE DEGREE OF
DOCTOR OF PHILOSOPHY

UNIVERSITY OF FLORIDA
1997

ACKNOWLEDGMENTS

I would like to sincerely thank my advisor Dr. D. Yogi Goswami for his constant support, assistance and suggestions, which encouraged me throughout my work. The encouragement and advice provided by Dr. S. A. Sherif are greatly appreciated. I owe a great deal of thanks to Dr. J. E. Peterson, C. K. Hsieh and B. L. Capehart for their time and effort devoted as part of the dissertation review committee. I would also like to thank Ms. Barbara Walker, Mr. Charles Garretson and Mr. John West for all the help and support they have rendered during my study at the Solar Energy and Energy Conversion Laboratory.

Deep appreciation is extended to my family for the support and inspiration they have always provided. Finally, I am grateful to my wife Hong and son Tom. This would not have been possible solely by myself.

TABLE OF CONTENTS

page

NOMENCLATURE

A	Helmholtz free energy
C_p	Specific heat
Ex	Exergy
f	Fugacity
G	Gibbs free energy
H	Enthalpy
h	Enthalpy per unit mass
m	Polarity factor
n	Index
P	Pressure
P_B	Reference pressure, $P_B = 10$ bar
R	Gas constant
S	Entropy
s	Entropy per unit mass
T	Temperature
T_B	Reference temperature, $T_B = 100$ K
V	Volume
v	Specific volume

w	Eccentric factor
x	Ammonia mass fraction
x'	Ammonia mole fraction
y	Ammonia vapor mass fraction
y'	Ammonia vapor mole fraction
Z	Compressiblity factor

Subscripts

0	Reference state
*	Ideal gas state
a	Ammonia
b	Bubble point
c	Critical point
cw	Critical point of water
cm	Critical point of mixture
d	Dew point
f	Saturated liquid
g	Saturated vapor
m	Mixture
r	Reduced property
v	Vaporization
w	Water

Supscript

E	Excess property
g	Vapor state
L	Liquid state

Abstract of Dissertation Presented to the Graduate School
of the University of Florida in Partial Fulfillment of the
Requirements for the Degree of Doctor of Philosophy

ANALYSIS OF A NOVEL COMBINED THERMAL POWER AND COOLING CYCLE USING AMMONIA-WATER MIXTURE AS A WORKING FLUID

By

Feng Xu

August 1997

Chairman: D. Yogi Goswami
Major Department: Mechanical Engineering

A combined thermal power and cooling cycle is proposed. Ammonia-water mixture is used as a working fluid. The proposed cycle combines Rankine cycle and absorption refrigeration cycle. It can provide power output as well as refrigeration with power generation as a primary goal. The concept of this cycle is based on the varying temperature boiling of a multi-component working fluid. The boiling temperature of the ammonia-water mixture increases as the boiling process proceeds until all liquid is vaporized, so that a better thermal match is obtained in the boiler. The proposed cycle takes advantage of the low boiling temperature of ammonia vapor so that it can be expanded to a low temperature while it is still in a vapor state or a high quality two phase state. This cycle can be used as a bottoming cycle using waste heat from a topping cycle

and can be used as an independent cycle using low temperature sources such as geothermal and solar energy.

Thermodynamic properties of the ammonia-water mixture are of technical importance to predict the performance of the proposed cycle. A new method is developed using Gibbs free energy equations to compute the pure component of ammonia and water properties, using bubble and dew point temperature equations developed from the experimental data in the literature for the mixture phase equilibrium calculations. Results have shown very good agreement with the experimental data and other literature data.

This study has also conducted the first and second law thermodynamic analyses of the proposed cycle. The mass composition of binary working fluid is considered in the second law analysis while most of the studies in the literature treat a binary working fluid as a simple fluid in the second law analysis. A comparison of the proposed cycle and the conventional Rankine cycle under the same thermal boundary conditions shows the advantage of the proposed cycle using ammonia-water mixture as a working fluid.

A completed cycle simulation program is developed and shows the performance of the proposed cycle with different parameters.

CHAPTER 1
INTRODUCTION

Thermal power cycle efficiencies have been steadily improving over the past 100 years. A number of methods have been used to improve the thermal efficiency of a power cycle. Raising the temperature of the heat source, using different working fluids, improving the system design and lowering the temperature of heat rejection are the most common ways.

The second law of thermodynamics sets an upper limit on the efficiencies of power cycles operating between fixed temperatures. The main reason that the maximum efficiency of a power cycle can not equal the efficiency of a Carnot cycle is due to irreversibilities in the system. Therefore, one way to increase the efficiency of a cycle with a fixed temperature heat source and sink is to reduce the cycle irreversibilities.

Considering the limitation of the second law of thermodynamics, a new power cycle combined with a cooling cycle has been proposed. Ammonia-water mixture is used as a working fluid in this cycle. A new system design will exploit the unique thermodynamic properties of ammonia-water mixtures to reduce the system irreversibilities. The proposed cycle will produce power while providing cooling as well. This cycle will be able to use low quality heat sources such as solar energy, geothermal heat and waste heat

while achieving high thermal efficiency. It may be used as an independent cycle or as a bottoming cycle in a combined cycle system.

1.1 Power Cycle

A thermal power cycle can be generally categorized by the working fluid as a vapor power cycle or a gas power cycle. In a vapor power cycle, the working fluid usually changes its phase from liquid to vapor and back to liquid in the cycle. In a gas power cycle, the working fluid remains a gas.

A typical vapor power cycle using steam as a working fluid is the Rankine Cycle as shown in figure 1-1:

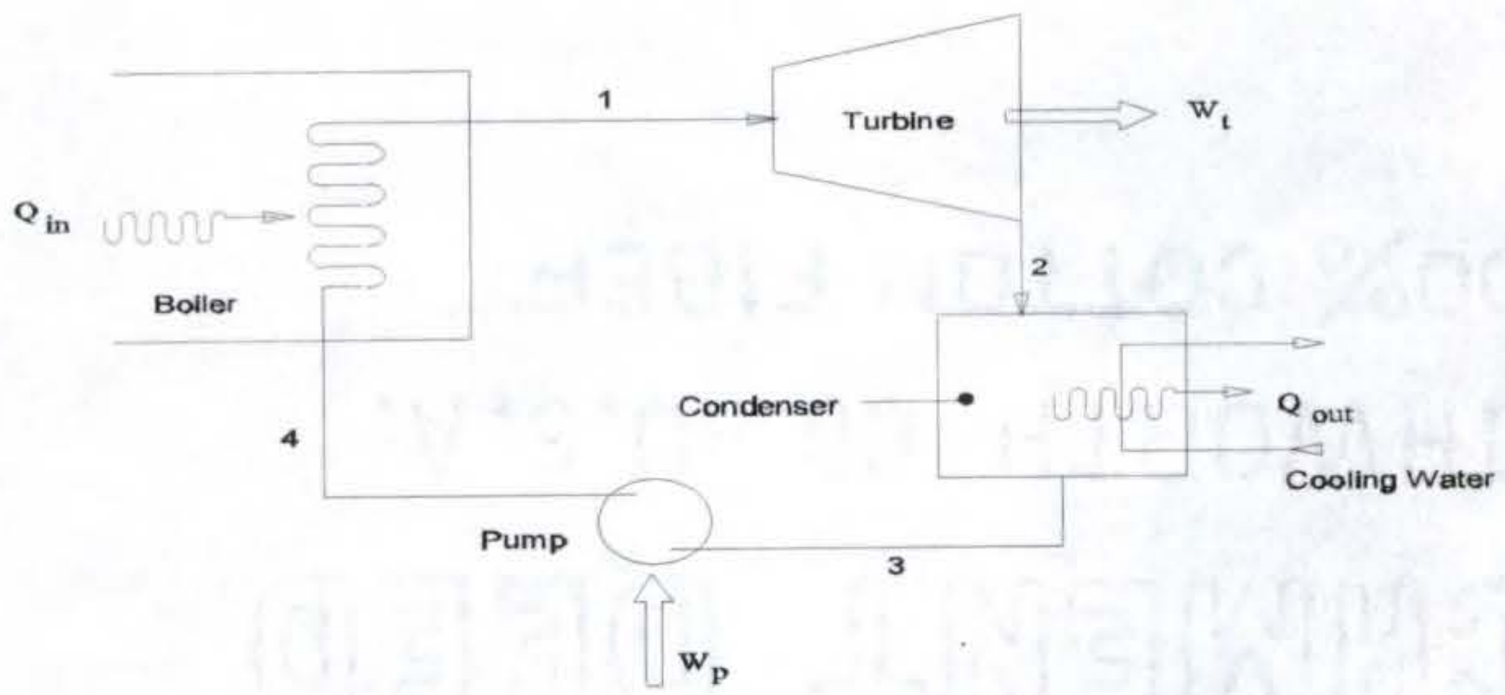

Figure 1-1 Rankine cycle

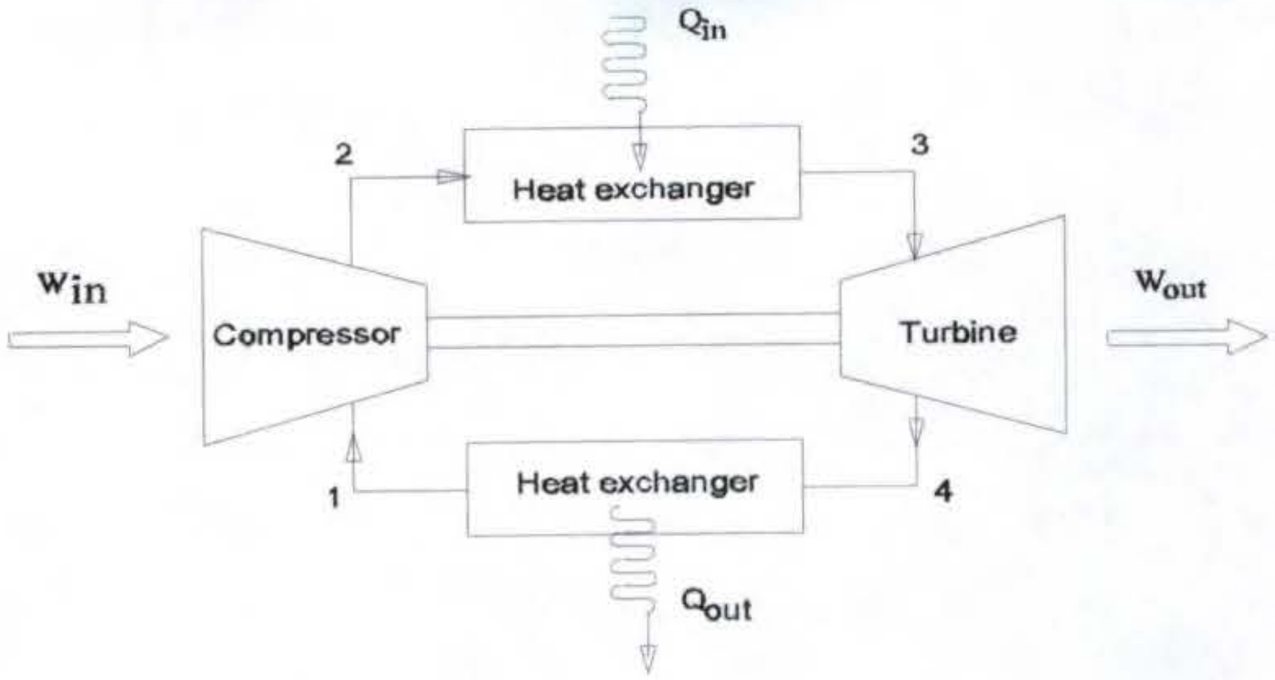

Figure 1-2 Brayton cycle

A typical gas power cycle using air as a working fluid is Brayton cycle as shown in figure 1-2. Both cycles have similar working theories: heat is added to the working fluid at the boiler or combustion chamber; the high temperature, high pressure working fluid passes through a turbine and becomes low temperature and low pressure fluid; the result is power output from the turbine. The fluid from the turbine goes through a heat exchanger to further lower its temperature before going through a pump or compressor to elevate its pressure.

It is well known that the higher the temperature of the working fluid at the turbine inlet, the more efficiently the power cycle performs. There are limits of temperature and pressure range for a vapor power cycle, which needs to operate between the ranges of two phases. High temperature vapor causes high pressure which requires piping that can withstand great stresses at elevated temperatures. For a gas power cycle, the high gas temperature is also restricted by metallurgical limitations imposed by the materials used to fabricate the turbine and other components.

Various modifications of the basic cycles are usually incorporated to improve the overall performance under the allowable material conditions and other limitations. Superheat, reheat and regeneration are the common modifications for vapor power cycles. Reheat, regeneration and compression with intercooling are the common modifications for gas power cycles.

An advantage of using a gas power system is that gas turbines tend to be lighter and more compact than the vapor power systems. In addition, the favorable power output-to-weight ratio and much higher turbine inlet temperatures make them well suited for certain applications. But a high turbine inlet temperature also results in a high turbine outlet temperature (i.e. a lot of heat has to be rejected). This is the main reason that makes a gas power system function at a low second law efficiency. To solve this problem a combined cycle is introduced. A combined cycle uses a gas power cycle as a topping cycle and a vapor power cycle as the bottoming cycle to utilize the waste energy in the relatively high temperature exhaust gas from the gas power cycle.

In this work, we are focusing on a vapor power cycle as an independent power cycle or as a bottoming cycle.

1.2 Vapor Power Cycle

Since the first electric generating station in the United States, the Brush Electric Light Company in Philadelphia, went into service in 1881, engineers have been working to improve the efficiency of the Rankine Cycle for power production (Babcock & Wilcox, 1978). The additions of superheat, multiple reheat and supercritical cycles have helped

push the thermal efficiency from 7% to approximately 38% (Bejan, 1988). The introduction and improvement of equipment such as air heaters, economizers and regenerative feedwater heaters have also contributed to an increase in thermal efficiency. Advances in metallurgy coupled with the previously mentioned improvements in cycle and equipment have raised the steam generator outlet conditions from 10×10^6 Pa (140psig) and 500 K (440 °F) in the 1880s, to today's 2.4×10^7 Pa (3500psig) and 865 K (1100 F) range typical of units such as the Cleveland Electric Illuminating Company's Avon Lake Station Unit #8 (Bannister and Silvestri., 1989; Duffy, 1964). However one item has remained constant since the Hero of Alexandria's engine, the use of water as the working fluid.

One of the methods of increasing the thermal efficiency of a vapor power cycle is the binary cycle. In this system the heat exchanger with the higher boiling point fluid serves as the boiler for the lower boiling point fluid. As early as the 1920s several binary cycles were being explored. Some of the fluids being looked at were mercury, aluminum bromide, zinc ammonium chloride and diphenyloxide (Gaffert, 1946). Mercury/water binary cycles have the most operating experience. It should be noted that the New Hampshire Public Service Shiller plant went on line in the early 1950s with a heat rate commendable by today's standards, 9700 kJ/kWh (9200 Btu/kWh) (Zerban and Nye, 1957). It was decommissioned in the late 1970s. Metallurgical and safety concerns on the mercury portion curtailed further development. A similar cycle receiving attention lately is the patented Anderson Power Cycle(Patent No. 4,660,511, 1987; Patent No. 4,346,561, 1982). In the Anderson cycle the water condenser serves as boiler for the R-

22 refrigerant. It is important to remember that in these binary cycles the two components are totally segregated.

The multi-component working fluid power cycle that this investigation is developing is different from the previously mentioned binary cycles in that the working fluids progress through the cycle; compression, vaporization, expansion and condensation; together in the same flow stream. More than two fluids can be employed.

1.3 Multi-Component Working Fluid Research

A review of the literature shows that the studies of multi-component cycles are very recent as compared to the conventional Rankine cycle. Kalina is recognized for introducing the multi-component working fluid power cycle and for bringing it to it's current state(Kalina, 1983, 1984; Kalina and Tribus, 1990; Kalina et al., 1986). However, Back in 1953, Maloney and Robertson (1953) from Oak Ridge National Laboratory studied an absorption-type power cycle using a mixture of ammonia and water as the working fluid. Avery (1980) investigated ammonia-water mixtures as the heat exchange media for power generation in the Ocean Thermal Energy Conversion (OTEC). Maloney and Robertson, and Avery encountered difficulties in getting the thermodynamic properties of ammonia-water mixtures in their systems analysis.

Kalina, Tribus and El-Sayed have collaborated on several publications. A comparison of the multi-component cycle to the Rankine cycle by El-Sayed and Tribus shows a 10% to 20% improvement in thermal efficiency (El-Sayed and Tribus, 1985b).

Marston (1990) conducted a detailed discussion of multi-component cycle behavior to date. It includes the effect of turbine inlet NH_3 mass fraction on cycle efficiency as well as the associated change in mass fraction in separator flow. Also investigated was the effect of varying the separator temperature on the cycle efficiency and separator inlet flow. All work was done at one separator pressure. Turbine inlet conditions were 773.15 K and 1.0×10^7 Pa. Marston found that the temperature at the separator and composition at the turbine inlet are the key parameters for optimizing the Kalina cycle.

Ibrahim and Klein (1996), and Park and Sonntag (1990a) also analyzed the Kalina cycle. Their studies show the advantages of Kalina cycle over the conventional Rankine cycle under certain conditions. Park and Sonntag pointed out that since the Kalina cycle uses many heat exchangers and separators for the distillation condensation process, the parameters (such as temperatures and pressures between heat exchangers) have small differences. This makes the simulation of Kalina cycle very difficult. Ibrahim and Klein (1996) concluded that Kalina cycle will have advantage over the conventional Rankine cycle only when heat exchanger NTU is greater that 5.

Since Kalina cycle uses the conventional condensation process by exchanging heat with the environment, it puts a constraint on the lowest temperature of the working fluid exiting the turbine. This constraint can be relaxed if absorption condensation process is employed.

Rogdakis and Antonopoulos (1991) proposed a triple stage power cycle which is similar to the Kalina cycle. However, they replaced the distillation condensation of the Kalina cycle with the absorption condensation process. Kouremenos el al. (1994) applied this absorption type of power cycle as a bottoming cycle in connection with a gas turbine

topping cycle. The absorption condensation process in this power cycle removes the need to use too many heat exchangers and simplifies the ammonia-water power cycle. Since this cycle still uses ammonia-water vapor mixtures going through turbine, the exit temperature must be relatively high in order to avoid condensation in the turbine. In their cycle, Rogdakis and Antonopoulos (1991) used about 400 C heat source and triple stage turbines to achieve high efficiency.

In this study a new cycle as proposed by Goswami (1995, 1996) is analyzed, that retains the advantages of the Kalina cycle but removes the constraints of the Kalina cycle and the Rogdakis and Antonopoulos cycle as identified above. The new cycle uses ammonia-water mixtures as the working fluids but uses very high concentration ammonia vapor in the turbine which allows it to expand the fluid in the turbine to a much lower temperature without condensation. The new cycle also uses absorption condensation process with its advantages as explained before.

1.4 Combined Cycle

A combined cycle is a synergistic combination of cycles operating at different temperatures, in which each cycle could operate independently. The cycle which operates at the higher temperature is called a topping cycle and the cycle which operates at the lower temperature is called a bottoming cycle. The topping cycle rejects heat at a high enough temperature to drive the bottoming cycle. The heat rejected from the topping cycle is recovered and used by the bottoming cycle to produce additional power to improve the overall efficiency of the combined cycle. Combined cycles which have been

proposed or commercialized include several combinations: diesel-steam, mercury-steam, gas-steam, steam-organic fluid, gas-organic fluid, and MHD-steam.

Combined cycle systems have been recognized as efficient power systems. A typical combined cycle system consists of a gas turbine cycle and a steam Rankine cycle which uses the exhaust gas from the gas turbine as the high temperature source. The exhaust gas provides the available energy for the bottoming cycle (the Rankine cycle) to improve the efficiency of the combined cycle system over the gas turbine cycle alone.

The efficiency of the overall system is a function of the temperature and pressure of the exhaust gas, the sink temperature of the bottoming cycle, and the type of the bottoming cycle itself.

1.5 The Proposed Cycle

The proposed ammonia-based power/cooling cycle, first suggested by Dr. Yogi Goswami(1995, 1996), combines two thermodynamic cycles, the Rankine cycle and the ammonia-absorption refrigeration cycle. This novel cycle uses a mixed working fluid (such as ammonia-water) with different compositions at different stages, therefore, it cannot be shown on a single thermodynamic diagram (i.e. pressure-enthalpy chart). However, by evaluating the features of the individual Rankine and ammonia-absorption refrigeration cycles, the features that apply to the overall cycle can be discussed.

1.5.1 Rankine Cycle Processes

An ideal Rankine cycle, shown in Figure 1-1, is a power generating cycle that has been used in steam power plants. The process involves pumping a liquid to a high

pressure, heating it to a superheated vapor state in a boiler, expanding it through a turbine to generate power while at the same time bringing the vapor to a saturated state, condensing the fluid back to a saturated liquid, and finally pumping the liquid back to the boiler.

1.5.2 Ammonia Absorption Refrigeration Cycle Processes

An ideal cycle for the vapor compression refrigeration is essentially a Rankine cycle in reverse. The ammonia-absorption refrigeration cycle differs from the vapor-compression cycle in the manner in which compression is achieved. In the ammonia-absorption refrigeration cycle(Figure 1-3), low-pressure ammonia vapor from the evaporator is absorbed in water and the liquid solution is pumped to a high pressure. The liquid solution is then heated and ammonia vapor is separated from the water. The ammonia vapor passes through a condenser where it is converted to a liquid and then through an expansion valve to reduce its pressure. At this point the liquid enters an evaporator, draws heat, and exits as a low pressure ammonia vapor.

1.5.3 Combined Power and Cooling Cycle Processes

The similarities in the Rankine and ammonia-absorption refrigeration cycle to the proposed ammonia-based power and cooling cycle are evident as seen in Figure 1-4. Within this one cycle, the Rankine cycle process of expanding a superheated vapor to produce work is present, as are most of the absorption refrigeration cycle processes.

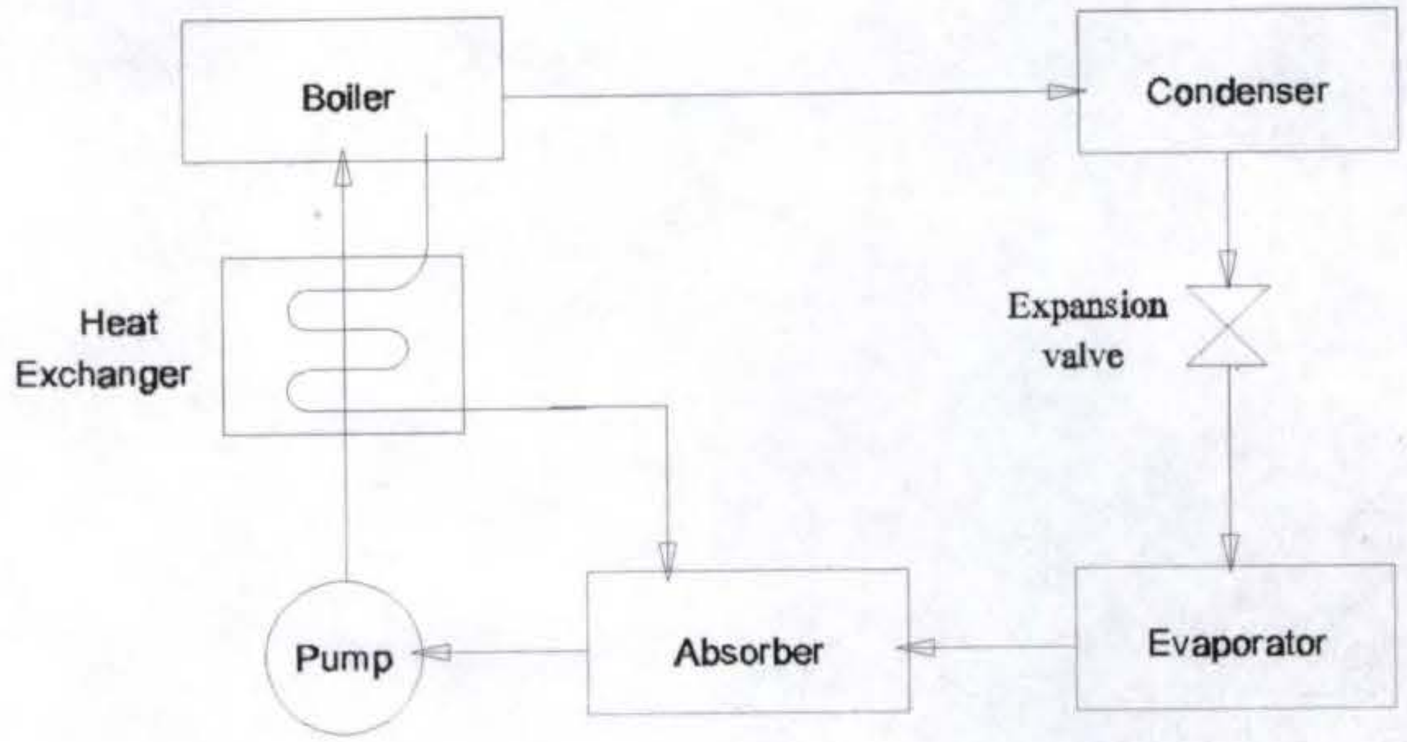

Figure 1-3 Ammonia-absorption refrigeration cycle

1.6 Thermodynamic Properties of Ammonia-Water Mixtures

Ammonia-water mixtures have been in use for several decades as working fluids of absorption-refrigeration cycles where ammonia is the refrigerant and water is the absorbent. Since 1980, ammonia-water mixtures have been investigated as potential working fluids for power cycles.

Consistent and accurate thermodynamic properties data of ammonia-water mixtures are very important for the power cycle analysis. In the past, properties of ammonia-water mixtures were of interest in the operating range of the absorption refrigeration cycle. As ammonia-water mixtures become attractive as power cycle working fluids, we need to extend their properties data to a high pressure and temperature range. Computer

programs are also needed to generate these properties. The important properties required are vapor pressure, equilibrium composition of the components, bubble and dew point temperature, saturation enthalpy and entropy. Data over the region of compressed liquid and superheated vapor are also required.

The literature survey shows that there are mainly three methods to compute the pure ammonia and water properties: 1. free energy method(Gibbs or Helmholtz free energy); 2. a generalized equation method; and 3. use of basic thermodynamic relationships (El-Sayed and Tribus method).

In chapter 2, these three methods are studied and evaluated. A method is developed which combines the advantages of the available methods. This new method is faster than the existing methods because it requires less iterations and it also provides a better match with the available experimental data. The results from this study are compared with the most recent experimental data.

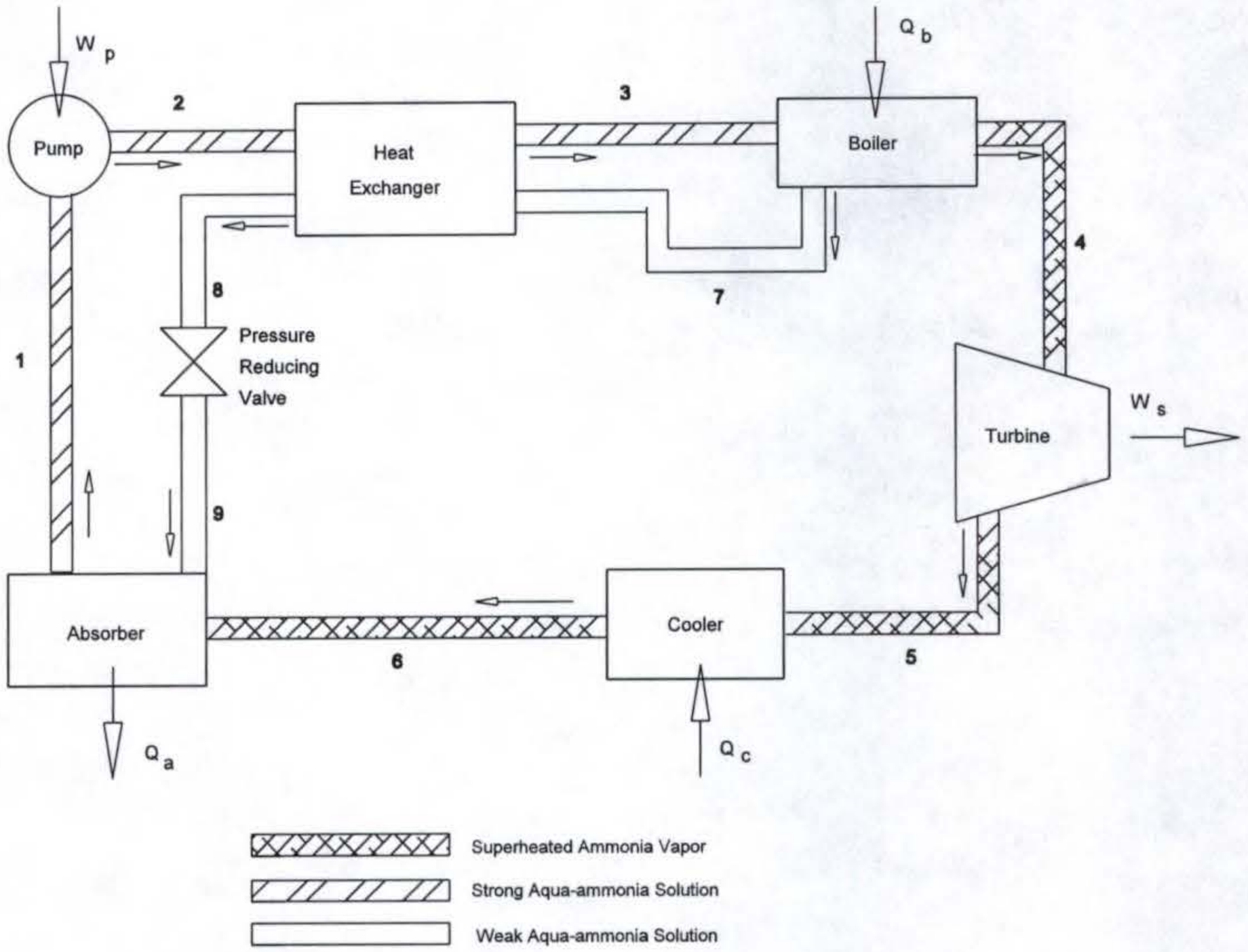

Figure 1-4 Ammonia-based combined power/cooling cycle

CHAPTER 2
THERMODYNAMIC PROPERTIES OF AMMONIA-WATER MIXTURES

2.1 Introduction

The thermodynamic properties of ammonia and water mixtures are of technical importance since ammonia-water mixtures have been in use for several decades as working fluids in absorption-refrigeration cycles. Use of multi-component working fluids for power cycles has been investigated more recently over the last two decades. Ammonia-water mixtures have been considered as potential working fluids for this purpose because of relatively high expected coefficients of performance for this combination.

For the power cycle analysis, the temperature and pressure range is much higher than that of absorption-refrigeration cycles. So a consistent and extended set of thermodynamic data for ammonia-water mixtures at higher temperatures and pressures is required. The motive of this study is a lack of enthalpy and entropy data over the range of variables needed. Also, it is necessary to use computer simulation to investigate ammonia-water mixtures as potential working fluids for a power cycle.

Many studies of the vapor-liquid equilibrium and thermodynamic properties of ammonia-water mixtures are cited in the literature. The temperature and pressure ranges of thermodynamic properties of the majority of the data in the literature are suitable for absorption-refrigeration cycle applications. Institute of Gas Technology (IGT) tables (Macriss et al. 1964) cover the range up to a pressure of 34 bar and its corresponding saturation temperature. Using the IGT data, Schultz (1972) developed equations of state for a pressure range of 0.01 to 25 bar and a temperature range of 200 to 450 K. Ziegler and Trepp (1984) presented a new correlation of equilibrium properties of ammonia-water mixtures. They used an equation of state that is based on that developed by Schultz and extended the range of applicability to 500 K and 50 bar. Ibrahim and Klein (1993) used the form of the equation of state given by Ziegler and Trepp for pure ammonia and pure water. They modified the correlation given by Ziegler and Trepp for the Gibbs excess energy to include Gillespie et al. (1987) experimental data at higher temperatures and pressures. The correlations by Ibrahim and Klein (1993) cover vapor-liquid equilibrium pressures of 0.2 to 110 bar and temperatures of 230 to 600 K.

A study of power cycles using ammonia-water mixtures was recently initiated by Kalina (1983). For power cycles, thermodynamic data of ammonia-water mixtures at higher temperatures and pressures than those presented by IGT are required. Gillespie et al. (1987) published vapor-liquid equilibrium measurements for five isotherms between 313 and 588 K. Corresponding pressures ranged from 0.1 to 210 bar. Herold et al. (1988) developed a computer program for calculation of the thermodynamic properties of ammonia-water mixtures using the Ziegler and Trepp correlation. El-Sayed and Tribus (1985a) presented a method for computing the thermodynamic properties of mixtures

from the properties of pure components to extend the property correlation to higher temperatures and pressures. Derived properties cover pressures of 0.1 to 110 bar and temperatures between 300 and 770 K. Kalina et al. (1986) presented a similar method to predict the thermodynamic properties of two miscible-component mixtures for the purpose of power-cycle analysis. Park and Sonntag (1990b) published a set of thermodynamic data of ammonia-water mixtures based on a generalized equation of state. The pressure and temperature ranges are extended to 200 bar and 650 K respectively.

Based on the above discussion it is clear that methods developed by Ibrahim and Klein (1993), Park and Sonntag (1990b) and El-Sayed and Tribus (1985a) cover all of the modeling efforts reported in the literature. The following section gives detailed discussions of these methods.

2.2 El-Sayed and Tribus method

El-Sayed and Tribus method starts with the thermodynamic properties of pure components, and mixes them according to certain assumptions. In the liquid region, below the bubble point temperature, and in the vapor region, above the dew point temperature, the enthalpy and entropy of the mixture are calculated by summing the product of the thermodynamic properties and mass fractions of the pure components.

The bubble point temperature is defined as the temperature at which the first bubbles of gas appear. The dew point temperature is the temperature at which condensate first appears.

El-Sayed and Tribus use a group of equations developed exclusively for ammonia-water mixtures based on vapor-liquid equilibrium data of Gillespie et al. (1987). The advantage of these equations is that they allow us to determine the start and end of the phase change of the mixture and compute the mass fractions of ammonia and water liquid and vapor phase respectively. This avoids the complicated method of calculating fugacity coefficient of a component in a mixture to determine the bubble and dew point temperatures.

2.2.1 Computational Procedure

The basic equations are given below.

Bubble temperature $T_b = T(P, x)$ 2-1

Dew temperature $T_d = T(P, x)$ 2-2

Equation of state $P = P(T)$ 2-3

$$T_b = T_c - \sum_{i=1}^{7}(C_i + \sum_{j=1}^{10} C_{ij}x^j)(\ln(\frac{P_c}{P}))^i \quad 2\text{-}4$$

where

$$T_c = T_{cw} - \sum_{i=1}^{4} a_i x^i \quad 2\text{-}5$$

$$P_c = P_{cw} \exp(\sum_{i=1}^{8} b_i x^j) \quad 2\text{-}6$$

P in psia and T in ^oF

$$T_d = T_c - \sum_{i=1}^{6}(a_i + \sum_{j=1}^{4} A_{ij}(\ln(1.0001 - x))^j(\ln(\frac{P_c}{P}))^i \quad 2\text{-}7$$

P in psia and T in ^{o}F.

Since El-sayed and Tribus used English units in their research, their equations are kept in English units in this study. In the program, English units are converted to SI units.

1. Pure ammonia liquid:

$$C_p = A + BT + C(T_c - T)^{-1/2} \qquad 2\text{-}8$$

$$h = \left[AT + 0.5BT^2 - 2C(T_c - T)^{1/2}\right]_{T_1}^{T_2} \qquad 2\text{-}9$$

where A = 3.14894

B = -0.0006386

C = 16.66345

T_c = ammonia critical temperature, 405.5 K

T = temperature, K

T_1 = Reference temperature, 195.40 K

T_2 = Final temperature, K

Coefficients A, B and C were found in Haar and Gallagher (1978).

$$C_P = T\frac{ds}{dT} \qquad 2\text{-}10$$

$$A + BT + C(T_c - T)^{-1/2} = T\frac{ds}{dT} \qquad 2\text{-}11$$

$$s = \left[A\ln T + BT + \frac{C}{T_c^{1/2}} \ln \left| \frac{(T_c - T)^{1/2} - (T_c)^{1/2}}{(T_c - T)^{1/2} + (T_c)^{1/2}} \right| \right]_{T_1}^{T_2} \qquad 2\text{-}12$$

2. Ammonia vaporization

$$H_{v2} = H_{v1} \left[\frac{1 - T_{r2}}{1 - T_{r1}} \right]^n \qquad 2\text{-}13$$

where H_{v1} = Known enthalpy of vaporization at a reference temperature T_1, cal/g mole

H_{v2} = Enthalpy of vaporization, cal/g mole

T_c = Ammonia critical temperature, 405.5 K

T_{r1} = Reduced temperature, at temperature T_1

T_{r2} = Reduced temperature, at temperature T_2

n = Constant

Equation 2-13 is transformed as follows:

$$H_{v2} = C_1 (1 - T_{r2})^n \qquad 2\text{-}14$$

where

$$C_1 = \frac{H_{v1}}{(1 - T_{r1})^n}$$

The above equation can be set up in the form y = a + bx

$$\ln H_{v2} = \ln C_1 + n \ln(1 - T_{r2}) \qquad 2\text{-}15$$

where $y = \ln H_{v2}$

$$a = \ln C_1$$

$$b = n$$

$$x = \ln(1 - T_{r2})$$

Values of H_{v2} and T_{r2} from 0.1 bar to 112 bar were taken from published literature(Haar and Gallagher, 1978) to find n as 0.38939. C_1 is found by

$$\ln C_1 = \ln H_{v2} - n\ln(1 - T_{r2}) \qquad 2\text{-}16$$

The value of C_1 used in this investigation was taken by averaging 11 values over the previously mentioned range of pressures. It is

$$C_1 = 7906.555$$

The enthalpy of vaporization equation used was found by using known values of C_1 and n in equation 2-14.

$$H_v = 7906.555 \times (1 - T/T_c)^{0.38939} \qquad 2\text{-}17$$

The entropy of vaporization is

$$S_v = H_v / T \qquad 2\text{-}18$$

3. Ammonia vapor

Integrating the heat capacity equation 2-19 and comparing the results with published enthalpy data did not yield good agreement.

$$C_p = A + BT + CT^2 + DT^3 \qquad 2\text{-}19$$

As the pressure increased the agreement worsened. Therefore, a pressure compensation term was added to obtain equation 2-20. In addition, the original coefficients (A, B, C and D) were changed as reflected in equation 2-21. Coefficients were taken from Haar and Gallagher (1978).

$$C_p = C_{po} + EPT^{-G} \qquad 2\text{-}20$$

where $$C_{po} = A + BT + CT^2 + DT^3 \qquad 2\text{-}21$$

$A = 3.70315$

$B = 2.8074 \times 10^{-3}$

$C = 4.4199 \times 10^{-6}$

$D = -6.3441 \times 10^{-9}$

$E = 1.73447 \times 10^{10}$

$G = 4.3314$

P = pressure, bar

T = temperature, K

$$h = \left[AT + \frac{BT^2}{2} + \frac{CT^3}{3} + \frac{DT^4}{4} + \frac{EPT^{(1-G)}}{(1-G)} \right]_{T1}^{T2} \qquad 2\text{-}22$$

$$s = \left[A\ln T + BT + CT^2 + DT^3 - \frac{EPT^{-G}}{G} \right]_{T1}^{T2} \qquad 2\text{-}23$$

where T_1 = Saturation temperature, K

T_2 = Final temperature, K

4. Water liquid

The liquid enthalpy is found using the enthalpy of vaporization of H_2O and the H_2O vapor enthalpy. Figure 2-1 illustrates the use of these two values in finding the liquid enthalpy.

Temperature T_1 in figure 2-1 is the reference temperature, chosen for this work to be 273.15 K. The straight, horizontal segment, line 1-2, is the enthalpy of vaporization.

This now places the computations on the saturated vapor curve. Liquid enthalpies at other temperatures are found by first "traveling" the H_2O saturated vapor curve. Segment 2-3 is the H_2O vapor enthalpy difference between the reference temperature and the temperature of interest, T_2. Point 3 is the H_2O vapor enthalpy at temperature T_2. The liquid enthalpy is found by subtracting the enthalpy of vaporization from the saturated vapor enthalpy. This is point 4 in figure 2-1. Point 5 is the critical temperature. Segment 5-6 is superheated vapor.

The liquid entropy of H_2O was found in a manner similar to the enthalpy. In this case the entropy of vaporization was used with the vapor entropy to find the liquid entropy. Again use figure 2-1 as a reference.

5. Water vaporization

Enthalpy of vaporization H_{v2} at temperature T_2 is found from the following equation:

$$\frac{H_{v2}}{H_{v1}} = \left[\frac{T_c - T_2}{T_c - T_1}\right]^n \qquad 2\text{-}24$$

In this equation, the known enthalpy of vaporization, H_{v1} at temperature T_1, and the power coefficient, n, were found from Reid et al. 1987, resulting in the following equation:

$$H_{v2} = C_1(1 - \frac{T}{T_c})^{C_2} \qquad 2\text{-}25$$

where $C_1 = 13468.42$

$C_2 = 0.380$

$T_c = H_2O$ critical temperature, 647.3 K

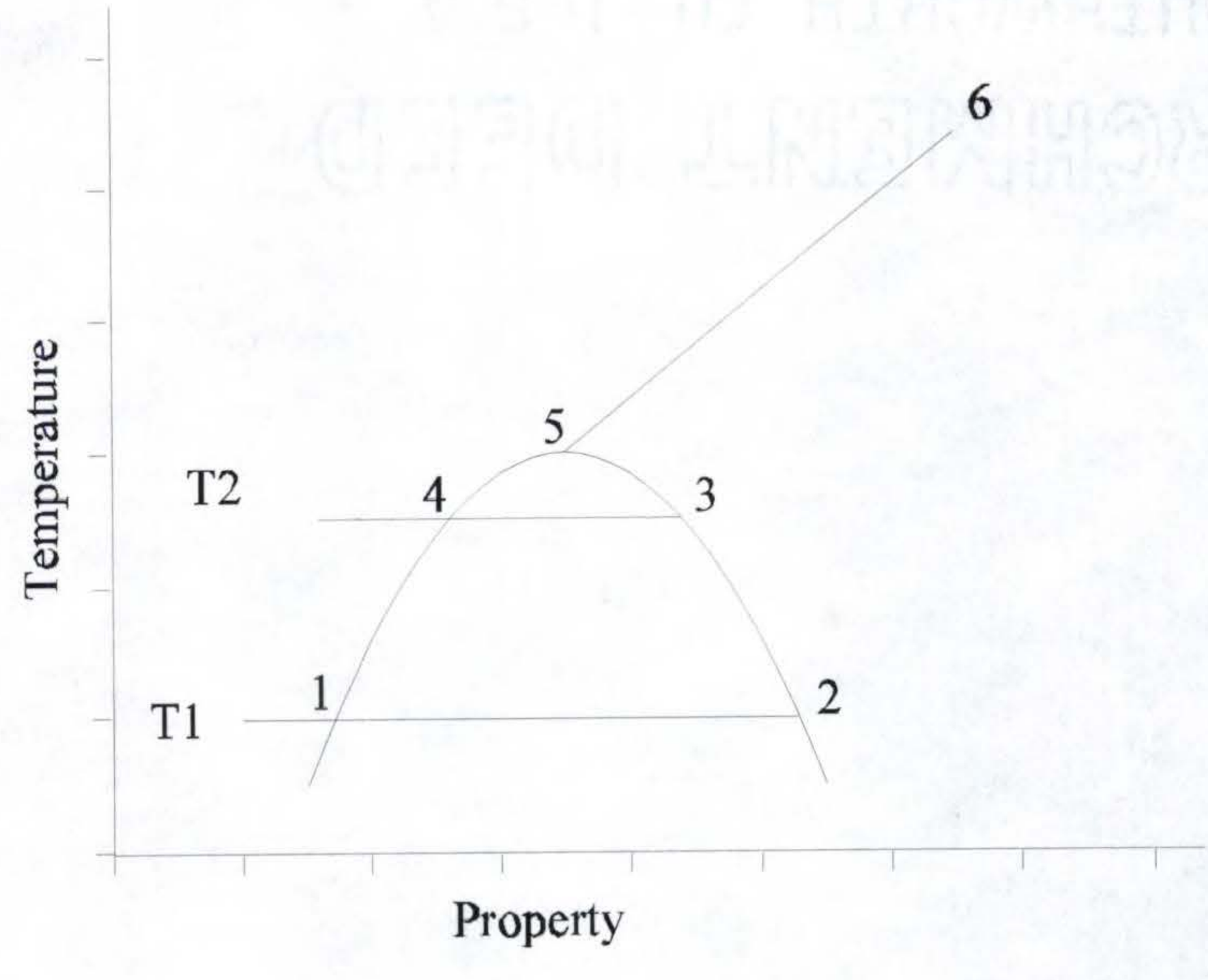

Figure 2-1 A generic diagram of water property (enthalpy or entropy) against temperature

6. Water vapor

$$C_p = A + BT + CT^2 + DT^3 \qquad 2\text{-}26$$

where $A = 32.24$

$B = 1.924 \times 10^{-3}$

$C = 1.056 \times 10^{-5}$

$D = -3.596 \times 10^{-9}$

$$h = \left[AT + \frac{BT^2}{2} + \frac{CT^3}{3} + \frac{DT^4}{4} \right]_{T_1}^{T_2} \qquad 2\text{-}27$$

$$s = \left[A\ln T + BT + \frac{CT^2}{2} + \frac{DT^3}{3} \right]_{T1}^{T2} \qquad 2\text{-}28$$

where T_1 = Saturation temperature, K

T_2 = Final temperature, K

2.2.2 Ammonia-Water Mixtures

1. Liquid

The ammonia-water mixture is in the liquid phase when the temperature is below its bubble point temperature.

$$h_m = xh_{NH3,f} + (1 - x)h_{H2O,f} \qquad 2\text{-}29$$

$$s_m = xs_{NH3,f} + (1 - x)s_{H2O,f} - R_m(x'\ln x' + (1 - x')\ln(1 - x') \qquad 2\text{-}30$$

where x = ammonia mass fraction

x' = ammonia mole fraction

R_m= gas constant of the mixture

2. Two phase region

The two phase region is the region between the bubble point and dew point.

$$h_m = amv \times x_g h_{NH3,g} + amv(1 - x_g)h_{H2O,g} + aml \times x_f h_{NH3,f} + aml(1 - x_f)h_{H2O,f} \quad 2\text{-}31$$

$$s_m = amv \times x_g s_{NH3,g} + amv(1 - x_g)s_{H2O,g} + aml \times x_f s_{NH3,f} + aml(1 - x_f)s_{H2O,f} - R_m(x_g'\ln x_g' + (1 - x_g')\ln(1 - x_g')) - R_m(x_f'\ln x_f' + (1 - x_f')\ln(1 - x_f')) \quad 2\text{-}32$$

where aml, amv = mass fractions of liquid and vapor in the mixture

x_g and x_g' = mass and mole fraction of ammonia of vapor mixture

x_f and x_f' = mass and mole fraction of ammonia of liquid mixture

3. Vapor

The ammonia-water mixture is in the vapor phase when temperature is above its dew point temperature.

$$h_m = xh_{NH3,g} + (1 - x)h_{H2O,g} \quad 2\text{-}33$$

$$s_m = xs_{NH3,g} + (1 - x)s_{H2O,g} - R_m(x'\ln x' + (1 - x')\ln(1 - x')) \quad 2\text{-}34$$

2.2.3 Discussion

The advantage of using the El-Sayed and Tribus method is that it is very convenient to calculate the bubble and dew temperatures, without having to compute the fugacity to determine the two phase region. The disadvantage is that it needs to calculate the saturation temperature to compute the enthalpy and entropy. And the saturation temperatures of pure components are different from the saturation temperatures of the mixtures, because the saturation temperature of a mixture changes even at the same pressure. Also, the coefficients of heat capacity equations can not fit a wide range. In the liquid region, the properties of two pure components cannot simply be mixed. Gibbs free energy is still needed to calculate the difference from the ideal condition.

2.3 Thermodynamic Properties of Ammonia-Water Mixtures by Gibbs Free Energy Method

2.3.1 Gibbs Free Energy for Pure Component

The fundamental equation of the Gibbs energy, G, of a pure component can be derived from known relations for volume and heat capacity as a function of temperature and pressure. The fundamental equation of the Gibbs energy is given in an integral form as

$$G = h_0 - Ts_0 + \int_{T_0}^{T} C_p dT + \int_{P_0}^{P} v dP - T\int_{T_0}^{T} \frac{C_p}{T} dT \qquad 2\text{-}35$$

where h_0, s_0, T_0 and P_0 are the enthalpy, entropy, temperature, and pressure at the reference state. The volume, v, and the heat capacity at constant pressure, C_p, for liquid phase are assumed to fit the following empirical relations proposed by Ziegler and Trepp(1984);

$$v^L = a_1 + a_2P + a_3T + a_4T^2 \qquad 2\text{-}36$$

$$C_P{}^L = b_1 + b_2T + b_3T^2 \qquad 2\text{-}37$$

For the gas phase, the corresponding empirical relations are

$$v^g = \frac{RT}{P} + c_1 + \frac{c_2}{T^3} + c_3T^{11} + \frac{c_4P^2}{T^{11}} \qquad 2\text{-}38$$

$$C_p{}^{g,o} = d_1 + d_2T + d_3T^2 \qquad 2\text{-}39$$

where the superscripts are L for liquid, g for gas, and o for the ideal gas state.

Integration leads to the following equations for the Gibbs energy for the pure components.

Liquid phase:

$$G_r^L = h_{r,o}^L - T_r s_{r,o}^L + B_1(T_r - T_{r,o}) + \frac{B_2}{2}(T_r^2 - T_{r,o}^2) + \frac{B_3}{3}(T_r^3 - T_{r,o}^3) - B_1T_r \ln(\frac{T_r}{T_{r,o}})$$
$$-B_2T_r(T_r - T_{r,o}) - \frac{B_3}{2}(T_r^2 - T_{r,o}^2) + (A_1 + A_3T_r + A_4T_r^2)(P_r - P_{r,o}) + \frac{A_2}{2}(P_r^2 - P_{r.o}^2) \qquad 2\text{-}40$$

Gas phase:

$$G_r^g = h_{r,o}^g - T_r s_{r,o}^g + D_1(T_r - T_{r,o}) + \frac{D_2}{2}(T_r^2 - T_{r,o}^2) + \frac{D_3}{3}(T_r^3 - T_{r,o}^3) - D_1 T_r \ln(\frac{T_r}{T_{r,o}})$$

$$-D_2 T_r(T_r - T_{r,o}) - \frac{D_3}{2}(T_r^2 - T_{r,o}^2) + T_r \ln(\frac{P_r}{P_{r,o}})$$

$$+C_1(P_r - P_{r,o}) + C_2(\frac{P_r}{T_r^3} - 4\frac{P_{r,o}}{T_{r,o}^3} + 3\frac{P_{r,o}T_r}{T_{r,o}^4}) + C_3(\frac{P_r}{T_r^{11}} - 12\frac{P_{r,o}}{T_{r,o}^{11}} + 11\frac{P_{r,o}T_r}{T_{r,o}^{12}})$$

$$+\frac{C_4}{3}(\frac{P_r^3}{T_r^{11}} - 12\frac{P_{r,o}^3}{T_{r,o}^{11}} + 11\frac{P_{r,o}^3 T_r}{T_{r,o}^{12}})$$

2-41

where the reduced thermodynamic properties are defined as

$T_r = T/T_B$

$P_r = P/P_B$

$G_r = G/RT_B$

$h_r = h/RT_B$

$s_r = s/R$

$v_r = vP_B/RT_B$

The reference values for the reduced properties are R = 8.314 kJ/kmole-K, T_B = 100 K and P_B = 10 bar.

2.3.2 Thermodynamic Properties of a Pure Component

The molar specific enthalpy, entropy, and volume are related to Gibbs free energy by

$$h = -T^2\left[\frac{\partial}{\partial T}(G/T)\right]_P \qquad 2\text{-}42$$

$$s = -\left[\frac{\partial G}{\partial T}\right]_P \qquad 2\text{-}43$$

$$v = \left[\frac{\partial G}{\partial P}\right]_T \qquad 2\text{-}44$$

In terms of reduced variables

$$h = -RT_B T_r^2 \left[\frac{\partial}{\partial T_r}(G_r / T_r)\right]_{P_r} \qquad 2\text{-}45$$

$$s = -R\left[\frac{\partial G_r}{\partial T_r}\right]_{P_r} \qquad 2\text{-}46$$

$$v = \frac{RT_B}{P_B}\left[\frac{\partial G_r}{\partial P_r}\right]_{T_r} \qquad 2\text{-}47$$

2.3.3 Ammonia-Water Liquid Mixtures

The Gibbs excess energy for liquid mixtures allows for deviation from ideal solution behavior. The Gibbs excess energy of the liquid mixture is expressed by the relation proposed by Redlich and Kister(Reid et al. 1987; Ziegler and Trepp 1984), which is limited to three terms and is given by

$$G_r^E = \left\{F_1 + F_2(2x-1) + F_3(2x-1)^2\right\}(1-x) \qquad 2\text{-}48$$

where

$$F_1 = E_1 + E_2P_r + (E_3 + E_4P_r)T_r + E_5/T_4 + E_6/T_r^2$$

$$F_2 = E_4 + E_8P_4 + (E_9 + E_{10}Pr)Tr + E_{11}/T_r + E_{12}/T_r^2$$

$$F_3 = E_{13} + E_{14}P_r + E_{15}/T_r + E_{16}/T_r^2$$

Table 2-1 Coefficients of equations 2-40 and 2-41

Coefficient	Ammonia	Water
A_1	$3.971423\ 10^{-2}$	$2.748796\ 10^{-2}$
A_2	$-1.790557\ 10^{-5}$	$-1.016665\ 10^{-5}$
A_3	$-1.308905\ 10^{-2}$	$-4.452025\ 10^{-3}$
A_4	$3.752836\ 10^{-3}$	$8.389246\ 10^{-4}$
B_1	$1.634519\ 10^{+1}$	$1.214557\ 10^{+1}$
B_2	-6.508119	-1.898065
B_3	1.448937	$2.911966\ 10^{-}$
C_1	$-1.049377\ 10^{-2}$	$2.136131\ 10^{-2}$
C_2	-8.288224	$-3.169291\ 10^{+1}$
C_3	$-6.647257\ 10^{+2}$	$-4.634611\ 10^{+4}$
C_4	$-3.045352\ 10^{+3}$	0.0
D_1	3.673647	4.019170
D_2	$9.989629\ 10^{-2}$	$-5.175550\ 10^{-2}$
D_3	$3.617622\ 10^{-2}$	$1.951939\ 10^{-2}$
$h_{r,o}^{L}$	4.878573	21.821141
$h_{r,o}^{g}$	26.468873	60.965058
$s_{r,o}^{L}$	1.644773	5.733498
$s_{r,o}^{g}$	8.339026	13.453430
$T_{r,o}$	3.2252	5.0705
$P_{r,o}$	2.000	3.000

Table 2-2 Coefficients of equation 2-48

E_1	-41.733398	E_9	0.387983
E_2	0.02414	E_{10}	0.004772
E_3	6.702285	E_{11}	-4.648107
E_4	-0.011475	E_{12}	0.836376
E_5	63.608967	E_{13}	-3.553627
E_6	-62.490768	E_{14}	0.000904
E_7	1.761064	E_{15}	24.361723
E_8	0.008626	E_{16}	-20.736547

The excess enthalpy, entropy, and volume for the liquid mixtures are given as

$$h^E = -RT_B T_r^2 \left[\frac{\partial}{\partial T_r} (G_r^E / T_r) \right]_{P_r, x} \qquad 2\text{-}49$$

$$s^E = -R \left[\frac{\partial G_r^E}{\partial T_r} \right]_{P_r, x} \qquad 2\text{-}50$$

$$v^E = \frac{RT_B}{P_B} \left[\frac{\partial G_r^E}{\partial P_r} \right]_{T_r, x} \qquad 2\text{-}51$$

The enthalpy, entropy, and volume of a liquid mixture are computed by

$$h_m^L = x_f h_a^L + (1 - x_f) h_w^L + h^E \qquad 2\text{-}52$$

$$s_m^L = x_f s_a^L + (1 - x_f) s_w^L + s^E + s^{mix} \qquad 2\text{-}53$$

$$s^{mix} = -R\{x_f \ln(x_f) + (1-x_f)\ln(1-x_f)\} \qquad 2\text{-}54$$

$$v_m^L = x_f v_a^L + (1-x_f) v_w^L + v^E \qquad 2\text{-}55$$

2.3.4 Ammonia-Water Vapor Mixture

Ammonia-water vapor mixtures are assumed to be ideal solutions. The enthalpy, entropy, and volume of the vapor mixture are computed by

$$h_m^g = x_g h_a^g + (1-x_g) h_w^g \qquad 2\text{-}56$$

$$s_m^g = x_g s_a^g + (1-x_g) s_w^g + s^{mix} \qquad 2\text{-}57$$

$$v_m^g = x_g v_a^g + (1-x_g) v_w^g \qquad 2\text{-}58$$

2.3.5 Vapor-Liquid Equilibrium

At equilibrium, binary mixtures must have the same temperature and pressure. Moreover, the partial fugacity of each component in the liquid and gas mixtures must be equal.

$$T^L = T^g = T \qquad 2\text{-}59$$

$$P^L = P^g = P \qquad 2\text{-}60$$

$$\hat{f}_a^L = \hat{f}_a^g \qquad 2\text{-}61$$

$$\hat{f}_w^L = \hat{f}_w^g \qquad 2\text{-}62$$

where P and T are the equilibrium pressure and temperature of the mixture, and $\hat{f}$ is the fugacity of each component in the mixture at equilibrium.

The fugacities of ammonia and water in liquid mixtures are given by Walas(1985)

$$\hat{f}_a^L = \gamma_a f_a^0 x \delta_a \qquad 2\text{-}63$$

$$\hat{f}_w^L = \gamma_w f_w^0 (1-x) \delta_w \qquad 2\text{-}64$$

where γ = activity coefficient

f^0 = standard state fugacity of pure liquid component corrected to zero pressure

δ = Poynting correction factor from zero pressure to saturation pressure of mixture

assuming an ideal mixture in the vapor phase, the fugacities of the pure components in the vapor mixtures are given by

$$\hat{f}_a^g = \phi_a P y \qquad 2\text{-}65$$

$$\hat{f}_w^g = \phi_w P (1-y) \qquad 2\text{-}66$$

where: ϕ = fugacity coefficient

2.3.6 Discussion

The Gibbs free energy method is relatively simple for calculation of the pure component thermodynamic properties. The reference temperature and pressure are fixed, you only need to know the temperature and pressure of interest to determine the mixtures properties.

2.4 Method by Park and Sonntag

The generalized equation of state approach is useful in predicting thermodynamic and volumetric properties of substances for which experimental data are scarce and a minimum number of data are available: critical temperature, critical pressure, critical volume, and eccentric factor.

In this study, thermodynamic and volumetric properties of ammonia-water mixtures are derived from three basic equations:

1. Helmholtz free energy equation for the ideal gas properties of water:

$$A^* = R\left[\sum_{i=1}^{6}\frac{a_i}{t^{i-1}} + 46\ln(T) - 1011.249\frac{\ln(T)}{t}\right] \qquad 2\text{-}67$$

where $t = 1000/T$

constants of ideal gas equation for water

Table 2-3 Coefficients of equation 2-67

a_1	1857.065	a_3	-419.465	a_5	-20.5516
a_2	3329.12	a_4	36.6649	a_6	4.85233

Similarly, for ammonia

$$A^* = RT\left[a_1\ln(T) + \sum_{i=2}^{11}a_i T^{i-3} + \ln(4.8180T) - 1\right] \qquad 2\text{-}68$$

2. The generalized equation of state based on a four-parameter corresponding state principle, which is expressed in terms of Z^0, Z^1, Z^2; functions of T_r and P_r; eccentric factor, w; and polarity factor, m, with appropriate correction term:

$$Z = Z^0 + wZ^1 + mZ^2 \qquad 2\text{-}69$$

$$Z^1 = \frac{1}{w^r}(Z^r - Z^0) \qquad 2\text{-}70$$

$$Z^2 = Z^w - \left\{Z^0 + \frac{w^w}{w^r}(Z^r - Z^0)\right\} \qquad 2\text{-}71$$

where Z^1 and Z^2 are the nonspherical and polar corrections, respectively.

Table 2-4 Coefficients of equation 2-68

a_1	-3.872727	a_7	$0.36893175\ 10^{-10}$
a_2	0.64463724	a_8	$-0.35034664\ 10^{-13}$
a_3	3.2238759	a_9	$0.2056303\ 10^{-16}$
a_4	-0.00213769925	a_{10}	$-0.6853420\ 10^{-20}$
a_5	$0.86890833\ 10^{-5}$	a_{11}	$0.9939243\ 10^{-24}$
a_6	$-0.24085149\ 10^{-7}$		

3. The pseudocritical constants method:

$$T_{cm} = \sum_i \theta_i T_{ci} + \sum_i \sum_j \theta_i \theta_j t_{ij} \qquad 2\text{-}72$$

where subscript cm refers to critical property of mixture.

$$V_{cm} = \sum_i \theta_i V_{ci} + \sum_i \sum_j \theta_i \theta_j v_{ij} \qquad 2\text{-}73$$

$$\theta_i = \frac{x_i V_{ci}^{2/3}}{\sum x_i V_{ci}^{2/3}} \qquad 2\text{-}74$$

$$P_{cm} = \frac{Z_{cm} R T_{cm}}{V_{cm}} \qquad 2\text{-}75$$

$$Z_{cm} = 0.2901 - 0.0879 w_m - 0.0266 m_m \qquad 2\text{-}76$$

$$w_m = \sum_i x_i w_i \qquad 2\text{-}77$$

$$m_m = \sum_i x_i m_i \qquad 2\text{-}78$$

4. Discussion

Park and Sonntag claim that using the generalized equation method provides a consistent way to calculate the thermodynamic properties of ammonia-water mixtures. But in the high pressure range, they don't have experimental data to verify the reliability of this method. This method needs to be further investigated.

2.5 An Alternative Method: Using Gibbs Free Energy Method for Pure Components, and Bubble and Dew Point Temperature Equations for Equilibrium Composition

The Gibbs free energy of the mixture is a function of temperature, pressure and mixture composition. The property data derived from such an equation of state are very consistent and convenient. One can easily calculate the thermodynamic properties of interest such as enthalpy, entropy, specific volume and vapor pressure without considering the phase state. Most of the researchers tend to use equation of state model in their properties calculation.

The criteria of phase equilibrium in a binary system is that the liquid fagucity (or chemical potential) of a pure component equals the vapor fagucity (or chemical potential) of that pure component. This requires several iterations to get the composition of each component of phase equilibrium. The accuracy and convergent time vary at different points. In a power cycle simulation, these iterations should be avoided for the accuracy and the computation time of the simulations. El-Sayed and Tribus (1985) developed bubble and dew point temperatures equations to calculate phase equilibrium. These equations reduce iterations during phase equilibrium calculations and their temperature ranges up to 770 K.

In the present study, a method that combines the advantages of Gibbs free energy method and bubble and dew point temperatures equations is presented. The results show a very good agreement with the available data based on experimental measurements and the computation time is reduced.

2.6 Results and Comparisons with Literature Data

The properties of pure ammonia and water can be calculated very precisely by using the Gibbs free energy equation. In order to calculate the properties of the mixtures it is very important to predict equilibrium state of vapor-liquid mixture.

For the vapor-liquid equilibrium, experimental data are used. Most experiments were done in the early 30s. IGT conducted their experiments in the 60s and combined most of the data from the early experiments to produce vapor-liquid equilibrium data and mixture properties data for temperature up to 500 K and pressure up to 34.45 bar. The

IGT data is accepted as a reliable source, and most computational data are compared with it.

Wiltec Research Co. (Gillespie et al. 1987) conducted measurements of the ammonia-water mixtures vapor-liquid equilibrium in the early 80s from 313 K and 589 K. Their data is used to extend the ammonia-water mixtures data to temperature up to 600 K and pressure up to 110 bar by Ibrahim and Klein (1993).

IGT and Wiltec data are used to make correlations to predict ammonia-water mixtures equilibrium state. The accuracy of computation depends on the mathematical models used to generate correlations, and computational methods used to compute the thermodynamic properties of ammonia-water mixtures. It is not surprising that studies reported in the literature have varying degrees of agreement with the IGT properties data.

2.6.1 Comparison of Bubble and Dew Point Temperatures

Figures 2-2 to 2-5 show that the bubble and dew point temperatures generated by this study compares favorably with the IGT data.

For the bubble point temperature at constant pressure, IGT has a complete set of data for pressures from 1 psia to 500 psia and ammonia mass concentration from 0 to 1 incremented by 0.1. The differences between our computed values and the IGT data are less than 0.3%. Ziegler and Trepp, Ibrahim and Klein reported to have differences up to 2% with the IGT data.

IGT data has dew point temperatures with only four different ammonia mass fractions of 0.9641, 0.9824, 0.9907 and 0.9953. The data for small moisture

concentrations are used primarily for the moisture effects of absorption refrigeration cycle. Our results match equally well for the bubble temperatures. An advantage of this comparison is that the working fluid used in the proposed power cycle also has a very small percentage of moisture content.

2.6.2 Comparison of Saturation Pressure at Constant Temperature

Figures 2-6 to 2-10 show the saturation vapor and liquid pressures of ammonia-water mixtures as compared with Gillespie et al. data.

For temperatures less than 406 K, the computation results fit the experimental data well, except at saturated liquid pressure. At higher temperatures, our computed values are within 5% of the Gillespie et al. (1987) data even at pressures higher than 110 bar, while Ziegler and Trepp have reported more than 15% difference. Ibrahim and Klein reported a less than 5% error under 110 bar and higher errors over 110 bar.

2.6.3 Comparison of Saturated Liquid and Vapor Enthalpy

1. Saturated liquid enthalpy

The enthalpy of saturated liquid of this work is compared with IGT data, as shown in figures 2-11 to 2-14. The differences are less than 2% for all the data.

2. Saturated vapor enthalpy

The saturated vapor enthalpy at constant pressure is shown in figures 2-15 to 2-18. The agreement with IGT data is within 3%. Ibrahim and Klein's model reported about a 5% maximum difference.

The ammonia mass fractions shown in these figures are not ammonia vapor concentrations. In fact, these are ammonia liquid mass fractions when the mixtures reach a saturated state. So in order to compute the saturated vapor enthalpy, the ammonia vapor mass fraction has to be determined first. This means that the model has to be accurate in predicting the ammonia compositions in saturated liquid and vapor.

2.6.4 Comparison of Saturated Liquid and Vapor Entropy

The value of entropy is very important in predicting the performance of a turbine in a power cycle. Entropy data is also essential to the second law analysis of thermal systems. Scatchard et al. (1947) published saturated liquid and vapor entropy data based on experimental data from Zinner (1934), Wucherer (1932) and Perman (1901). Park and Sonntag(1990b) published calculated entropy data based on their models and compared with the Scatchard et al. data. In the present study, saturated liquid entropy data are compared with Scatchard et al., and Park and Sonntag computational data. However, saturated vapor data are compared with Scatchard et al. data only.

1. Saturated liquid entropy

Figures 2-19 to 2-22 show saturated liquid entropy data as compared with Scatchard et al. data. Our data agree with the experimental data very well except in the region of ammonia mass fraction from 0.3 to 0.6. In figures 2-19, 2-21 and 2-22, computed data from Park and Sonntag (1990b) are also compared. It can be seen that the magnitude of Park and Sonntag's data are very low as compared to Scatchard's data; it is more than 50% lower at ammonia mass fraction of 0.5.

2. Saturated vapor entropy

Excellent agreement of our computed values with the Scatchard et al. data of the saturated vapor entropy is shown in figures 2-23 to 2-26. Data reported by Park and Sonntag (1990b) are consistently lower than the Scatchard's data. Since it is very difficult to identify Park and Sonntag's saturated vapor entropy data from the literature, we didn't compare our results with them. Since the behavior of ammonia-water mixtures in the vapor state is close to the ideal gas mixture, this results in a good match for our mixture vapor model.

2.7 Conclusion

Different methods for calculating the ammonia-water mixture properties are studied. A practical and accurate method is used in this study. This method uses Gibbs free energy equations for pure ammonia and water properties, and bubble and dew point temperature equations for vapor-liquid equilibrium. The iterations necessary for calculating the bubble and dew point temperatures by the fugacity method are avoided. This method is much faster than method of using fugacities or chemical potentials. The computational results have been compared with the accepted experimental data and show very good agreement.

With consistent and accurate thermodynamic properties data of ammonia-water mixtures, we can perform the first and second law analyses of the proposed power cycle.

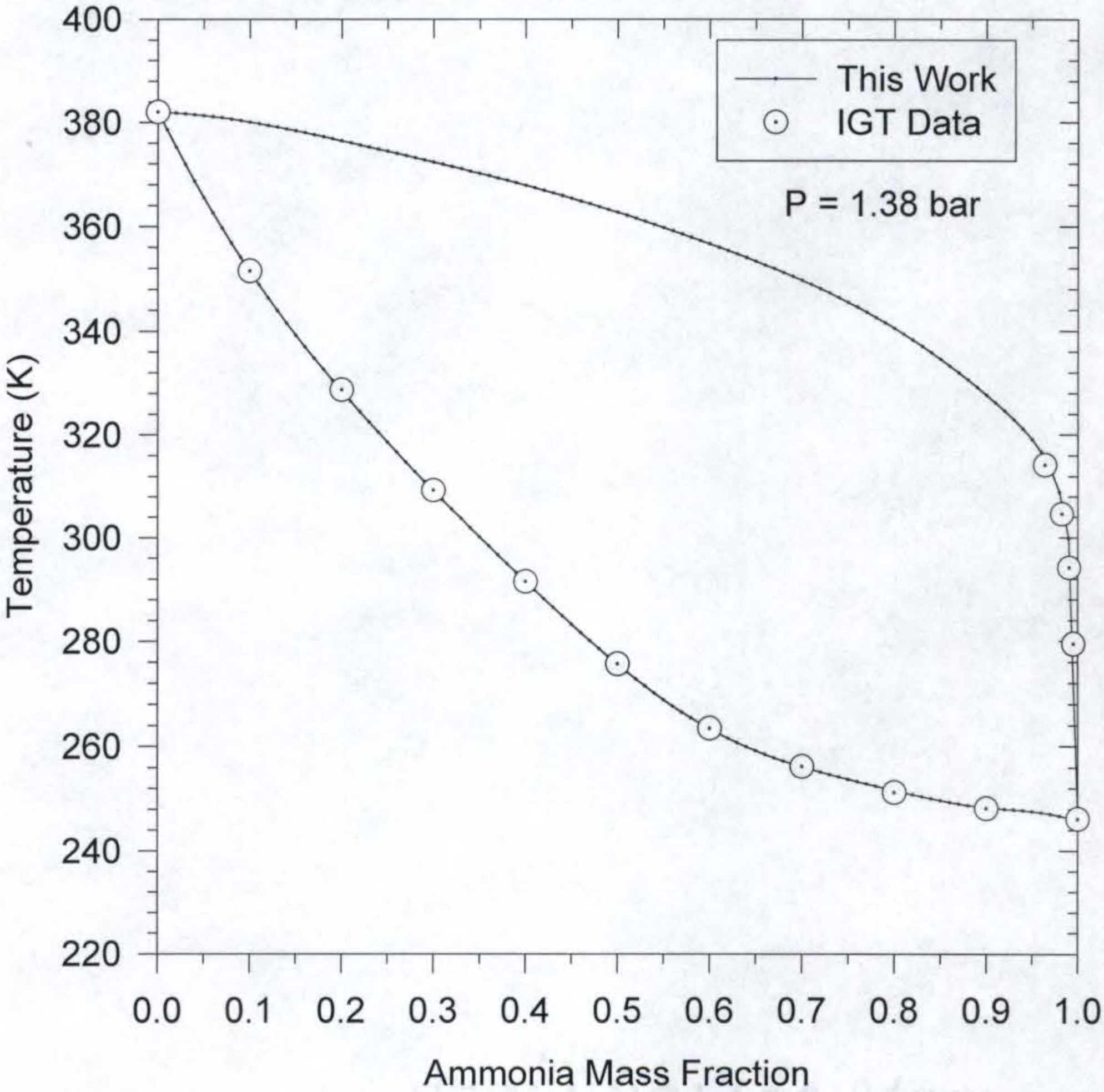

Figure 2-2 Bubble and dew point temperatures at a pressure of 1.38 bar

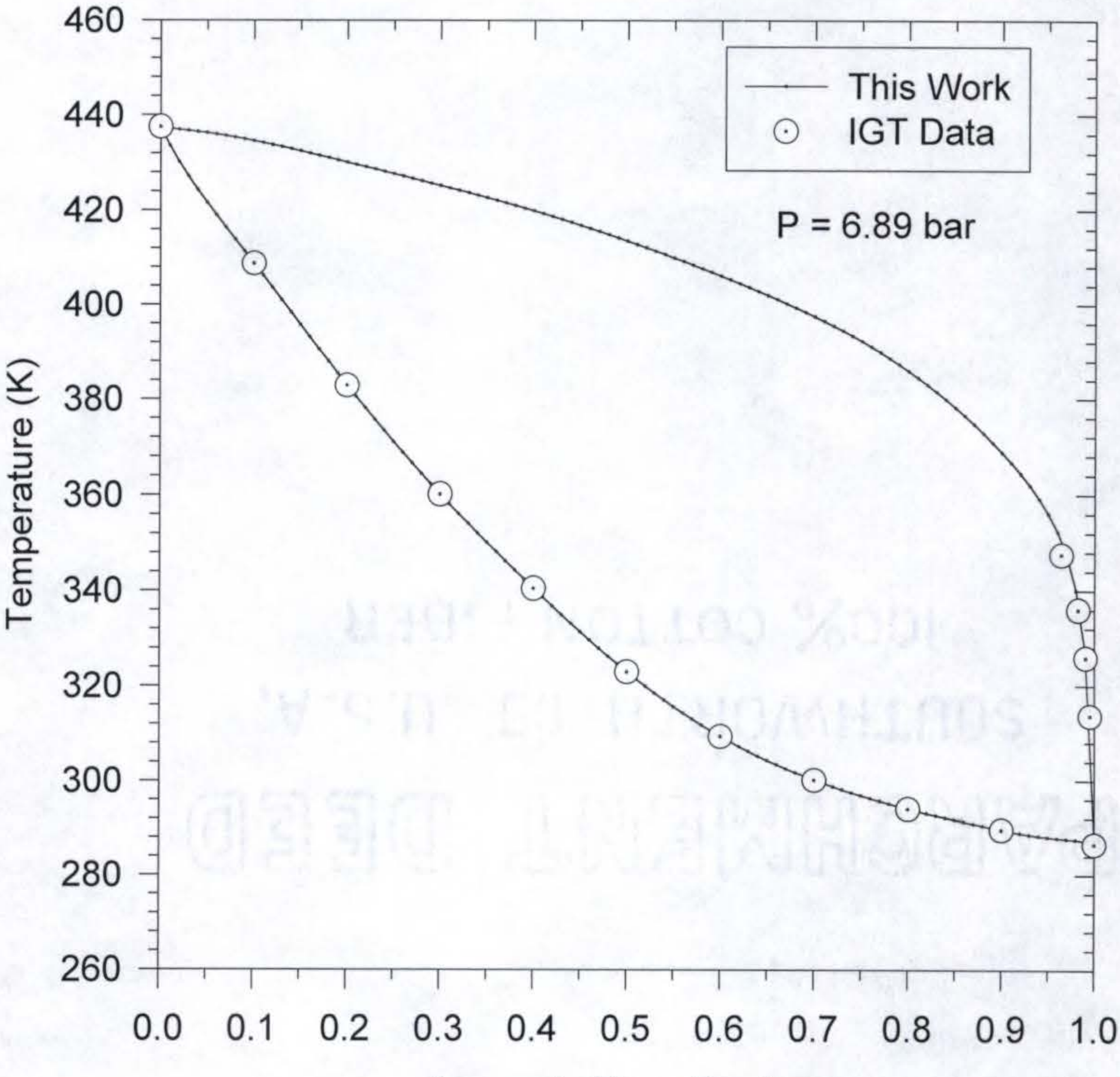

Figure 2-3 Bubble and dew point temperatures at a pressure of 6.89 bar

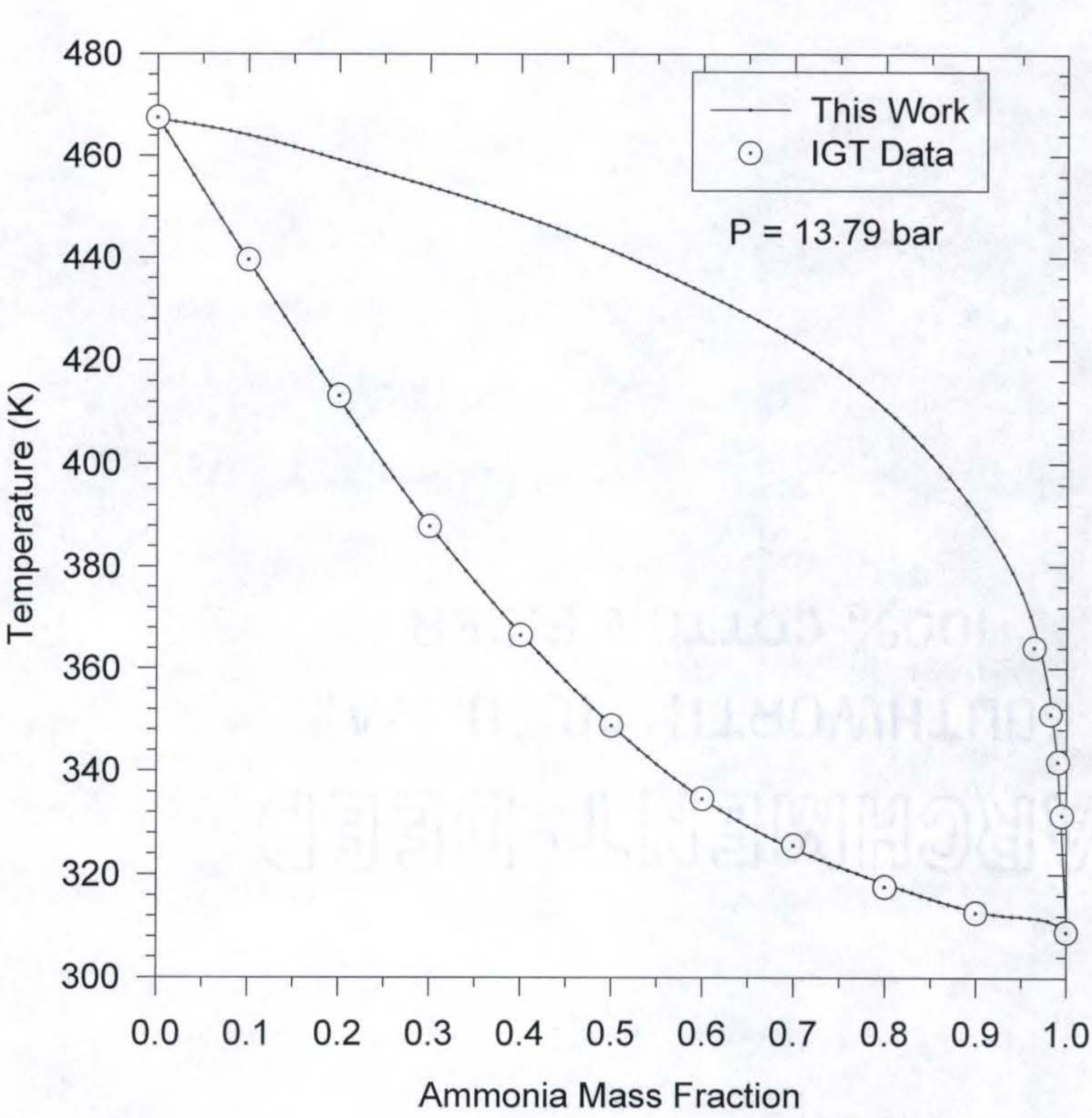

Figure 2-4 Bubble and dew point temperatures at a pressure of 13.79 bar

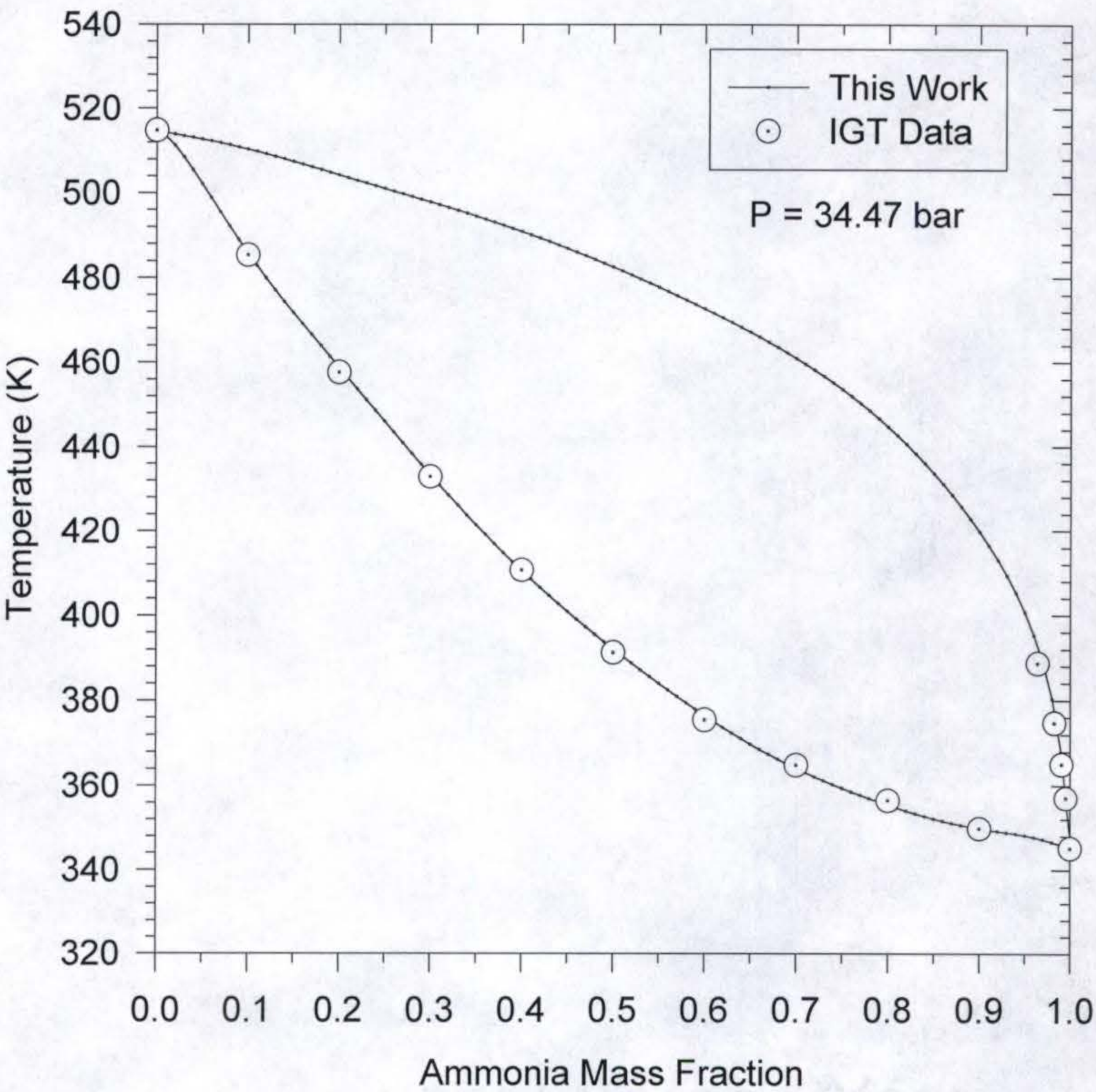

Figure 2-5 Bubble and dew point temperatures at a pressure of 34.47 bar

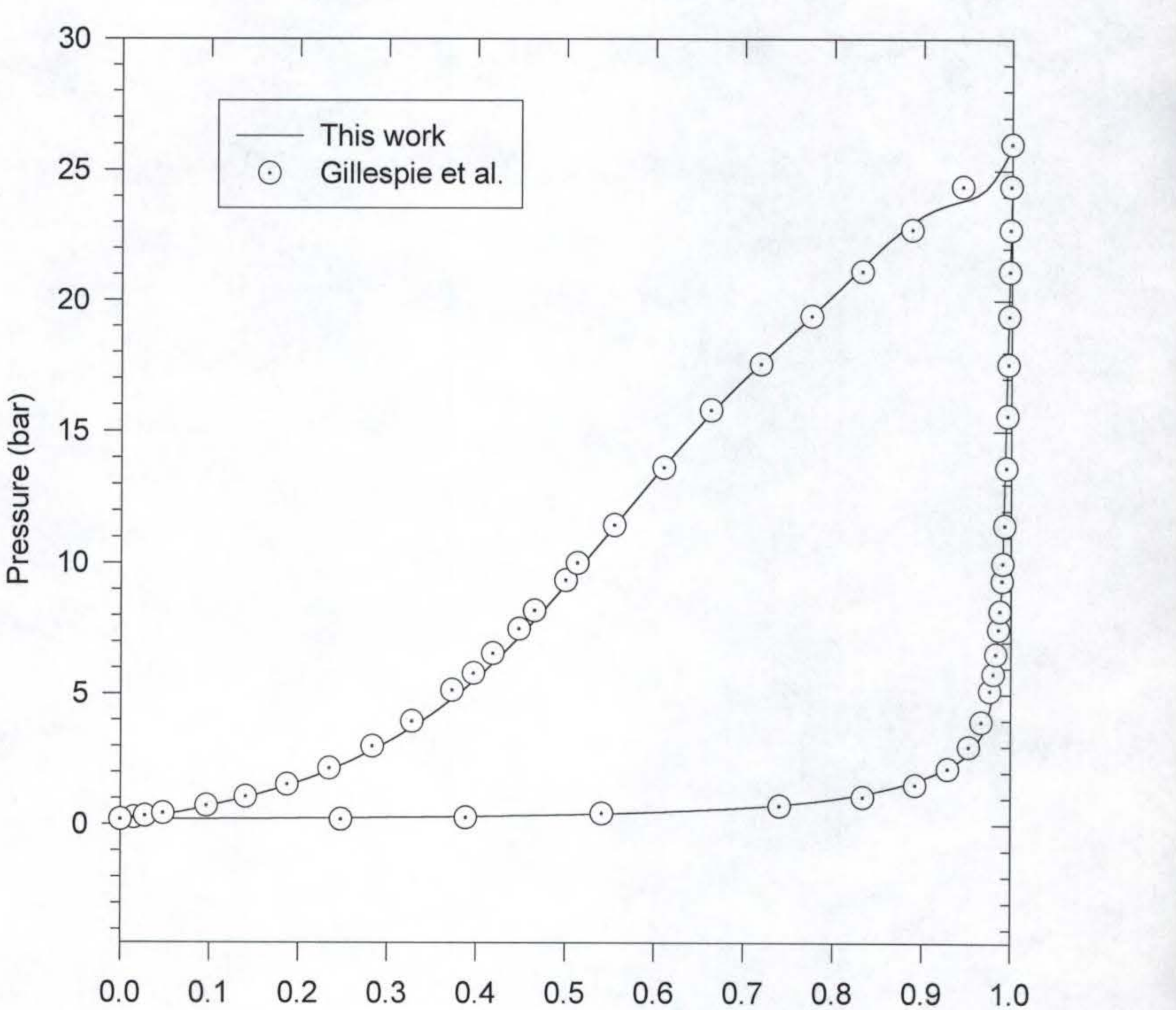

Figure 2-6 Saturated pressures of ammonia-water mixtures at 333.15 K

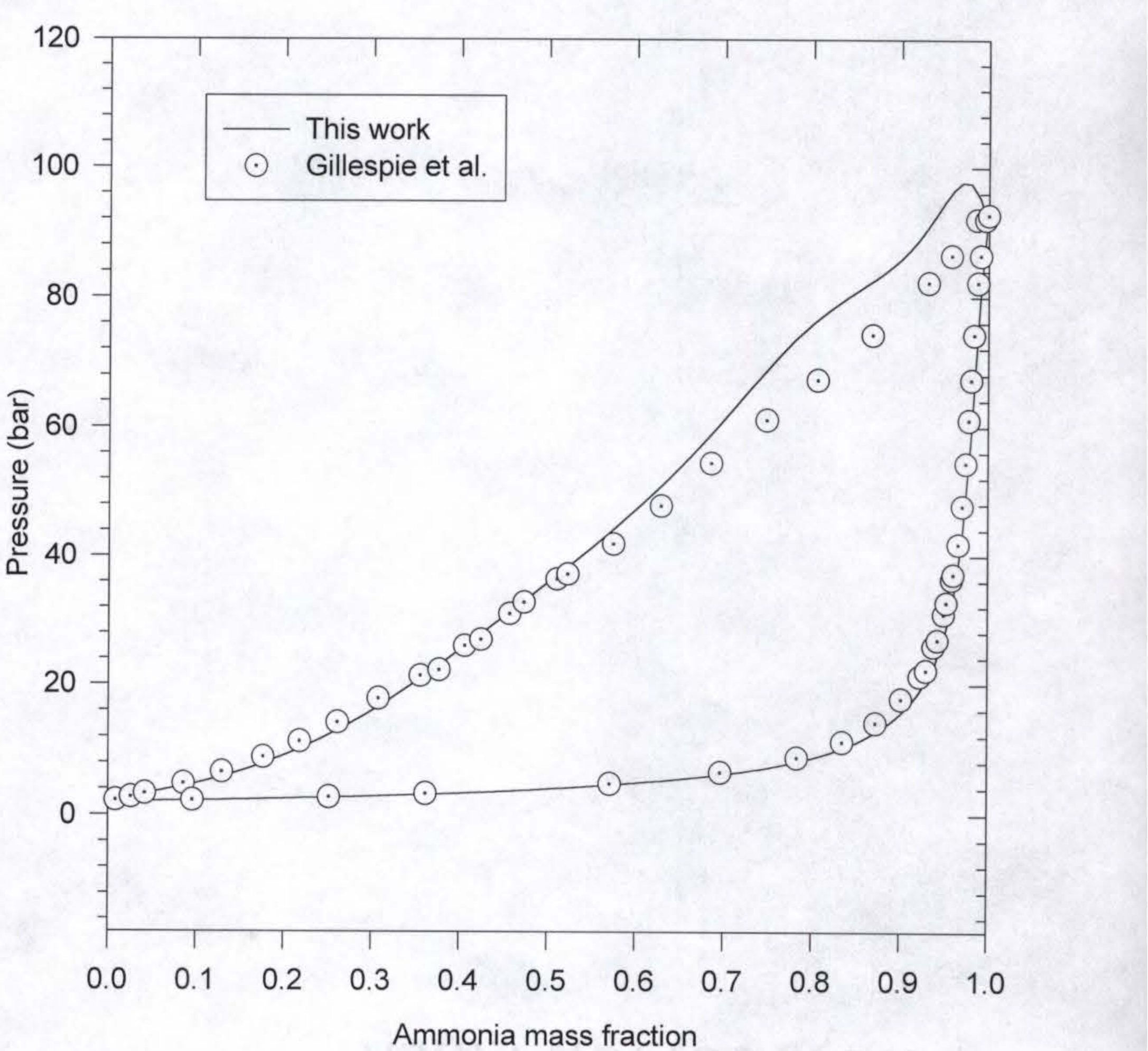

Figure 2-7 Saturated pressures of ammonia-water mixtures at 394.15 K

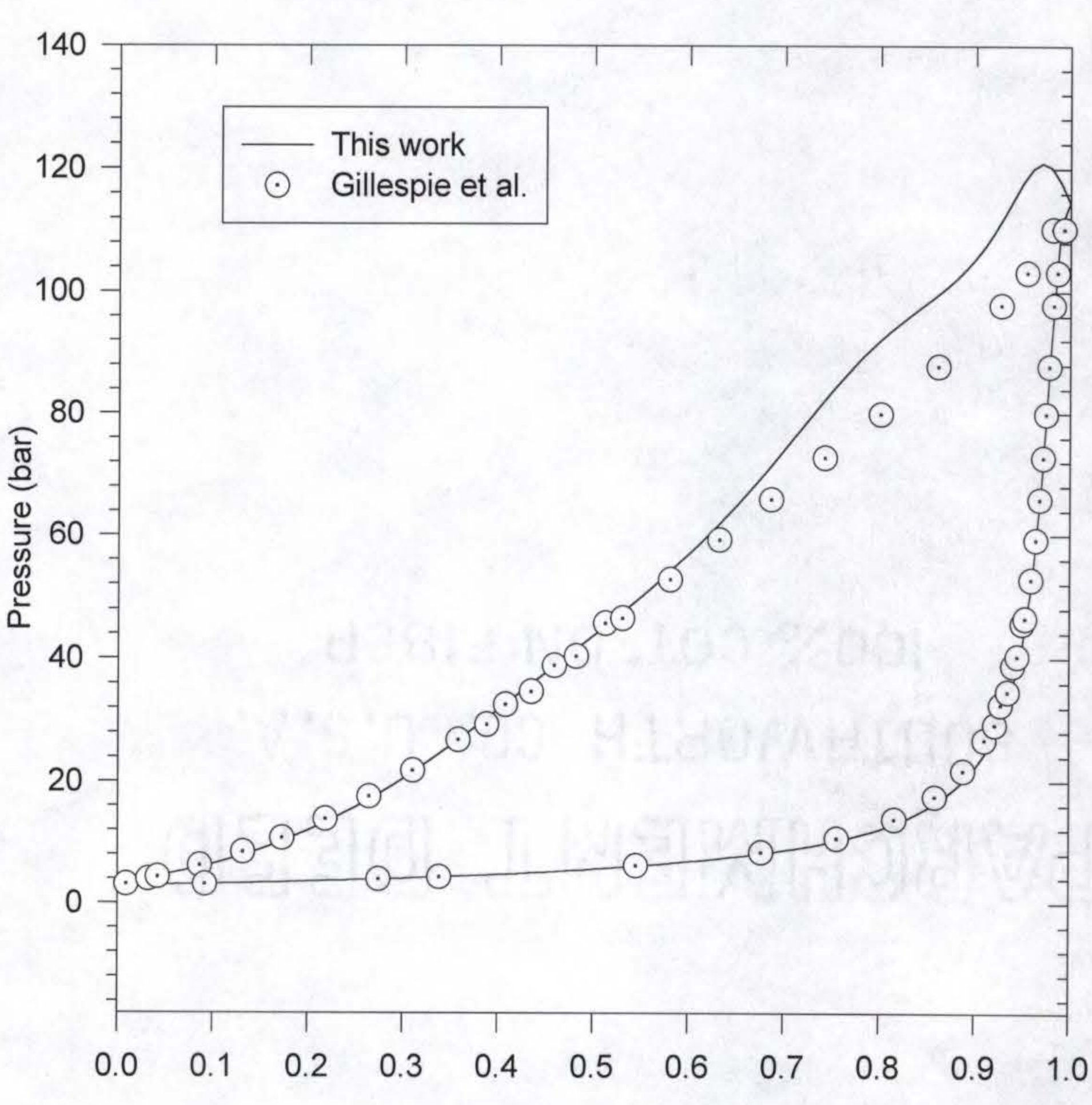

Figure 2-8 Saturated pressures of ammonia-water mixtures at 405.95 K

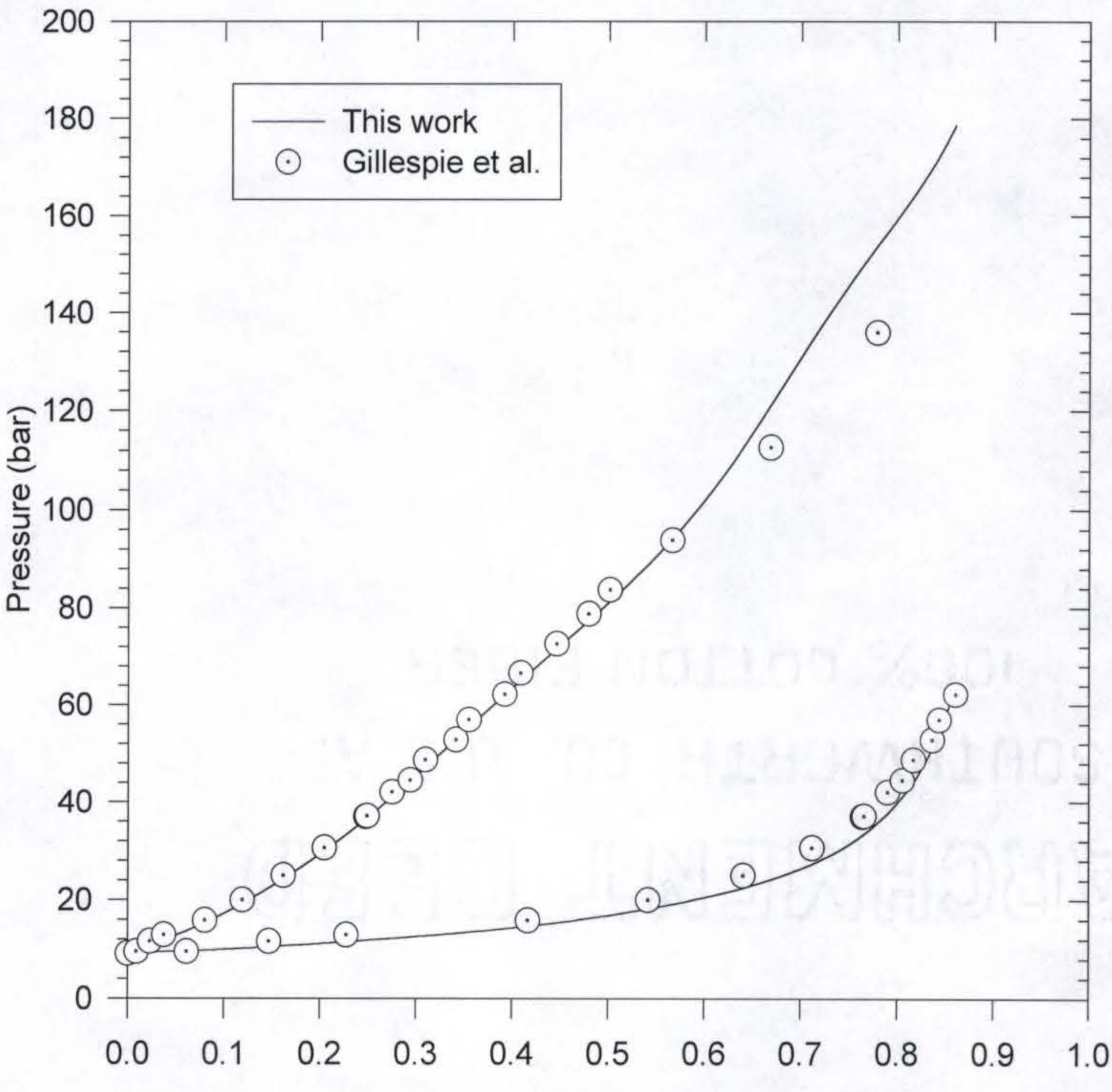

Figure 2-9 Saturated pressures of ammonia-water mixtures at 449.85 K

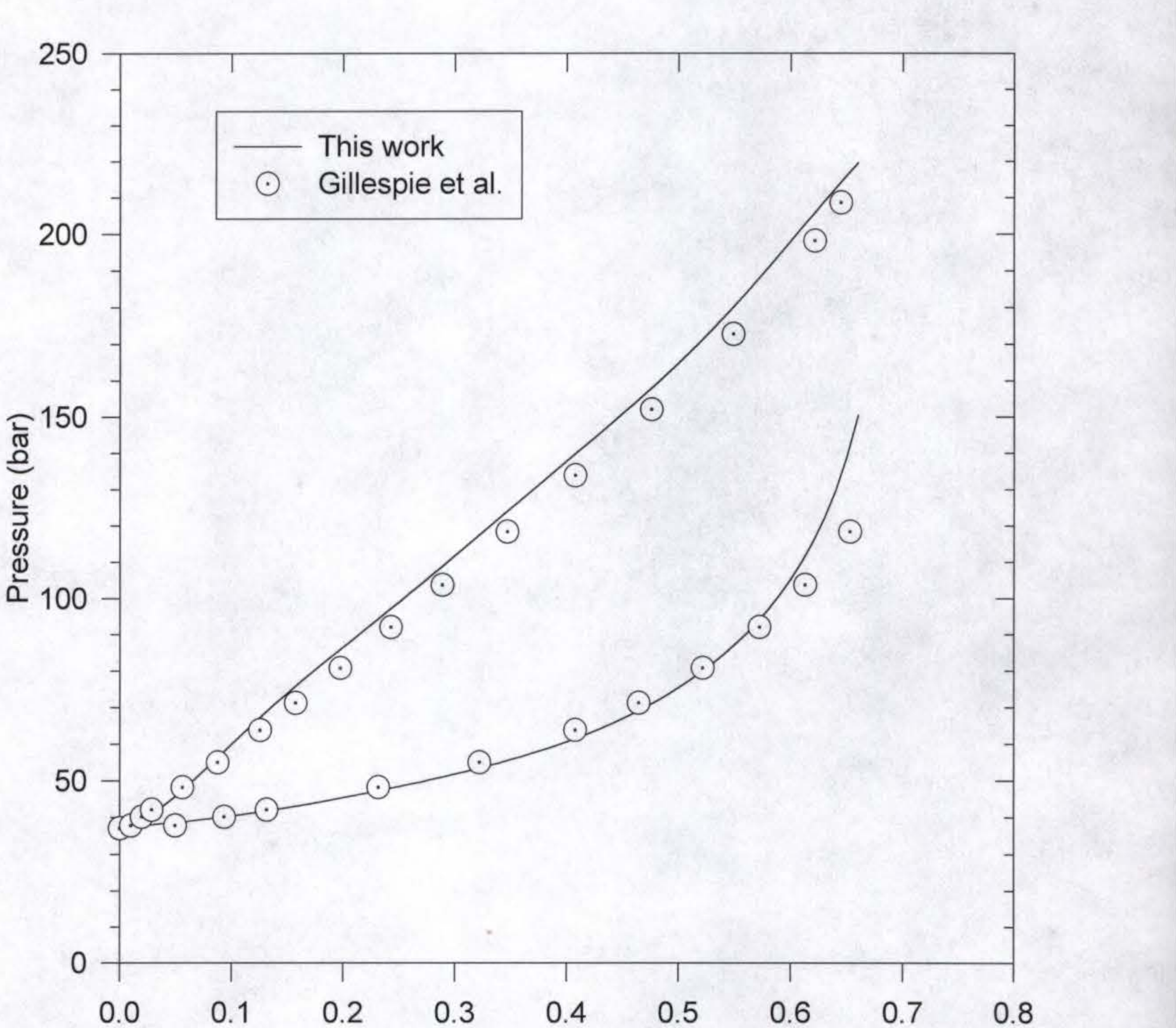

Figure 2-10 Saturated pressures of ammonia-water mixtures at 519.26 K

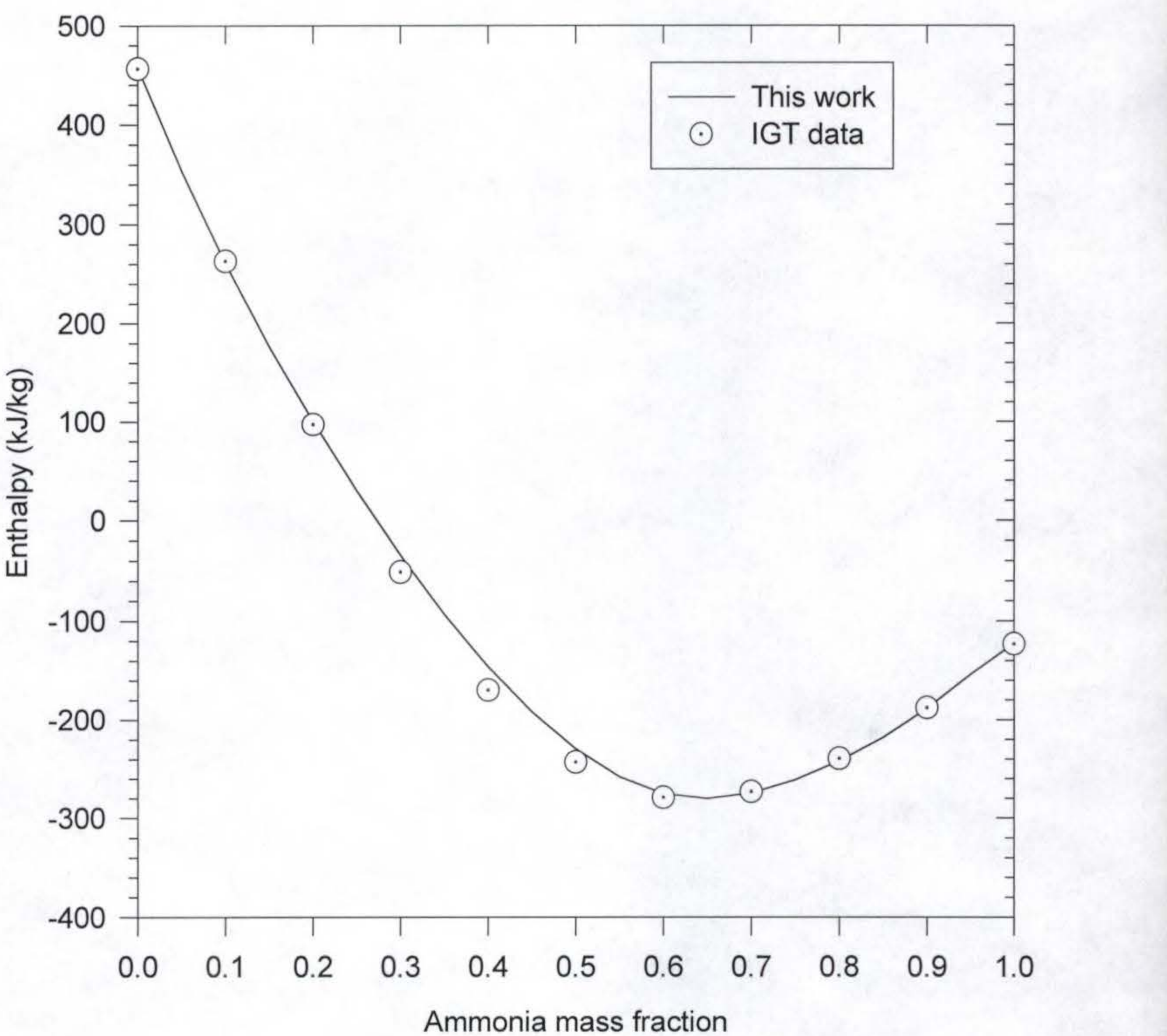

Figure 2-11 Saturated liquid enthalpy of ammonia-water mixtures at 1.38 bar

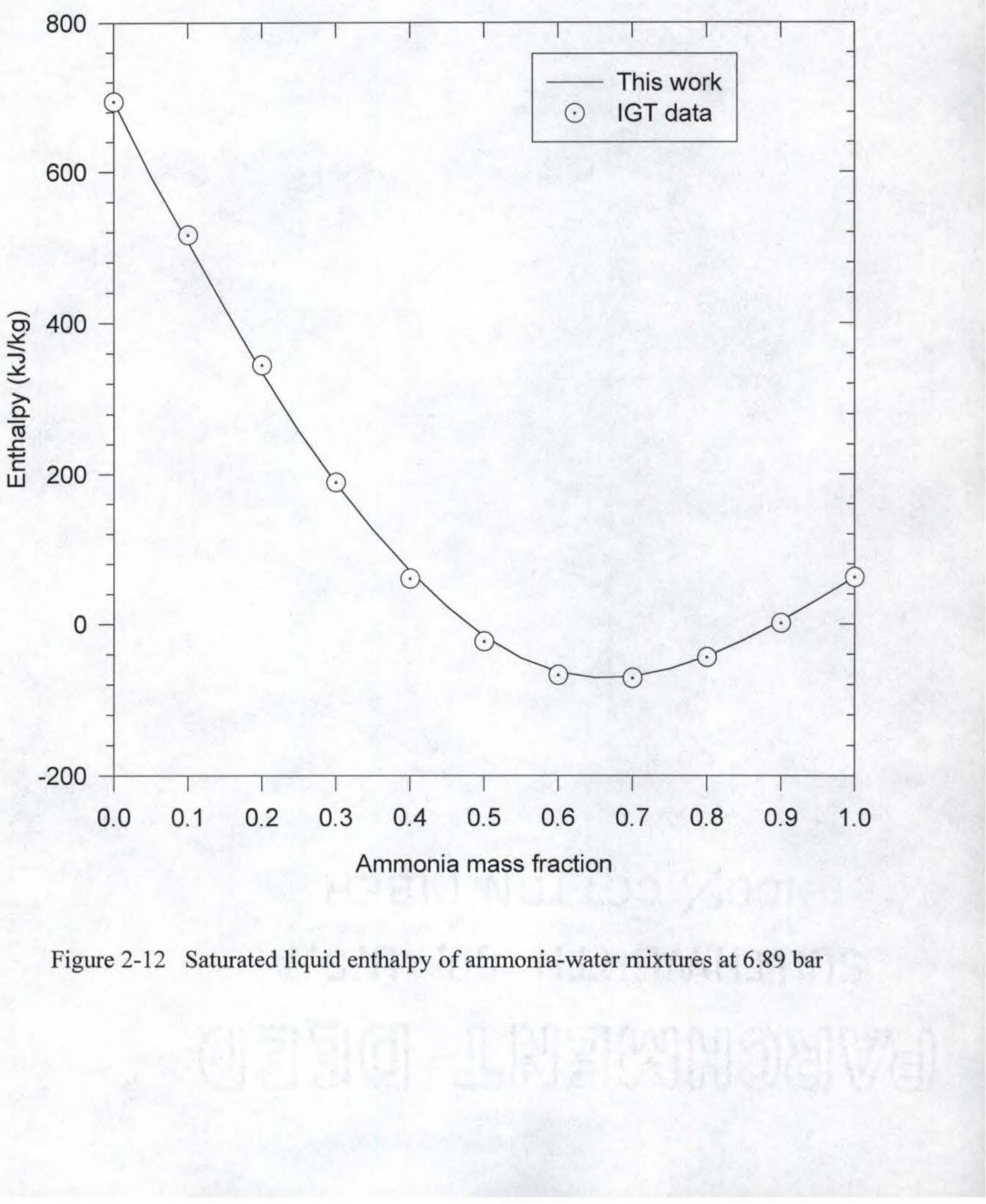

Figure 2-12 Saturated liquid enthalpy of ammonia-water mixtures at 6.89 bar

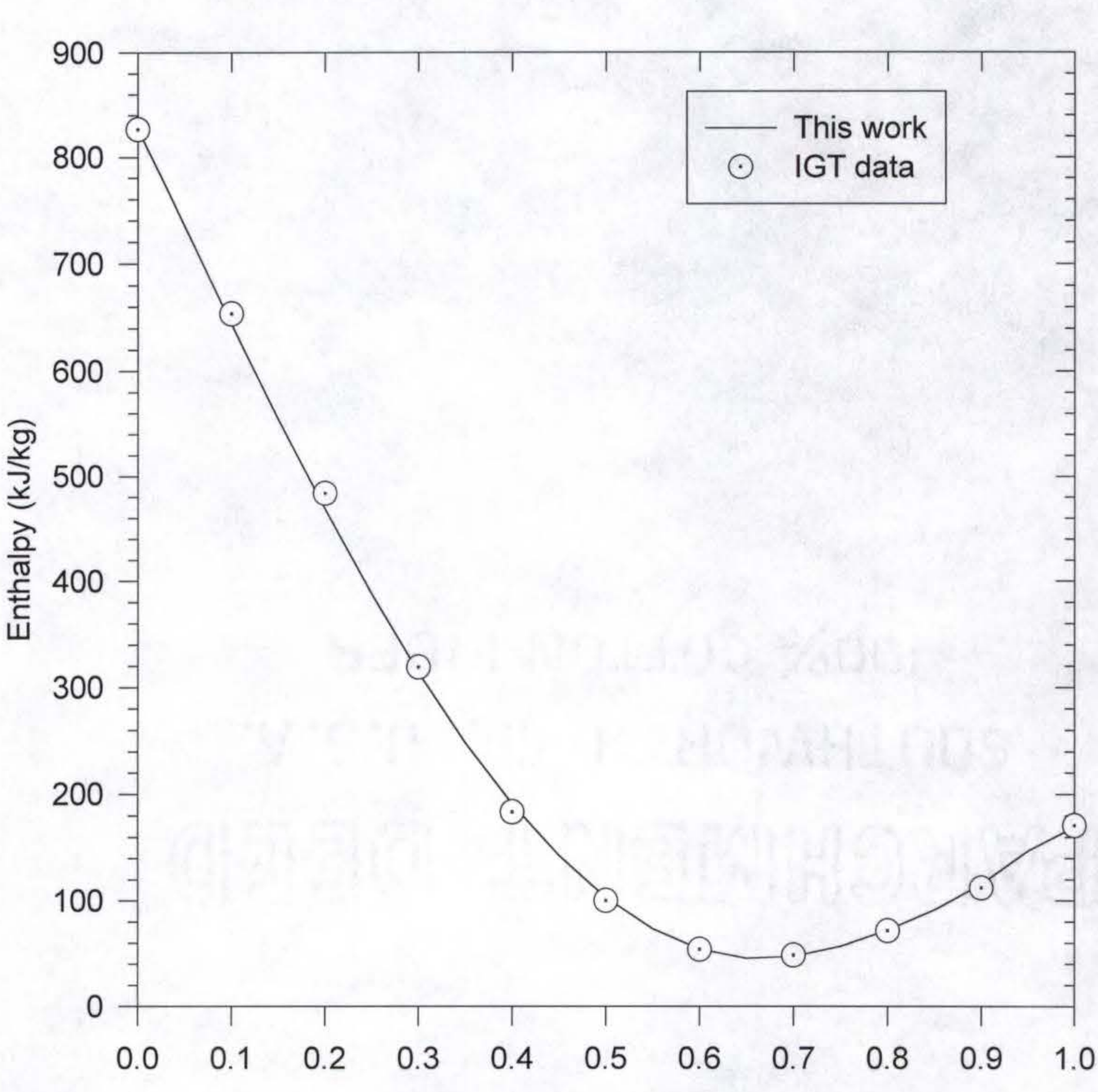

Figure 2-13 Saturated liquid enthalpy of ammonia-water mixtures at 13.79 bar

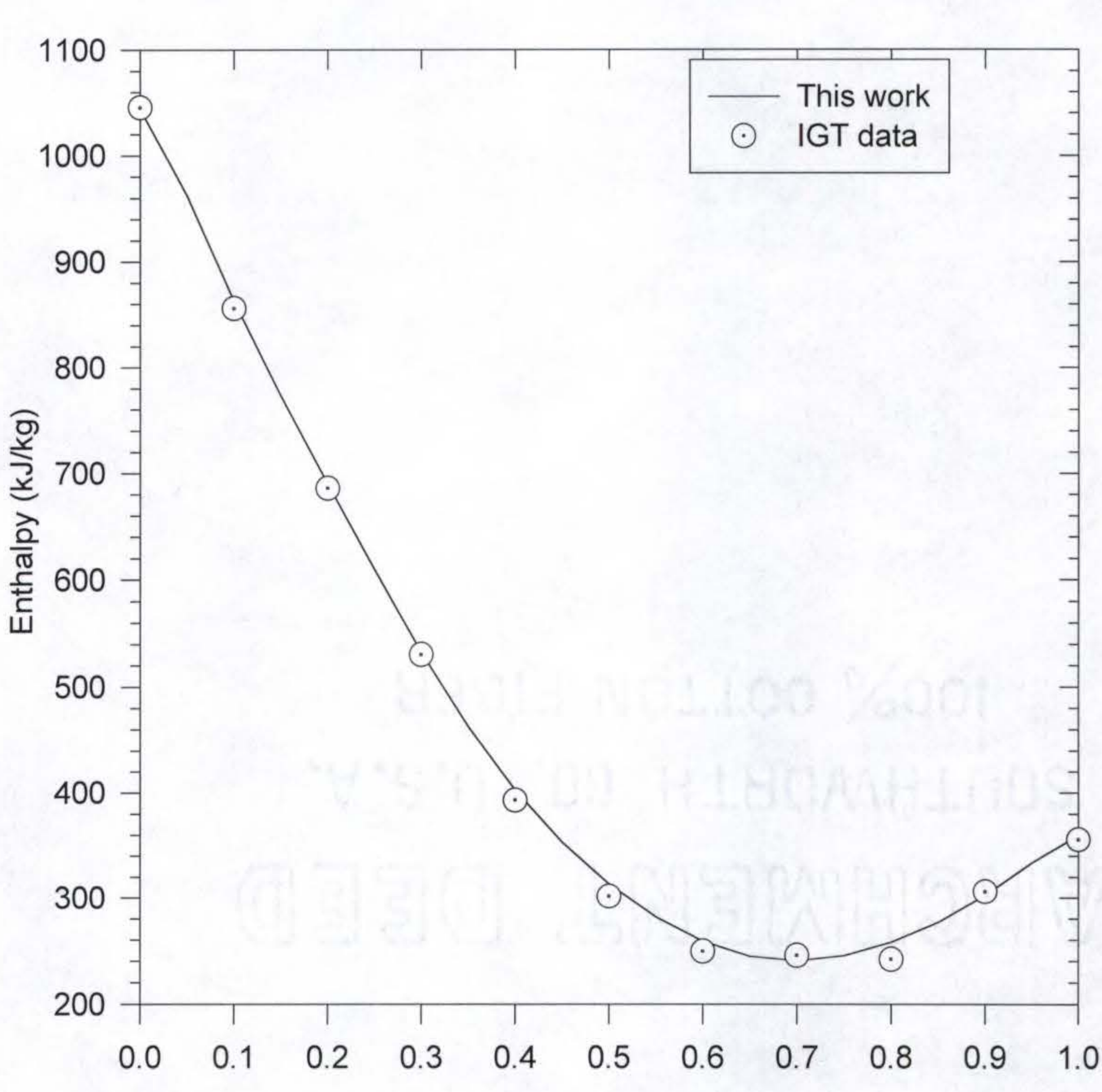

Figure 2-14 Saturated liquid enthalpy of ammonia-water mixtures at 34.47 bar

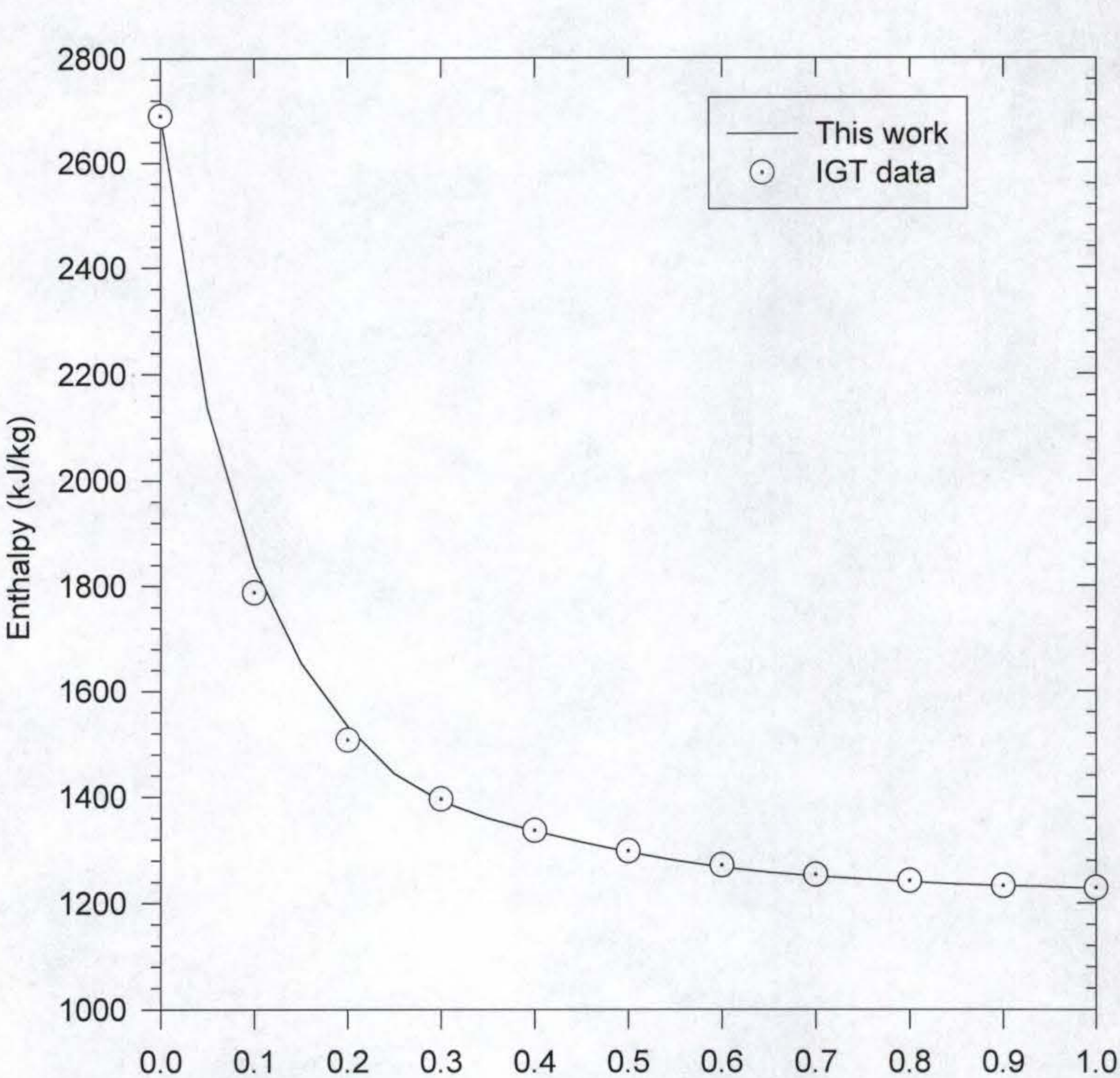

Figure 2-15 Saturated vapor enthalpy of ammonia-water mixtures at 1.38 bar

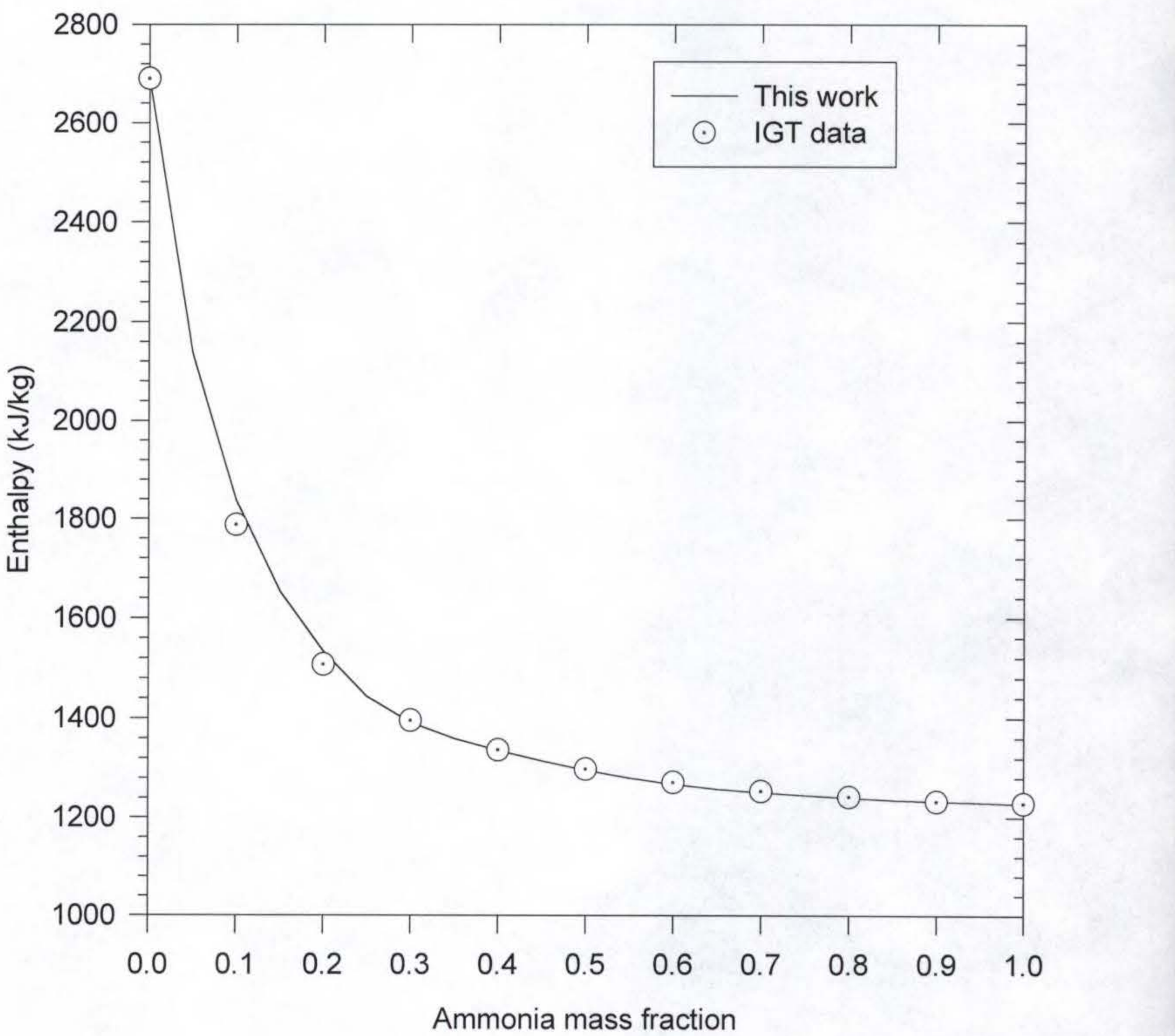

Figure 2-16 Saturated vapor enthalpy of ammonia-water mixtures at 6.89 bar

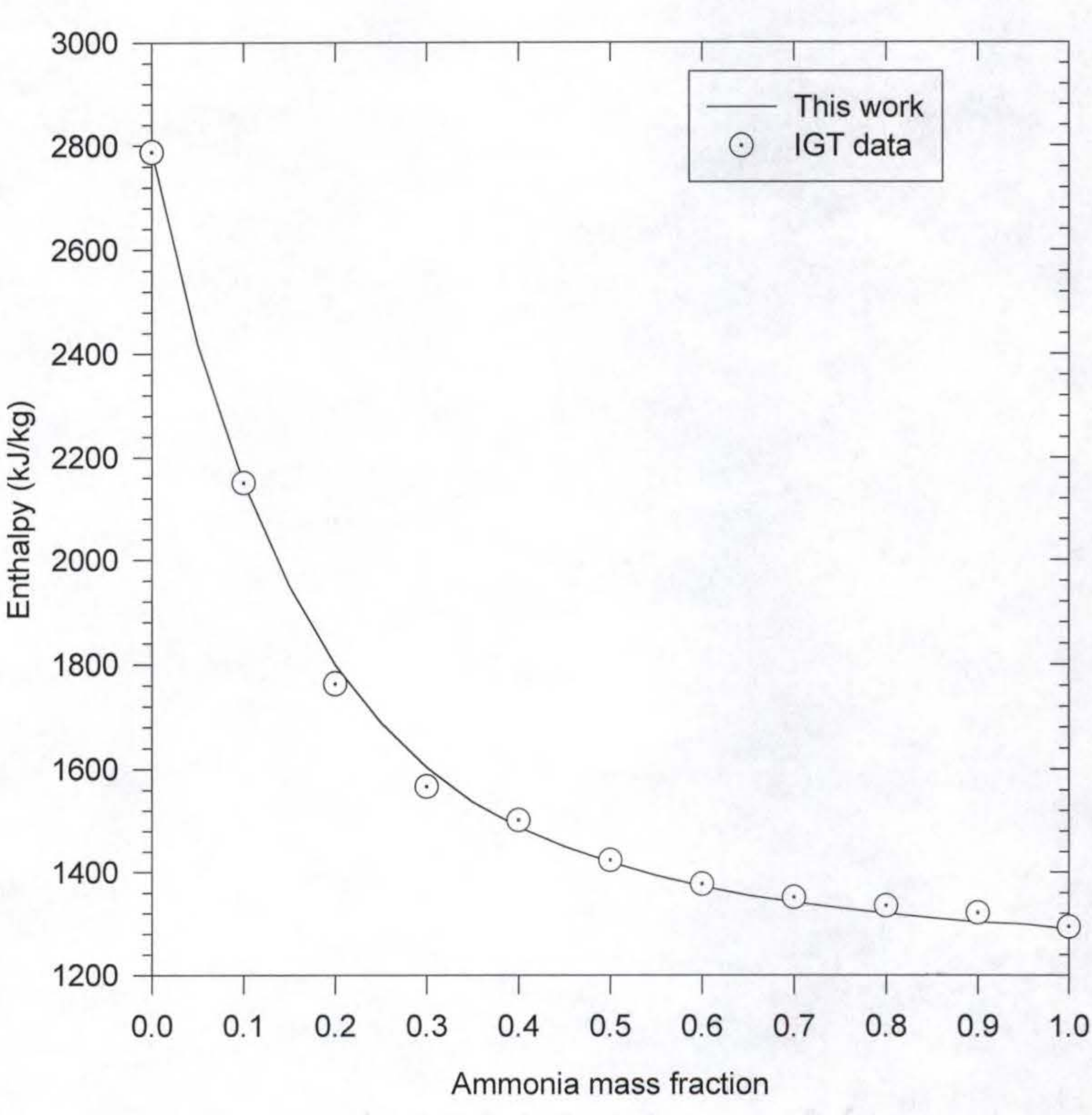

Figure 2-17 Saturated vapor enthalpy of ammonia-water mixture at 13.79 bar

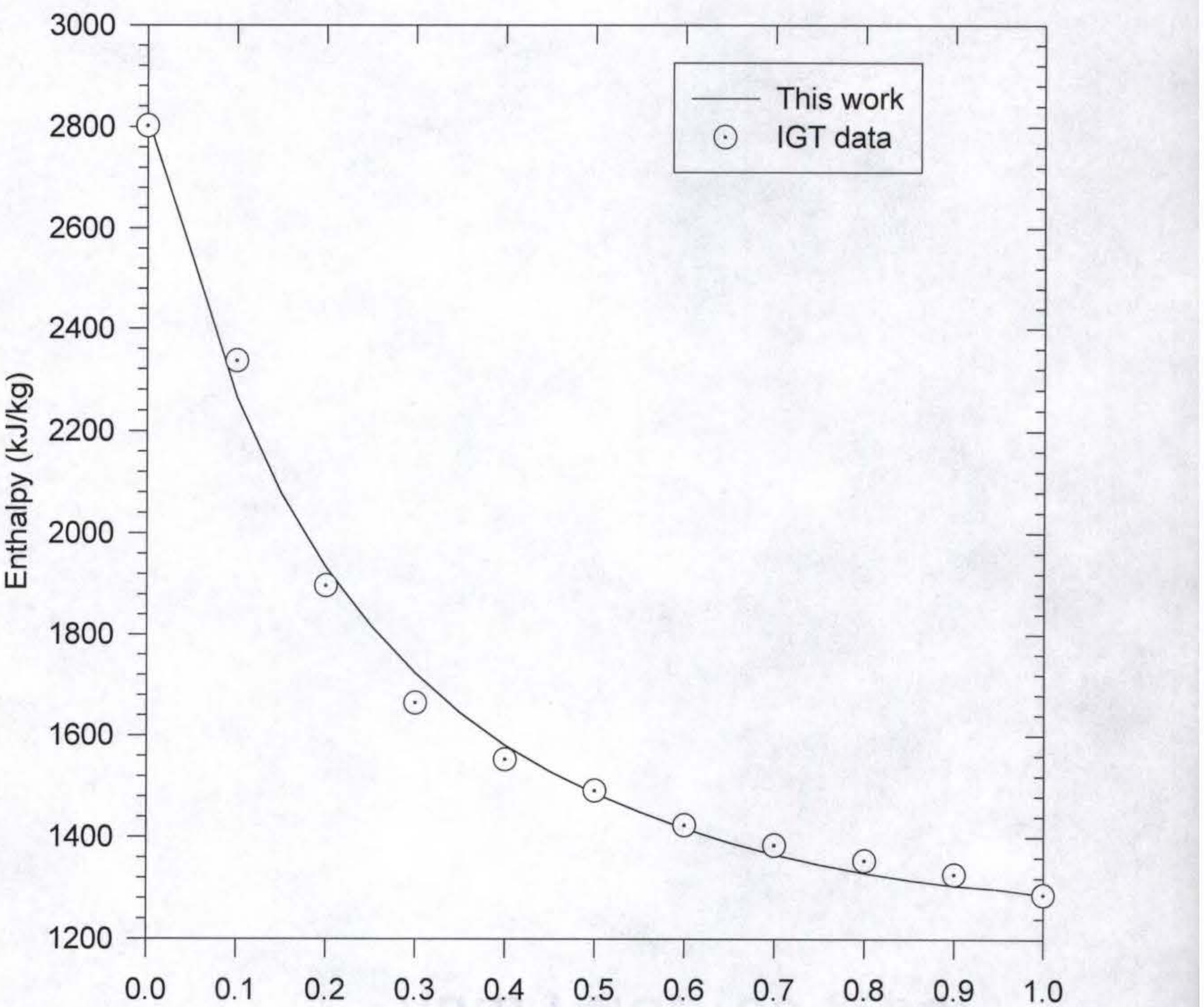

Figure 2-18 Saturated vapor enthalpy of ammonia-water mixtures at 34.47 bar

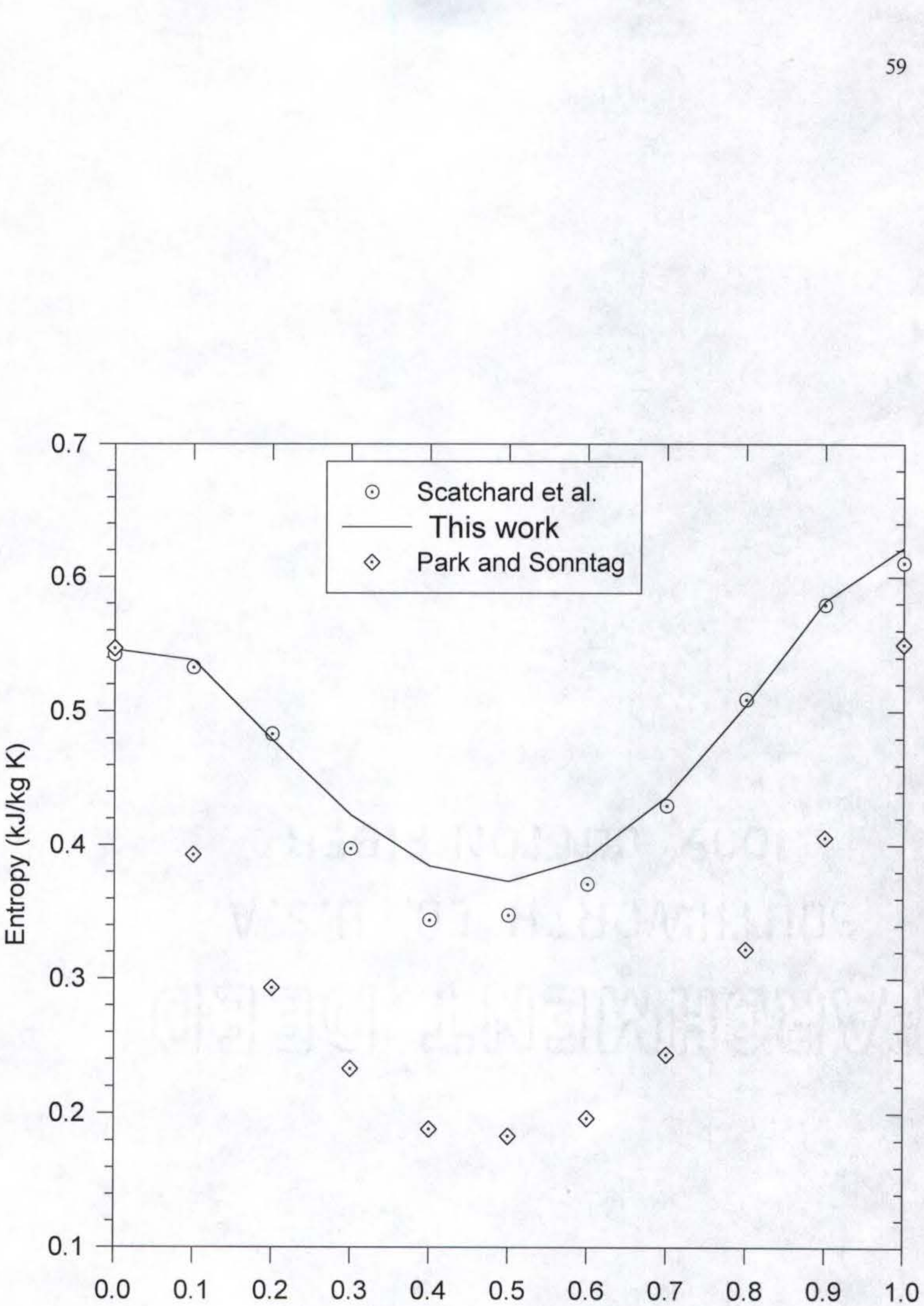

Figure 2-19 Entropy of Saturated liquid at 310.9 K

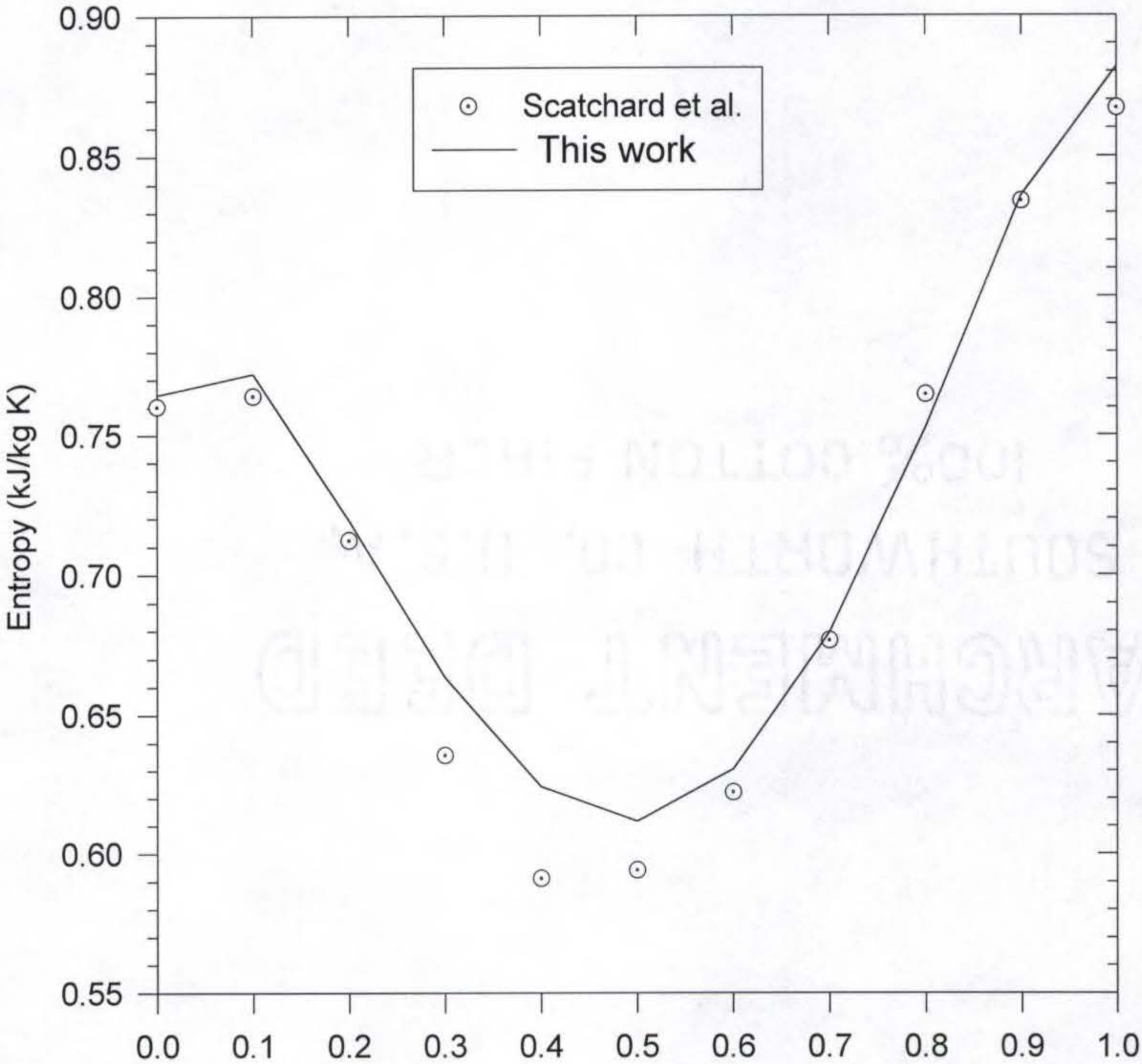

Figure 2-20 Entropy of Saturated liquid at 327.6 K

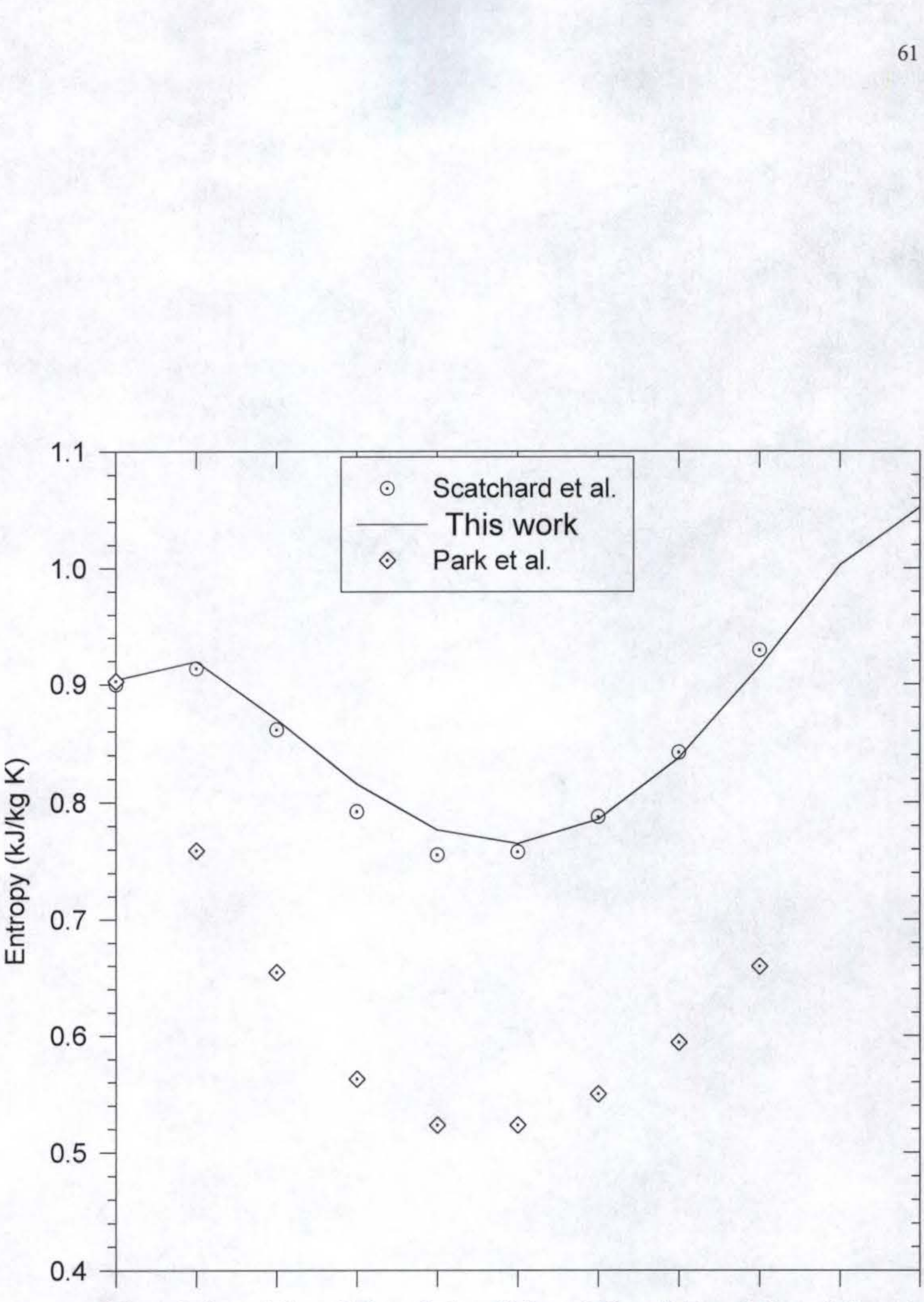

Figure 2-21 Entropy of Saturated liquid at 338.7 K

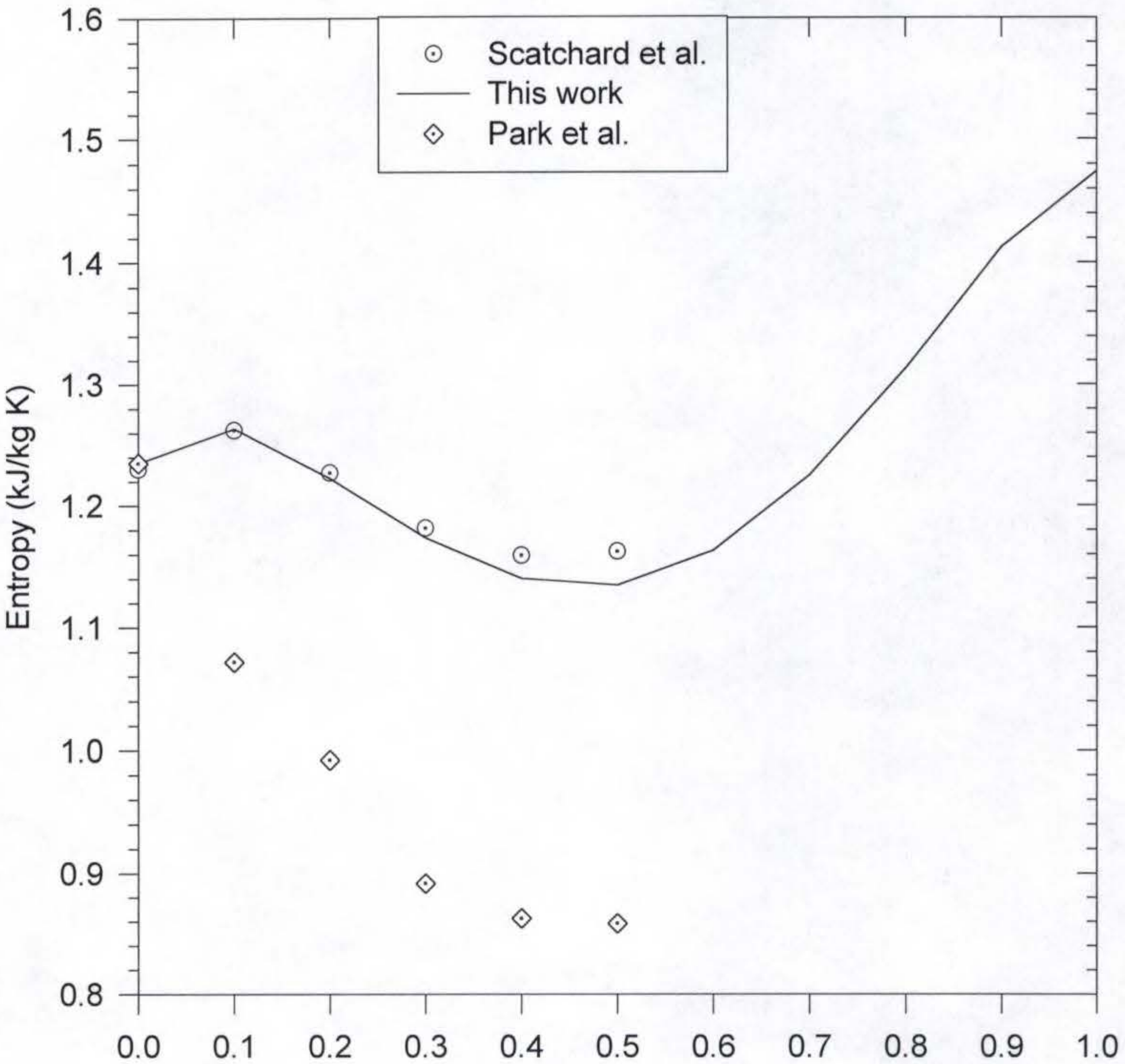

Figure 2-22 Entropy of Saturated liquid at 366.5 K

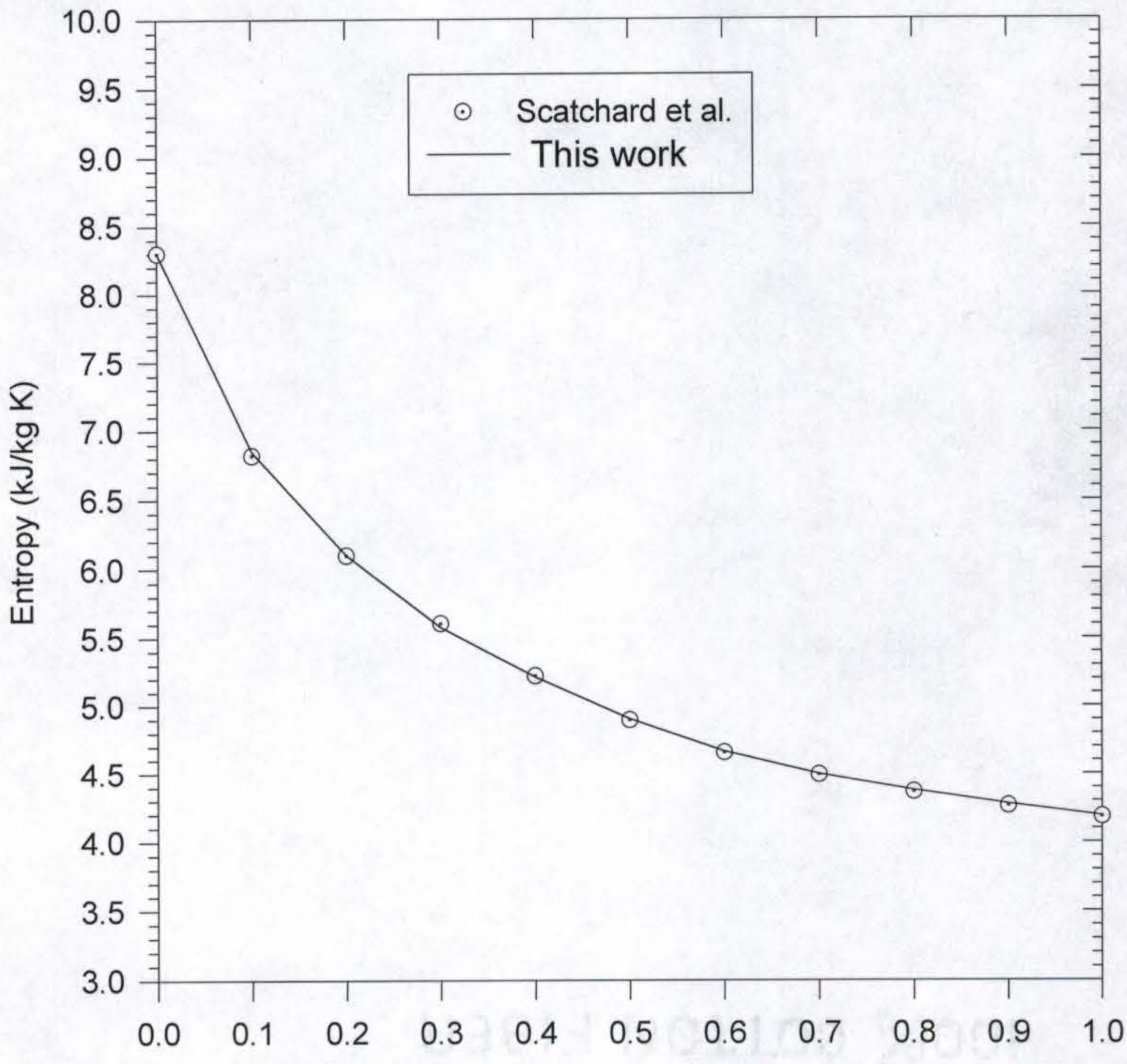

Figure 2-23 Entropy of Saturated vapor at 310.9 K

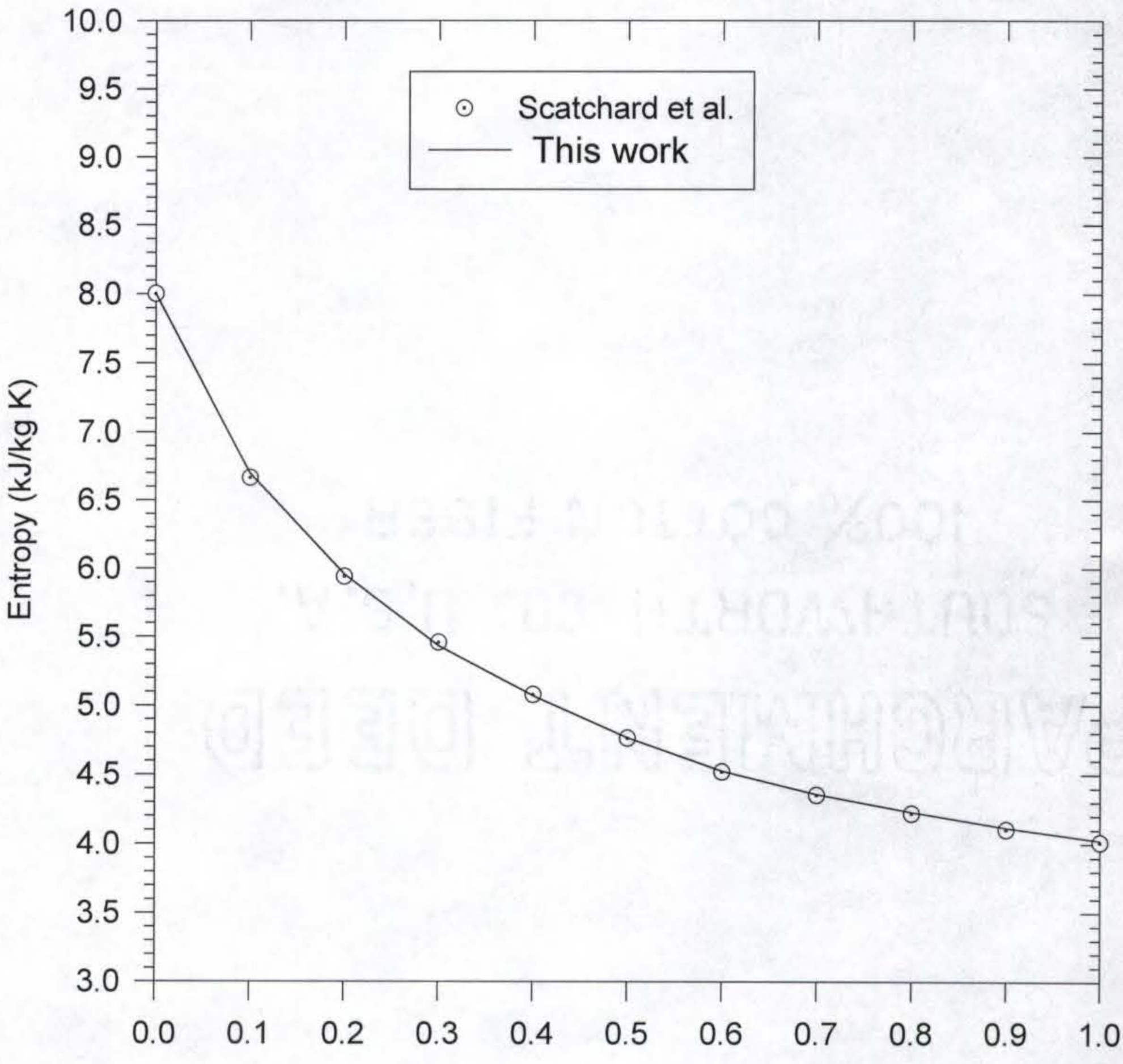

Figure 2-24 Entropy of Saturated vapor at 327.6 K

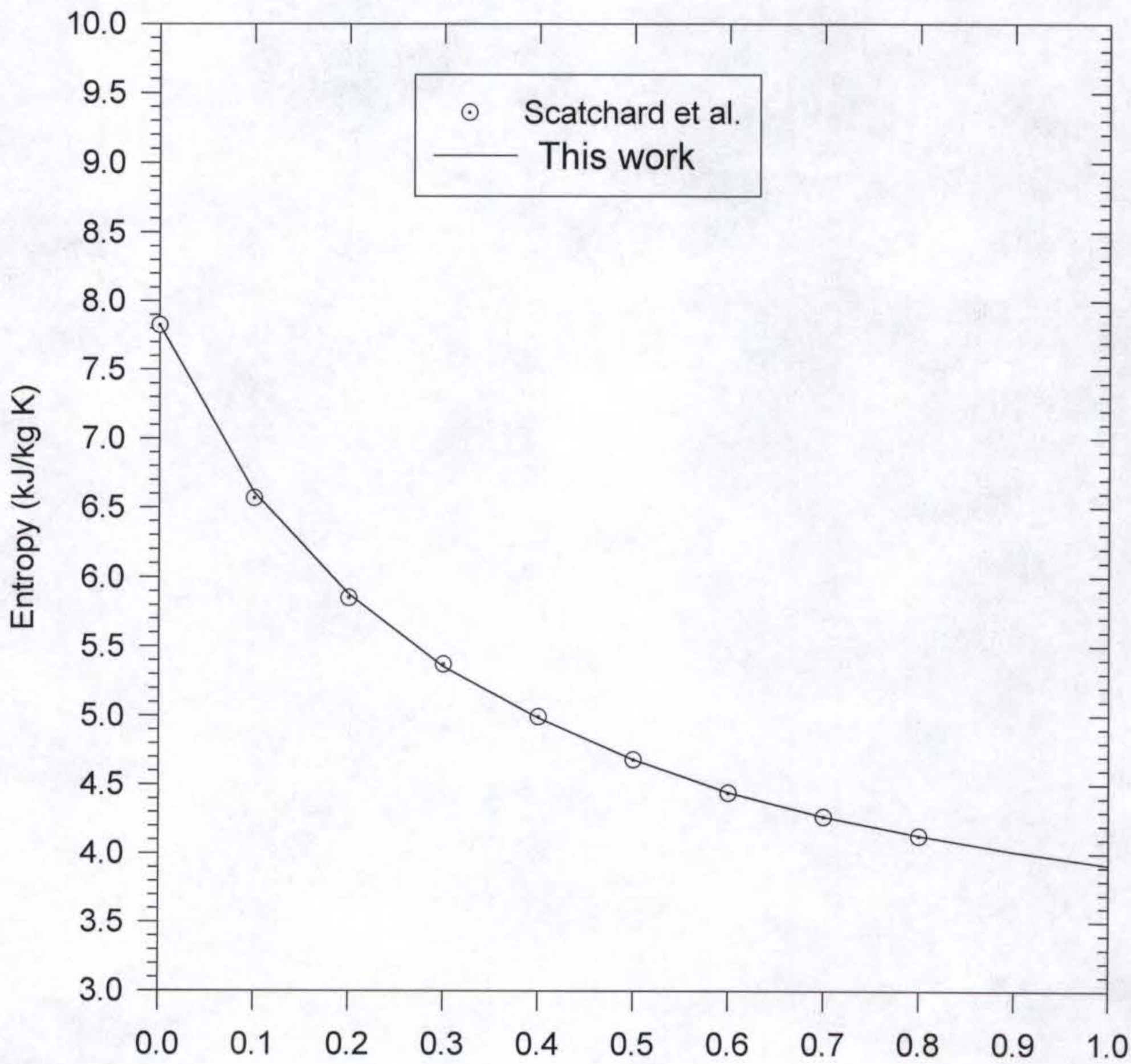

Figure 2-25 Entropy of Saturated vapor at 338.7 K

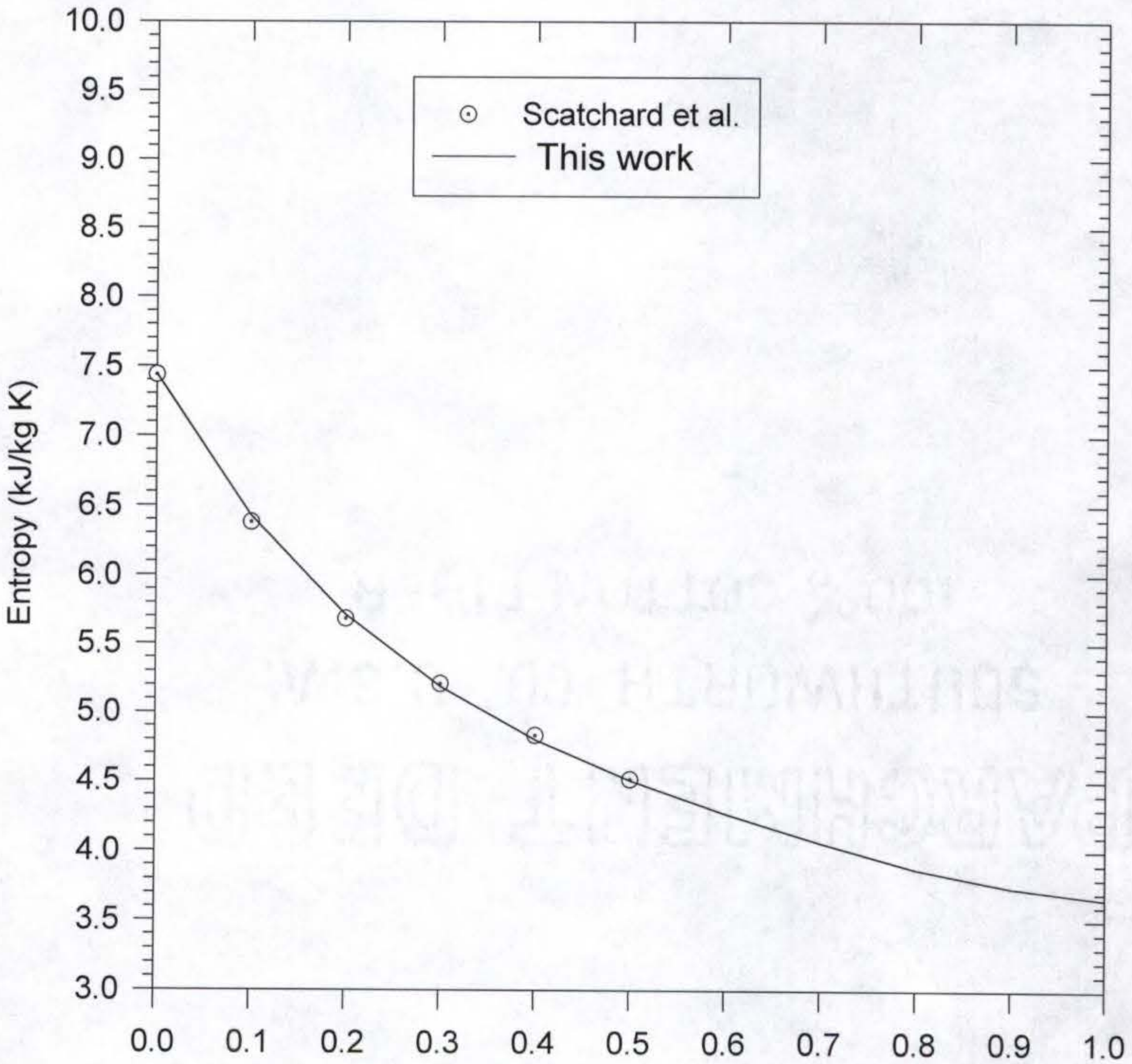

Figure 2-26 Entropy of Saturated vapor at 366.5 K

CHAPTER 3
AMMONIA-BASED COMBINED POWER/COOLING CYCLE

3.1 Introduction

Combined cycle systems have been recognized as efficient power systems. A typical combined cycle system consists of the gas turbine cycle(the Brayton cycle), which produces the base load, and the Rankine cycle, which uses the exhaust gas from the gas turbine as the high temperature source. The exhaust gas provides the available energy to the bottoming cycle (the Rankine cycle) to improve the efficiency of the combined cycle system over the gas turbine cycle alone.

The efficiency of the overall system is a function of the temperature and pressure of the exhaust gas, the sink temperature of the bottoming cycle, and the type of the bottoming cycle itself.

Most heat sources available to the bottoming cycles, such as hot exhaust gases, are sensible-heat sources because the temperature of the source is varying during the heat transfer process. The amount of the cooling medium at the sink temperature in reality is also limited so that the heat sink is sensible as well. This sensible heat does not satisfy

the isothermal process of the ideal cycle (the Carnot cycle). The ideal cycle to convert sensible heat to mechanical or electrical energy is therefore not the Carnot cycle.

The ideal cycle to convert sensible heat to mechanical or electrical energy is the Lorenz cycle (Lorenz 1894). This cycle has a triangular shape on a temperature and entropy diagram, generating the least entropy during the heat transfer process (Kalina 1984). The least production of entropy yields the highest thermodynamic efficiency. It is interesting to note that with respect to the combined cycle efficiency, the Carnot cycle is still the ideal cycle to produce overall maximum work at a given source temperature since the bottoming cycle of a triangular shape leads the overall combined cycle to the Carnot cycle, as seen in figure 3-1.

To increase the efficiency of the Rankine cycle working with sensible heat, two conventional ways have been proposed:

(1) Incorporation of a multi-pressure boiler

(2) Implementation of the supercritical cycle

The multi-pressure boiler is widely used in industry, but results in only moderate improvement in efficiency unless the number of boiler steps is very large. For the exhaust gas temperature range from 900-1000 ^{o}F(755 - 811 K), the cycle efficiency is 20-22% with a single pressure boiler and 23-25% with tri-pressure boiler (Foster-Pegg 1978). Since a significant increase in the number of boiler steps is technically and economically not feasible, the number of such steps does not usually exceed three (Kalina 1984). The implementation of a supercritical cycle can theoretically achieve a triangular shape cycle and thus high efficiency, but requires extremely high pressure in the boiler,

which in turn adversely affects the turbine performance (Kalina 1984). Milora and Tester (1976) have given a detailed discussion of the supercritical cycle.

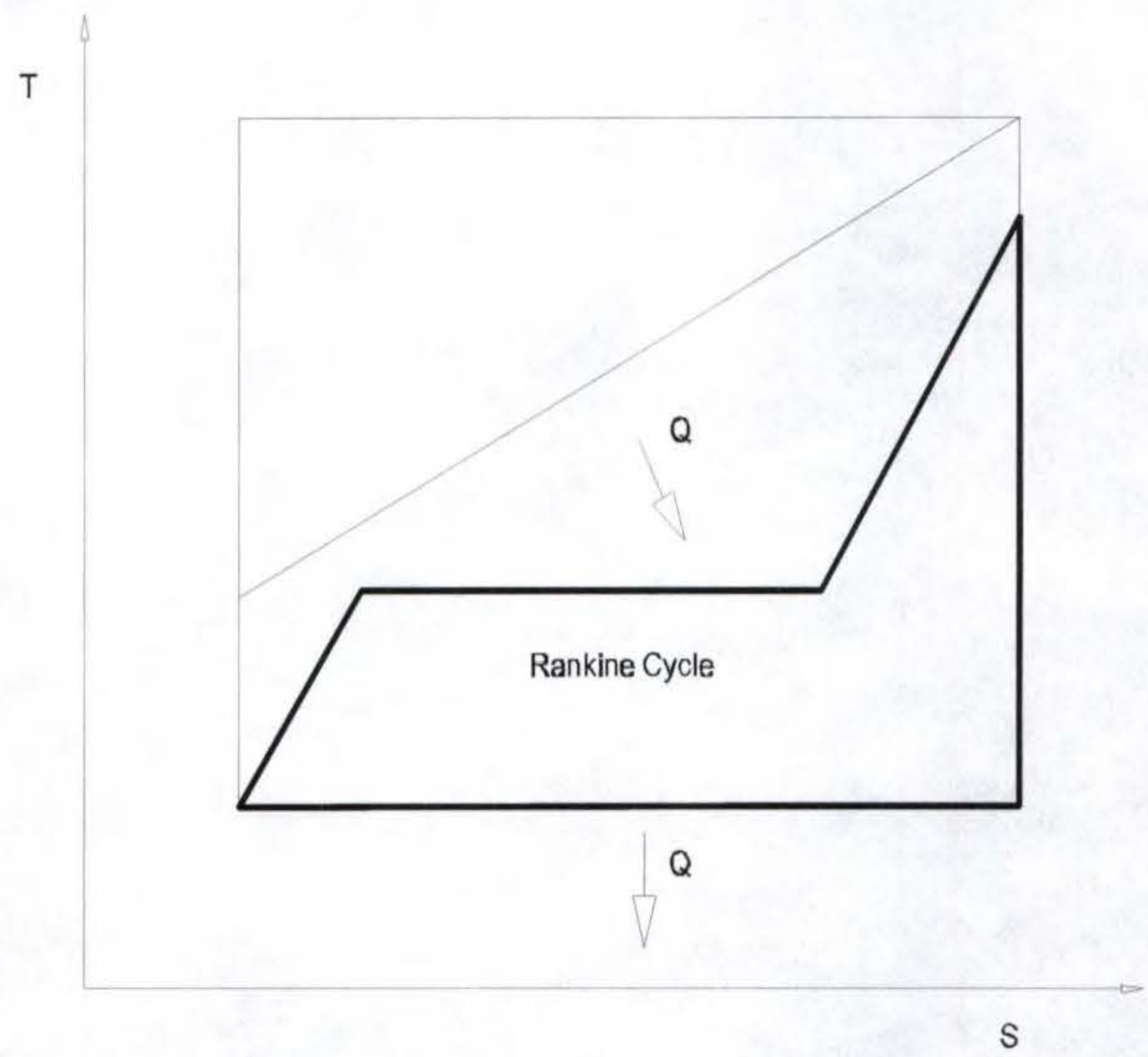

Figure 3-1 Schematic diagram of the Rankine cycle in connection with a combined cycle

An alternative way to increase the efficiency of the Rankine cycle working with a sensible heat source is to use a multi-component working fluid. A multi-component working fluid boils at a variable temperature with a change in the liquid composition of the components. This variable temperature boiling process yields a better thermal match with the sensible heat source than the constant temperature boiling process, and is close to a triangular shape. The better thermal match contributes to the improvement of thermodynamic efficiency in the boiler. Since the multi-component working fluid condenses at a variable temperature as well, a part of the gain of the variable temperature boiling is lost in the condenser. To reduce this loss, the simple condensation process is complemented by an absorption distillation process (Babcock and Wilcox, 1978).

Our novel power cycle is proposed by Goswami(1995, 1996). The cycle uses a multi-component working fluid and the condensing process of the Rankine cycle is replaced by the absorption process. This cycle meets both conditions for higher thermodynamic efficiency--a better thermal match in the boiler and a heat rejection system complemented by the absorption system.

The purpose of this work is to conduct a study of the novel power cycle system in connection with a combined cycle system as in Figure 3-2, comparing the novel cycle and the Rankine cycle at the same thermal boundary conditions with different internal conditions for the best performance of each cycle. This study is performed using the thermodynamic properties of ammonia-water mixtures developed in Chapter 2 in this study.

3.2 Characteristics of the Novel Cycle as a Bottoming Cycle

A bottoming cycle is a cycle which operates between the high temperature heat rejected by a topping cycle and the ambient. The cycle utilizes the available heat of the exhaust gas from the topping cycle. Most heat available to the bottoming cycle is sensible; the temperature varies during the heat transfer process. This sensible heat can not realize the isothermal heat supply process of the ideal cycle, the Carnot cycle. Therefore, the Carnot cycle is not the ideal bottoming cycle to convert sensible heat to mechanical energy or electrical energy. Rather, the ideal cycle working with sensible heat is the Lorenz cycle(Lorenz, 1894), which has a triangular shape in the temperature and entropy coordinates.

The Lorenz cycle is composed of four processes, as shown in Figure 3-2

(1) Heat supply at a variable temperature(1-2)

(2) Isentropic expansion(2-3)

(3) Isothermal heat rejection(3-4)

(4) Isentropic compression(4-1)

The Lorenz cycle is exactly the same as the Carnot cycle except for the process(1-2).

Possible ways to realize the Lorenz cycle are:

(1) Multi-pressure boiler

(2) Supercritical cycle

(3) The Kalina cycle

(4) The novel ammonia-based combined power/cooling cycle

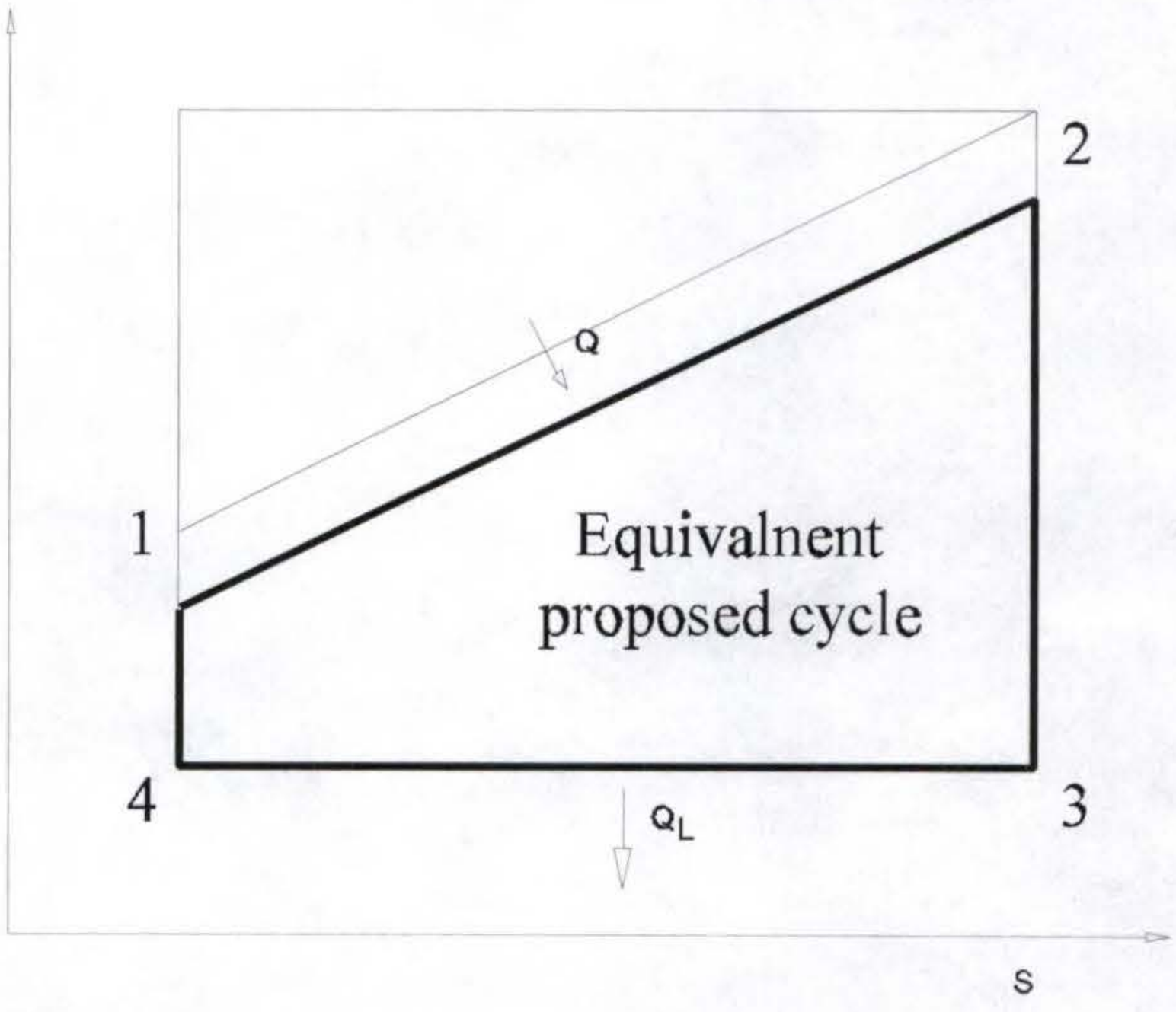

Figure 3-2 Schematic diagram of the novel cycle in connection with a combined cycle

The novel cycle combines two thermodynamic cycles, the Rankine cycle and the ammonia-absorption refrigeration cycle, as seen in figure 1-4. In Rankine cycle, ammonia-water mixture is pumped to a high pressure. The mixture is heated to boil off ammonia, and ammonia is separated from water. After expanding through a turbine to generate power, ammonia is brought to absorption refrigeration cycle. Low temperature ammonia provides cooling in the evaporator and then it is absorbed by water in an

absorber and becomes ammonia-water mixture liquid. As seen in figure 3-3, the novel cycle provides extra work (shade area) over Rankine cycle.

The novel cycle as a bottoming cycle is a creative way to realize the triangular shape of the T-S diagram. The concept of this cycle is based on the varying temperature boiling of a multi-component working fluid. The boiling temperature of the multi-component working fluid increases as the boiling process proceeds until all liquid is vaporized, so that a better thermal match is obtained in the boiler. This better thermal match yields a

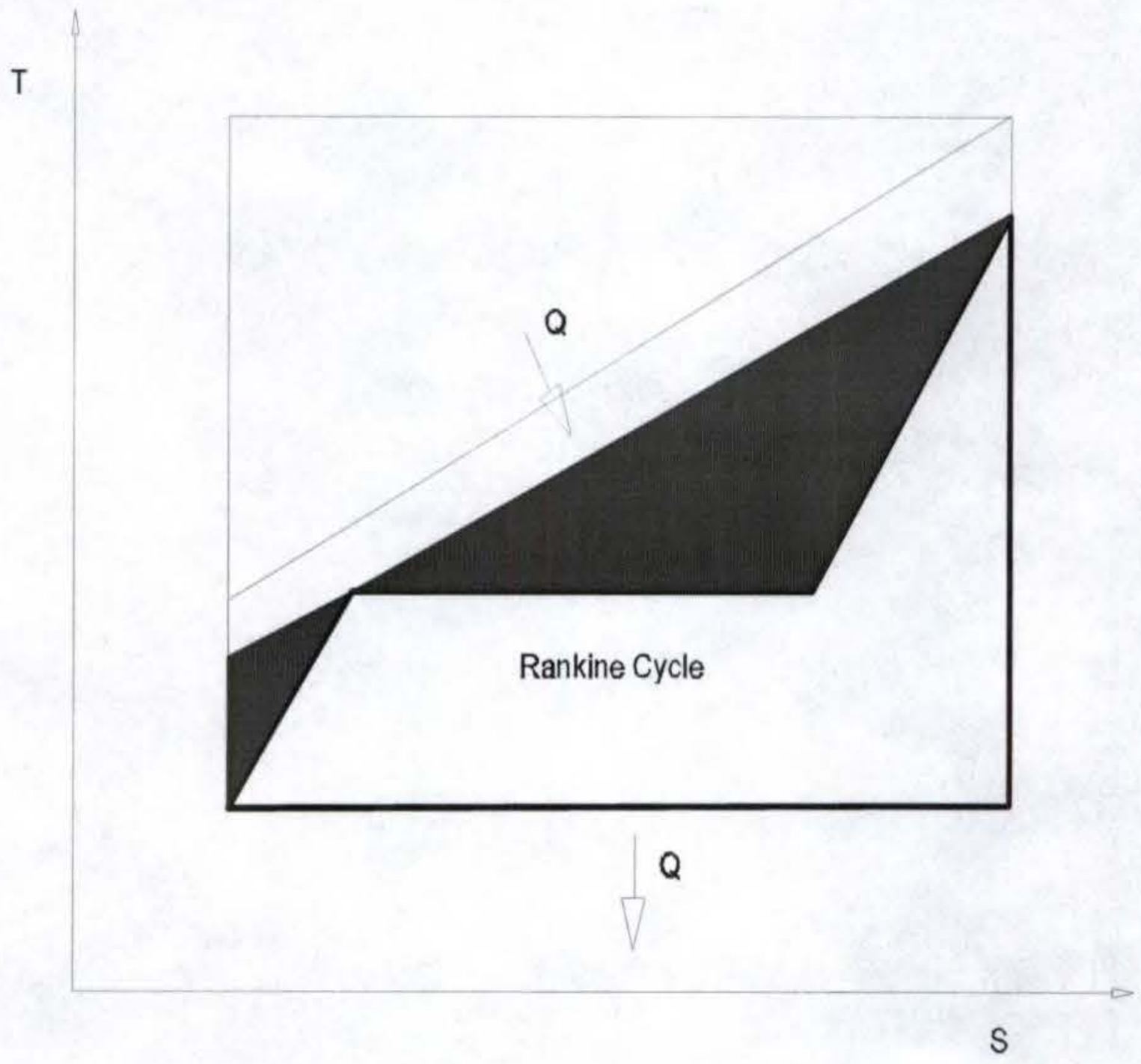

Figure 3-3 T-S diagram showing advantage of the novel cycle over a conventional Rankine cycle

better thermodynamic efficiency. The higher thermodynamic efficiency of the novel cycle as the bottoming cycle results from

(1) The multi-component working fluid, having a variable boiling temperature, provides significantly less available energy loss in the boiler, as the heat source has a variable temperature in the boiler as well.

(2) The working fluid starts boiling almost immediately after entering the evaporator, which increases the efficiency of the heat exchanger(boiler).

(3) The amount of heat rejected in the condenser is significantly smaller than that in the in the Rankine cycle arrangement.

3.3 Thermodynamic Analysis of the Proposed Cycle

As seen in Figure 3-3 , the proposed ammonia-based cycle is a combination of the Rankine and the ammonia-absorption refrigeration cycles. Within this one cycle, the Rankine cycle process of expanding a superheated vapor to produce work is present, as is part of the ammonia-absorption refrigeration cycle. A difference between this cycle and the ammonia-absorption refrigeration cycle is that ammonia vapor is not condensed and then expanded to provide refrigeration, but the ammonia vapor is used as the working fluid in a turbine.

This section gives a thermodynamic analysis of this novel cycle with assumed thermal boundary conditions as

1. Power output: 2.5 kW
2. Turbine inlet temperature: 400 K - 500 K
3. Turbine inlet pressure: 18 bar - 32 bar

At this stage, the thermodynamic state conditions of the proposed combined cycle are evaluated assuming a idealized cycle (that is , irreversibilities associated with real apparatus were neglected.) The idealized cycle does provide the analytical maximum limits for real processes and is necessary in determining the efficiency limits of a real system. The following list of assumptions was used in the initial analysis of the proposed cycle.

3.4 Thermodynamic Property Calculation

The thermodynamic properties of the working fluids were evaluated using the methods developed in Chapter 2. The following paragraphs explain the techniques used to determine the thermodynamic properties at each state in the cycle.

Three working fluids were considered, ammonia vapor, strong ammonia/water solution, and a weak ammonia water solution. Strong ammonia/water solution refers to the condition where ammonia vapor and the weak ammonia/water solution have been combined. Likewise, when the ammonia vapor is boiled off from the strong ammonia/water solution, the remaining solution is considered the weak ammonia/water

Table 3-1 Assumptions and parameters of the proposed cycle

	Assumptions	State characteristics
a	Strong ammonia/water mixture is pumped to 27.6 bar and heated to 466 K	$P_2 = 27.6$, $T_4 = T_7 = 466$ K
b	Superheated ammonia vapor is expanded through a turbine to 2.1 bar	$P_5 = 2.1$ bar
c	ammonia vapor exiting the turbine is used in a refrigeration application which brings its temperature to 277 K	$T_6 = 277$ K
d	Neglect pressure drops in components and pipelines.	$P_2 = P_3 = P_4 = P_7 = P_8 = 27.6$ bar $P_5 = P_6 = P_9 = P_1 = 2.1$ bar
e	Liquid solutions at states 1, 3, and 7 are saturated liquids	
f	Pump process is assumed to be reversible and adiabatic	$h_2 - h_1 = (P_2 - P_1)v_1$
g	Steady state, steady flow.	
h	Pure ammonia vapor leaves boiler.	$x_a = 1.0$
i	Turbine expansion is isentrophic (reversible, adiabatic)	$s_4 = s_5$
j	The pressure reducing valve is an adiabatic process	$h_8 = h_9$
k	Mass flow of weak aqua-ammonia solution is assumed	
l	Temperature of strong aqua-ammonia solution is 373 K after leaving the heat exchanger.	$T_3 = 373$ K

solution. Subscripts a, s, and w for the thermodynamic properties refer to the ammonia vapor, strong ammonia/water solution, and weak ammonia/water solution, respectively.

Since pressure drops in the components and pipelines are neglected, all pressures are established from the given assumptions; States between the pump and the turbine, or the pump and pressure relief valve are at 27.6 bar and the states between the turbine or pressure relief valve and the pump are at 2.1 bar.

The concentrations of ammonia in the aqua-ammonia mixtures are determined using the assumptions that the strong and weak liquids would be saturated at states 3 and 7, respectively. The concentrations are assumed as $x_s = 0.54$, $x_w = 0.125$ and $x_a = 1.0$.

Mass balance equations were used to determine the mass flow rates through the cycle. With the following two equations:

$$m_s = m_w + m_a,$$

$$m_s x_s = m_w x_w + m_a x_a$$

and assuming a value for one of the mass flow rates, the values of the other two flow rates can be determined.

Table 3-2 shows the thermodynamic state including enthalpy at each point.

Table 3-3 shows the energy balance of each component.

Table 3-2 Example of operating conditions for the proposed cycle

State	Description	Fluid	Phase	Temp K	Pressure bar	Enthalpy kJ/kg	Concentration kg NH_3/kg mix	Flowrate kg/s
1	Absorber Exit / Pump Inlet	strong aqua-ammonia solution	saturated liquid	280	2.1	-209.16	0.540	0.01141
2	Pump Exit / HEX Inlet	strong aqua-ammonia solution	liquid	280	27.6	-206.59	0.540	0.01141
3	HEX Exit / Boiler Inlet	strong aqua-ammonia solution	saturated liquid	373	27.6	223.22	.540	0.01141
4	Boiler Exit / Turbine Inlet	ammonia	superheated vapor	466	27.6	1682.37	1.000	0.00541
5	Turbine Exit / Cooler Inlet	ammonia	superheated vapor	262	2.1	1256.28	1.000	0.00541
6	Cooler Exit / Absorber Inlet	ammonia	superheated vapor	277	2.1	1290.98	1.000	0.00541
7	Boiler Exit / HEX inlet	weak aqua-ammonia solution	saturated liquid	466	27.6	760.95	0.125	0.006
8	HEX Exit / PRV Inlet	weak aqua-ammonia solution	subcooled liquid	288	27.6	-15.5	0.125	0.006
9	PRV Exit / Absorber Inlet	weak aqua-ammonia solution	subcooled liquid	288	2.1	-15.5	0.125	0.006

Table 3-3 Energy balance of each component

Component	Energy equations	Energy (kW)
Pump	$W_p = m_s(h_2 - h_1)$	0.030
Boiler	$Q_b = m_a h_4 + m_w h_7 - m_s h_3$	11.120
Turbine	$W_t = m_a(h_5 - h_4)$	-2.305
Cooler	$Q_c = m_a(h_6 - h_5)$	0.188
Absorber	$Q_a = m_a h_6 + m_w h_9 - m_s h_1$	-9.278

Turbine power output: $W_t = m_a(h_4 - h_5) = 2.305$ kW

Refrigeration: $Q_c = m_a(h_e - h_5) = 0.188$ kW

First law efficiency: $$\eta = \frac{W_t + Q_c}{Q_b} = \frac{2.305 + 0.188}{11.12} \text{x} 100\% = 22.42\%$$

3.5 A New Improved Design Cycle

The previous section has described the advantage of the conceptual proposed cycle as shown in figure 1-4. In that section it was assumed that the boiler produced pure ammonia vapor, however, the figure does not show how to generate highly concentrated ammonia vapor. Usually, the boiler generates vapor with about 90% ammonia mass fraction. At this ammonia mass fraction, vapor can not be expanded in a turbine to a very low temperature because a certain amount of condensation will be generated in the turbine. For an absorption refrigeration cycle, a condenser or rectifier is used to condense

part of the water vapor from the boiler. After the condenser, a highly concentrated ammonia vapor is generated. The ammonia composition after the condenser can be over 99%.

Since water vapor is condensed in the condenser/rectifier, heat of condensation is released. But this heat is not wasted, instead it is used to preheat the basic solution from the absorber.

Figure 3-4 shows a more detailed design of the proposed cycle. In this system, the boiler generates ammonia rich vapor (state 5). Before the vapor is superheated in a superheater (state 7), it passes through a condenser or rectifier (state 6) to get a higher concentration ammonia vapor. After expansion in the turbine, the ammonia vapor drops to a very low temperature. The cold ammonia vapor provides cooling by passing through the cooler (state 9). The ammonia vapor is then reunited with the weak solution from the boiler in the absorber to regenerate the basic solution (state 1). The basic solution is then pumped to a high pressure (state 2) to complete the loop. The basic solution coming out of the absorber is used as the cooling fluid for the condenser. At state 2, part of the solution goes through a solution heat exchanger, and another part goes to the condenser. These two streams mix before the boiler. So no heat is wasted while a highly concentrated ammonia vapor is obtained as a working fluid.

Table 3-4 shows typical operating conditions of the proposed cycle. Table 3-5 shows the performance of each component based on a unit mass of the basic solution at the conditions of table 3-4.

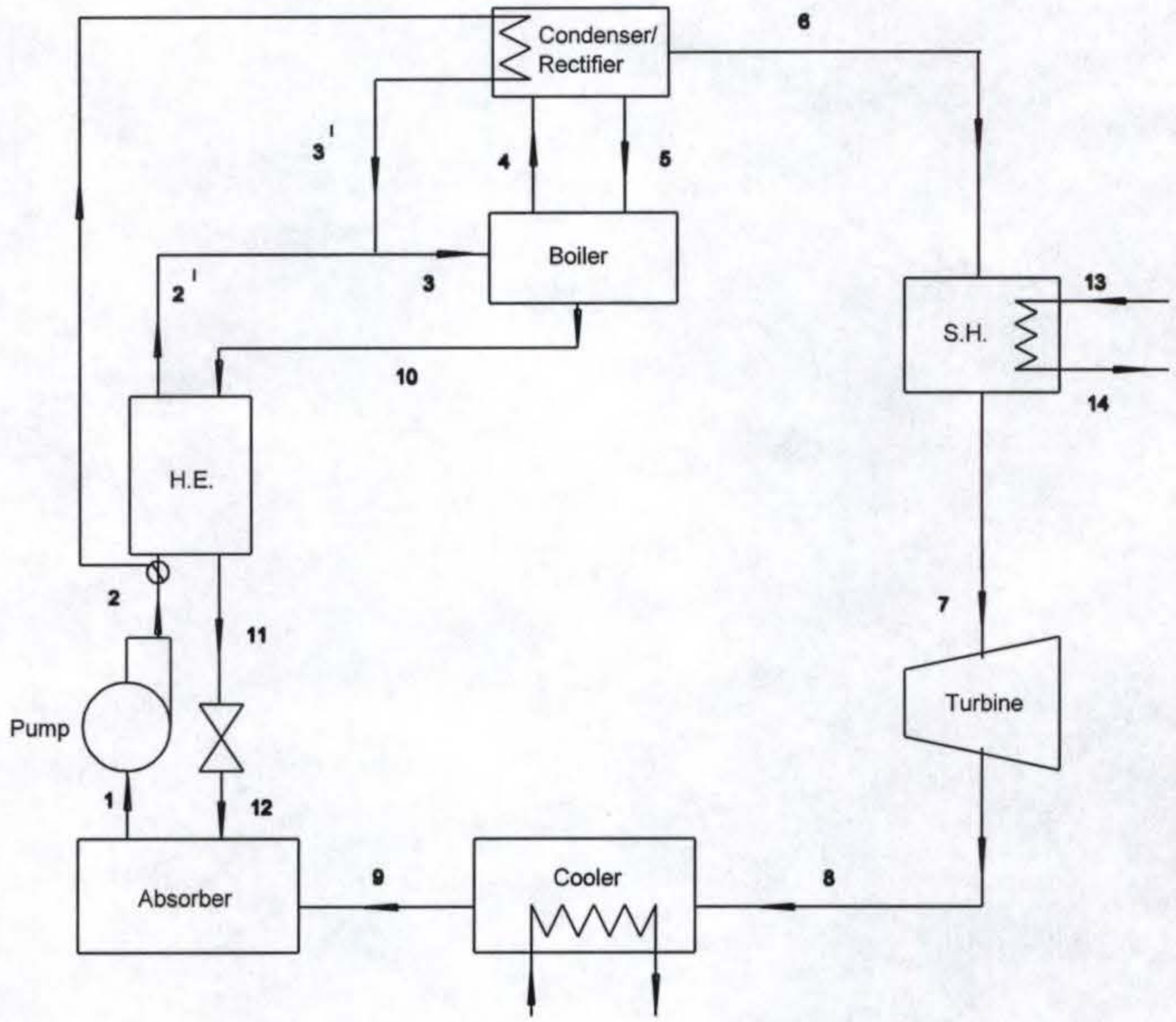

Figure 3-4 A modified ammonia-based combined power/cooling cycle

Table 3-4 Typical operating conditions

State	T (K)	p (bar)	h (kJ/kg)	s (kJ/kg K)	x	Flow rate m/m_1
1	280.0	2.0	-214.1	-0.1060	0.5300	1.0000
2	280.0	30.0	-211.4	-0.1083	0.5300	1.0000
3	378.1	30.0	246.3	1.2907	0.5300	1.0000
4	400.0	30.0	1547.2	4.6102	0.9432	0.2363
5	360.0	30.0	205.8	1.1185	0.6763	0.0366
6	360.0	30.0	1373.2	4.1520	0.9921	0.1997
7	410.0	30.0	1529.7	4.5556	0.9921	0.1997
8	257.0	2.0	1148.9	4.5558	0.9921	0.1997
9	280.0	2.0	1278.7	5.0461	0.9921	0.1997
10	400.0	30.0	348.2	1.5544	0.4147	0.8003
11	300.0	30.0	-119.0	0.2125	0.4147	0.8003
12	300.0	2.0	-104.5	0.2718	0.4147	0.8003

Table 3-5 Results from the table 3-4 state conditions

cycle high temperature and pressure are 410.0 K and 30.0 bar
cycle low temperature and pressure are 257.0 K and 2.0 bar
boiler heat input = 390.4
super heat input = 31.3
condenser heat reject = -83.8
absorber heat reject = -358.8
cooler cooling load = 25.9
turbine work output = 76.0
turbine liquid fraction = 0.0692
turbine vapor fraction = 0.9308
pump work input = 2.7
total heat input = 421.6
total work output = 73.33
cycle efficiency = 23.54%

All energy units are kW/kg basic solution

3.6 Conclusion

The initial thermodynamic analysis has shown that the ammonia-based combined power/cooling cycle has a promising application. In the case study of turbine inlet condition of 466 K and 27.6 bar, we obtain a pretty good first law system efficiency of 20.7%. At this condition, the steam is still a condensed liquid which means that the steam Rankine cycle can't even be used for such low temperature application. Further study with different turbine inlet temperature will also show that the proposed cycle will have better first law efficiency. The proposed cycle can be applied to many low temperature heat sources such as geothermal and solar energy heat sources.

An improved design of the proposed cycle is also presented in this chapter with detailed information. A second law analysis and system simulation based on this design are discussed in the following chapter.

CHAPTER 4
THE SECOND LAW THERMODYNAMIC ANALYSIS

4.1 Introduction

With the increasing cost of our most widely used fuels and the potential decrease in their availability in the future, the importance of effective use of our available energy resources is now receiving more and more attention. The location and degree of inefficient use of energy in our energy systems should be a primary factor in the design and performance analysis of the system. The second law analysis is directed to providing this information by a systematic approach.

To evaluate the effectiveness of energy use in different systems, a realistic measure of energy utilization must be applied. The exergy method of analysis will provide this true measure of effective energy use through its application of principles of both the first and second laws of thermodynamics.

4.2 Work and Availability

The final product of interest from the expenditure of energy resources is work which is used to perform tasks such as generating electricity, pumping water and moving

objects. Work is made available from the energy resources in many forms. For example, the combustion of oil or gas in a power plant provides high-pressure, high-temperature steam that is available to do work through a turbine and generator system. When the temperature and pressure of the steam are near the conditions of the surrounding environment(condensed liquid near ambient temperature), the work available in the steam has essentially disappeared. Another example is that, the water behind a dam on a river is available to do work by driving a hydraulic turbine and an electric generator. The available work in the water behind the dam reverts to zero when the water level falls to the level in front of the dam. So when the mass comes into equilibrium with the environment, no more changes of state will occur and the mass will not be capable of doing any work. Therefore, the steady-state condition of our surrounding environment is a reference state which a mass at a given state(such as high temperature and high pressure steam, water held in a dam) can achieve after a process to perform maximum available work. This concept of available work referenced to the surrounding environment is the basis of the exergy method of energy-systems analysis.

It is also a realistic method of comparing the efficient use of our energy resources. It should be noted that a fluid or gas that is not in equilibrium with the ambient surroundings has the potential to perform work as its condition reverts to the ambient surrounding conditions, as everything will do naturally. This means that a fluid that is colder than the ambient surroundings will be available to perform work as it warms up to the ambient surroundings just as a warm fluid is available to perform work in its passage to the ambient surrounding conditions.

4.3 Thermodynamic Processes and Cycles

Energy systems are made up of a series of individual processes that form closed or open cycles. Each process in a system or cycle can be analyzed separately from the system by performing a first-law energy balance around the component involved in the process.

As the available work in a system working fluid decreases through energy-related processes, there are losses in the available work since no transfer of heat or conversion between mechanical work and heat can be performed without some irreversibility in the process. In a system in which many processes are involved, the loss of work in the system will be distributed throughout the individual processes. It is important to establish the relative losses in each process if we are to effectively improve the system efficiency.

It should be noted that the conventional heat-balance method of evaluating system losses and system efficiency is misleading and not a true representation of system effectiveness. Only through an evaluation of the available work throughout the system can we have a true measure of the losses in the system processes, which is necessary for effective energy conservation in system design and operation.

4.4 Exergy

Exergy is defined as the work that is available in a mass as a result of conditions nonequilibrium relative to some reference condition. As we have described in the

previous paragraph, atmospheric condition generally is a reference condition. Useful work can be recovered during the cooling and expansion processes of steam through a steam engine or turbine and heat exchangers. The exergy that is not recovered as useful work is lost.

Exergy is an explicit property at steady-state conditions. Its value can be calculated at any point in an energy system from the other properties that are determined from an energy balance on each process in the system. Exergy is calculated at a point in the system relative to the reference condition by the following general equation:

$$\text{Exergy} = (u - u_0) - T_0(s - s_0) + P_0(v - v_0) + V^2/2g + g(z - z_0) + \Sigma(\mu_i - \mu_{io})x_i \qquad 4\text{-}1$$

Internal Energy | Entropy | Work | Momentum | Gravity | Chemical Potential

Where the subscript 0 denotes the reference condition and i denotes as i-th composition. There are variations of this general exergy equation, and in most systems analyses some, but not all, of the terms shown in equation 4-1 would be used. Since exergy is the work available from any source, terms can also be developed using electrical current flow, magnetic fields, and diffusion flow of materials.

4.5 Background of Dead State

The exergy method of analysis is a particular approach to application of the second law of thermodynamics to engineering systems. Another frequently used term is

availability analysis, which is often found in classical thermodynamic text books (Sonntag et al, 1994; Moran and Shapiro, 1992).

"Exergy is the maximum theoretical work that can be extracted from a combined system or system and environment as the system passes from a given state to equilibrium with the environment-that is, passes to the dead state." (Moran and Sciubba, 1994).

Environment or surroundings are often used as a reference state for availability analysis. When the mass comes into equilibrium with the environment, no change of state will occur. So the mass is incapable of doing any work or is in a dead state.

One standard atmospheric pressure is normally used as a reference pressure. Different reference environment temperature have been used by researchers such as 293 K (Aphornratana and Eames, 1995), 298 K (Egrican, 1988) and 300 K (Waked, 1991).

Krakow(1991) proposed a dead-state definition. He indicated that the reservoir of a system that is not the environment is defined as the system reservoir. The system reservoir serves as the source for engines and coolers and as the sink for heat pumps. The environment serves as the sink for engines and coolers and as the source for heat pumps. So instead of using universal ambient condition as a dead state, he proposed that one of the high-temperature and low-temperature reservoirs of the system to be considered as a reference state.

Since reservoirs of real systems are finite, their temperatures change during any heat transfer process. Therefore, the dead state temperature in a real process changes during the process. To account for the change in the dead state temperature in real processes,

Krakow defined an effective reservoir temperature for heat sources and sinks which is essentially the same as the entropic average temperature used by Herold (1989).

The effective reservoir temperature, which is used as the dead state for the reservoir, is defined as the temperature that will make its initial exergy equal to the final exergy. Neglecting the momentum, gravity and chemical exergies, the initial and final exergies of a reservoir are

$$Ex_1 = (h_1 - h_{ef}) - T_{ef}(s_1 - s_{ef}) \qquad 4\text{-}2$$

$$Ex_2 = (h_2 - h_{ef}) - T_{ef}(s_2 - s_{ef}) \qquad 4\text{-}3$$

where subscripts 1 and 2 stand for the initial and final conditions of the reservoir, and ef stands for the effective temperature condition.

T_{ef} is defined such that $Ex_1 = Ex_2$.

The entropic average temperature of a reservoir is defined as

$$T_{avg} = \frac{Q_{1-2}}{S} = \frac{Q_{1-2}}{\int_1^2 \frac{\delta Q}{T}} \qquad 4\text{-}4$$

where $Q_{1\text{-}2}$ is the heat exchanged with the reservoir.

Above methods and definitions can be used easily for single working fluids such as steam. However, it is difficult to define the dead state for mixtures such as LiBr/water and ammonia/water. Since a dead state composition must also be defined. In other words, it is important to know what work will be done by changing mixture composition at the same temperature and pressure, or will the composition change at all under the same temperature and pressure.

Koehler et al.(1988) proposed the following method to consider the mixture composition factor in exergy calculations for the LiBr/water mixtures.

$$Ex = Ex(T, P, x) = Ex(T, P) + Ex_0(x) \qquad 4\text{-}5$$

Ex(T, P) denotes the temperature and pressure dependent part of the exergy of mixtures at a given composition x, and $Ex_0(x)$ depends on x at the reference state.

To find $Ex_0(x)$ imagine mixtures at T_0, P_0 undergoing a change of state from a given x to the dead state at saturated mixtures state x_s by adding an amount of solution at T_0, P_0. And we have following equations:

$$Ex(T, P) = (h(T, P, x) - h_0(T_0, P_0, x)) - T_0(s(T, P, x) - s_0(T_0, P_0, x)) \qquad 4\text{-}6$$

$$Ex_0(x) = (h_x - h_s) - T_0(s_x - s_s) + \frac{x_s - x}{1 - x_s}[(h_{02} - h_s) - T_0(s_{02} - s_s)] \qquad 4\text{-}7$$

where $\frac{x_s - x}{1 - x_s} = \frac{m_s - m_x}{m_x}$

subscript 02 stands for the solute or solution being added

subscripts s and x stand for the saturated and actual concentration.

The exergy of the pure component can be obtained as

$$Ex(x = 0) = (h - h_s) - T_0(s - s_s) + \frac{x_s}{1 - x_s}[(h_{02} - h_s) - T_0(s_{02} - s_s)] \qquad 4\text{-}8$$

There are two main problems with this method. First, when a solution from a state T, P passes to a dead state T_0, P_0, the solution concentration may be over the level of saturation concentration. Then an amount of solute must be taken out from the solution. Koehler et al. did not mention this point. Secondly, equation 4-8 is not the equation for

the pure cycle working fluid exergy analysis, and therefore it should not be used for a pure component exergy calculation.

4.6 Exergy Analysis for the Proposed Cycle

The reservoir in a system that serves as the environment state should be used as a reference state. Our new cycle is a combined power and refrigeration cycle, therefore, both boiler and cooler are system reservoirs. The main purpose of this cycle is power generation, and the absorber serves as a condenser of the power cycle. Heat is rejected during the absorption process.

It is inappropriate to use water at ambient state as a reference for a mixture solution. Koehler et al.(1988) consider the mixture effect, but his method will create many reference states in the system as there are several different mixture compositions. Therefore, their method does not provide a common ground for exergy analysis.

Szargut et al. (1988) suggested a rule for the choice of reference levels for calculating exergy of mixtures. If the processes under consideration are only physical, a reference level can be assumed separately for each constituent involved in the process.

For a cyclic physical process involving a solution of changing composition, the following equation can be used for the thermal exergy related to the arbitrarily assumed reference level:

$$Ex = h - T_0 s - \Sigma(h_{0i} - T_0 s_i)x_i \qquad 4\text{-}9$$

For a binary solution, ammonia-water mixtures, equation 4-9 can be written as:

$$Ex = h - T_0 s - (h_{0w} - T_0 s_{0w})x_w - (h_{0a} - T_0 s_{0a})x_a \quad 4\text{-}10$$

$$x_w = 1 - x_a \quad 4\text{-}11$$

Substituting 4-11 in 4-10 gives

$$Ex = h - T_0 s + [-(h_{0w} - T_0 s_{0w})] + [(h_{0w} - T_0 s_{0w}) - (h_{0a} - T_0 s_{0a})]x_a \quad 4\text{-}12$$

Equation 4-12 can be written as

$$Ex = h - T_0 s + a + bx \quad 4\text{-}13$$

where $a = -(h_{0w} - T_0 s_{0w})$

$$b = (h_{0w} - T_0 s_{0w}) - (h_{0a} - T_0 s_{0a})$$

In Equation 4-13, x is the ammonia mass fraction, a and b are constants that depend on the choice of the dead state.

For a closed cycle, the values of a and b will not have any effect on the exergy analysis since eventually they will be canceled out. So a and b can be chosen such that all the exergies in a cycle are positive.

For pure component analysis, x is either 0 or 1. In that case equation 4-12 takes the following form:

$$Ex = h - T_0 s + c \quad 4\text{-}14$$

where c is a constant.

Equation 4-11 is a general form for a pure component exergy analysis.

The following is an exergy analysis of the proposed cycle as shown in figure 3-4.

Assumptions used in the study are:

1. Ammonia-water solutions in the boiler and the absorber were assumed to be in equilibrium at their respective temperatures and pressures.

2. Pressure losses due to the friction in heat exchangers and pipe lines are neglected.

3. The reference temperature T_0 has been chosen as 280 K, which is the absorber temperature usually used in this study. Constants a and b are chosen as 10 kJ/kg and 536 kJ/kg so that all the points have positive exergy.

Boiler exergy change:

$$\Delta E_{boiler} = m_4E_4 + m_{10}E_{10} - m_3E_3 - m_5E_5$$

Condenser exergy change:

$$\Delta E_{cond} = m_5E_5 + m_6E_6 + m_{3'}E_{3'} - m_4E_4 - m_3E_2 \qquad 4\text{-}15$$

Superheater exergy change:

$$\Delta E_{S.H.} = m_7E_7 - m_6E_6 \qquad 4\text{-}16$$

Cooler exergy change:

$$\Delta E_{cooler} = m_9E_9 - m_8E_8 \qquad 4\text{-}17$$

Absorber exergy change:

$$\Delta E_{absorber} = m_1E_1 - m_9E_9 - m_{12}E_{12} \qquad 4\text{-}18$$

Solution heat exchanger exergy change:

$$\Delta E_{H.E.} = m_{2'}E_{2'} + m_{11}E_{11} - m_{2'}E_2 - m_{10}E_{10} \qquad 4\text{-}19$$

Throttling valve exergy change:

$$\Delta E_{valve} = m_{12}E_{12} - m_{11}E_{11} \qquad 4\text{-}20$$

Exergy change due to mixing at point 3:

$$\Delta E_{mixing} = m_3E_3 - m_{2'}E_{2'} - m_{3'}E_{3'} \qquad 4\text{-}21$$

Turbine exergy change:

$$\Delta E_{turbine} = m_3E_8 + m_7E_7 \qquad 4\text{-}22$$

Pump exergy change:

$$\Delta E_{pump} = m_2E_2 + m_1E_1 \qquad 4\text{-}23$$

Table 1 Typical state points

State	Temperature (K)	Pressure (bar)	Enthalpy (kJ/kg)	Entropy (kJ/kg K)	Ammonia mass frac.	Flow rate m/m_1	Exergy (kJ/kg)
1	280.0	2.0	-209.7	-0.0636	0.5000	1.0000	86.1
2	280.0	23.0	-207.6	-0.0649	0.5000	1.0000	88.6
2'	374.0	23.0	263.5	1.4282	0.5000	0.7299	141.6
3	372.5	23.0	234.5	1.3441	0.5000	1.0000	136.1
3'	360.0	23.0	156.0	1.0761	0.5000	0.2701	132.7
4	400.0	23.0	1590.7	4.8285	0.9227	0.2784	743.3
5	360.0	23.0	168.6	1.0992	0.5738	0.0436	178.4
6	360.0	23.0	1409.5	4.3613	0.9876	0.2347	727.6
7	500.0	23.0	1793.4	5.2631	0.9876	0.2347	859.1
8	276.1	2.0	1250.5	5.2631	0.9876	0.2347	316.2
9	280.0	2.0	1264.1	5.3159	0.9876	0.2347	315.0
10	400.0	23.0	357.2	1.5718	0.3504	0.7653	115.0
11	300.0	23.0	-92.1	0.2826	0.3504	0.7653	26.7
12	300.0	2.0	-94.0	0.2838	0.3504	0.7653	24.4

Table 2 Exergy change of each component

	Exergy Change	Exergy input	Exergy loss	Exergy loss(%)	Work Output
Boiler	151.0	151.0			
Superheater	30.8	30.8			
Condenser	-16.4		16.4	28.97%	
Absorber	-6.5		6.5	11.49%	
Solution H.E.	-28.9		28.9	51.06%	
Throttling Valve	-1.8		1.8	3.18%	
Mixing	-3.0		3.0	5.30%	
Turbine	-127.4				127.4
Cooler	-0.3				0.3
Pump	2.5				-2.5
Total	0	181.8	56.6	100%	125.2

The second law efficiency is

η_{II} = (exergy output) / (exergy input) = 125.5 / 181.8 = 68.9%

4.7 Discussion

It can be seen that the condenser, solution heat exchanger and absorber are the three major components that lose exergy. While absorber and condenser lose about the same amount of exergy, solution heat exchanger makes up the biggest loss of exergy. The exergy analysis has identified the components of the cycle that must be targeted for

further improvement in the cycle efficiency. To reduce the amount of exergy loss in condenser , the condenser temperature must be increased so that less vapor is condensed. But this will increase the moisture content in the ammonia vapor and cause problems in the turbine expansion process. The condenser temperature can be increased to reduce the exergy loss in the condenser, as long as the turbine exit condition of less than 10% moisture(liquid) can be maintained.

4.8 Conclusion

A second law analysis of the new power cycle is presented. This analysis has used the thermodynamics properties of ammonia-water mixtures developed in this research. Different methods proposed in the literature to choose dead state conditions for exergy analysis are discussed. This paper proposes a reference state at ambient pressure and saturated liquid state of the basic solution in the cycle, so that the mixture effect is considered in the reference state.

Performances of the proposed cycle are evaluated. The exergy analysis shows more detailed information than the first law analysis. The exergy analysis shows how the energy is utilized and which components waste the available energy, so that improvements in system design can be recommended.

CHAPTER 5
A THEORETICAL COMPARISON OF THE PROPOSED CYCLE AND RANKINE CYCLE

5.1 Introduction

The new power cycle using ammonia-water mixtures as a working fluid was introduced in the chapter 3. The new power cycle can operate as an independent cycle as well as a bottoming cycle. Most heat sources available to the bottoming cycles, such as hot exhaust gases, are sensible-heat sources because the temperature of the source varies during the heat transfer. The amount of cooling medium at the sink temperature in reality is also limited so that the heat sink is sensible as well. This sensible heat transfer does not fit the isothermal process of the conventional Rankine cycle using a pure working fluid because there is a pinch point during the heat transfer process.

In this chapter, a detailed performance of the new cycle and the Rankine cycle will be investigated and contrasted. An objective of this study is to determine under what circumstances one cycle has an advantage over the other.

Maloney and Robertson(1953) studied a similar ammonia-water power cycle using ammonia-water mixtures as a working fluid. They compared the ammonia-water power cycle with Rankine cycle and concluded that the efficiency of the ammonia-water cycle is less than that of a steam cycle.

5.2 Cycle Description

In the Rankine cycle the heat rejection occurs in a simple heat exchanger(condenser), and the heat addition also occurs in a simple heat exchanger(boiler or steam generator). In the proposed cycle the heat rejection occurs in an absorber, and the heat addition includes solution heat exchanger, boiler and rectifier. When comparing different power cycles, regardless of the details of the balance of the system, heat source and heat sink are the two major criteria for comparison. The ability to add heat in the cycle at the heat source temperature and reject heat at the heat sink temperature is a decisive factor in achieving a better cycle efficiency.

Figure 5-1 shows a simplified power cycle model used to compare the proposed cycle and the Rankine cycle.

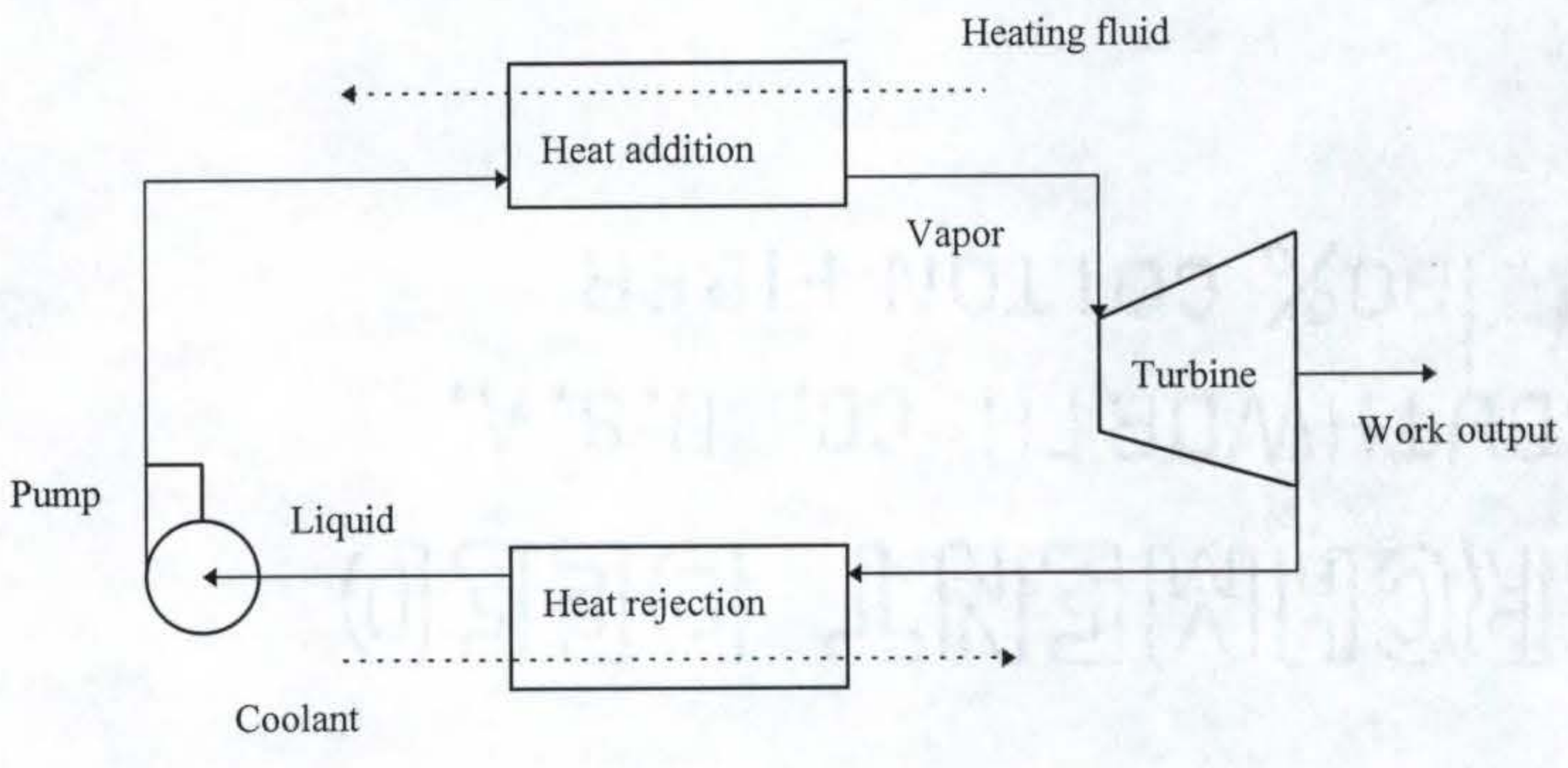

Figure 5-1 A simplified power cycle

The working fluid is heated to a vapor state in the heat addition heat exchanger. The vapor expands in the turbine and produces useful work. The fluid condenses to liquid state in the heat rejection heat exchanger. The liquid is pumped to a high pressure to complete the cycle. In the following paragraph, a theoretical comparison of using ammonia-water mixtures and steam as working fluids in this cycle is studied. The results will show the advantage of the proposed cycle over the Rankine cycle.

5.3 Thermal Boundary Conditions

As mentioned in the chapter 3, this cycle can be used as a bottoming cycle as well as an independent power cycle using low temperature heat sources such as solar energy and geothermal energy. The heating fluid is taken to be at 520 K and the cooling sink is taken to be at 280 K. The heating fluid has a constant thermal capacity of 1 kJ/kg K.

If a stream of hot gases is taken to flow without friction and is cooled to sink temperature under constant composition, it is found that the maximum mechanical power that could be produced is 220 kJ/kg of gases. This is referred to as 100% of the exergy. The destruction of this exergy will be investigated in both the cycles.

5.4 Temperature Limitation in the Heat Addition Exchanger

The first limitation is due to thermal properties and heat transfer. If water at 280 K and 20 bar is introduced in the steam generator and if the heat transfer surface is infinite

in area, it is found that the temperature profile of water can not match the temperature profile of the hot gases. At one point in the heat exchanger, the water boiling point temperature can at most be equal to the hot fluid temperature. This is the so-called "pinch point". Figure 5-2 shows the heat transfer profile of a steam generator of Rankine cycle.

At the exit the temperature can at most be equal to the inlet temperature of the hot gases. If the maximum pressure of steam is 20 bar and the water inlet temperature is 280 K, it is found that a large amount of hot fluid energy remains unused in the heat exchanger. The exit temperature of hot gases will be 470 K, which means 67.5% of the availability remains unused and therefore wasted. The availability gained by the steam is 27.9%, and 4.6% availability is destroyed during the heat transfer process. Figure 5-4 shows the exergy diagram of a steam generator assuming the outlet steam temperature equals the inlet hot fluid temperature and pinch point temperature difference is zero.

In the proposed cycle ammonia-water mixture is a working fluid. When the mixture enters the vapor generator, light substance ammonia tends to boil off early. The mixture composition changes during the heating process and the boiling point rises. Figure 5-3 shows a typical temperature profile of ammonia-water mixtures and hot gases in a heat exchanger.

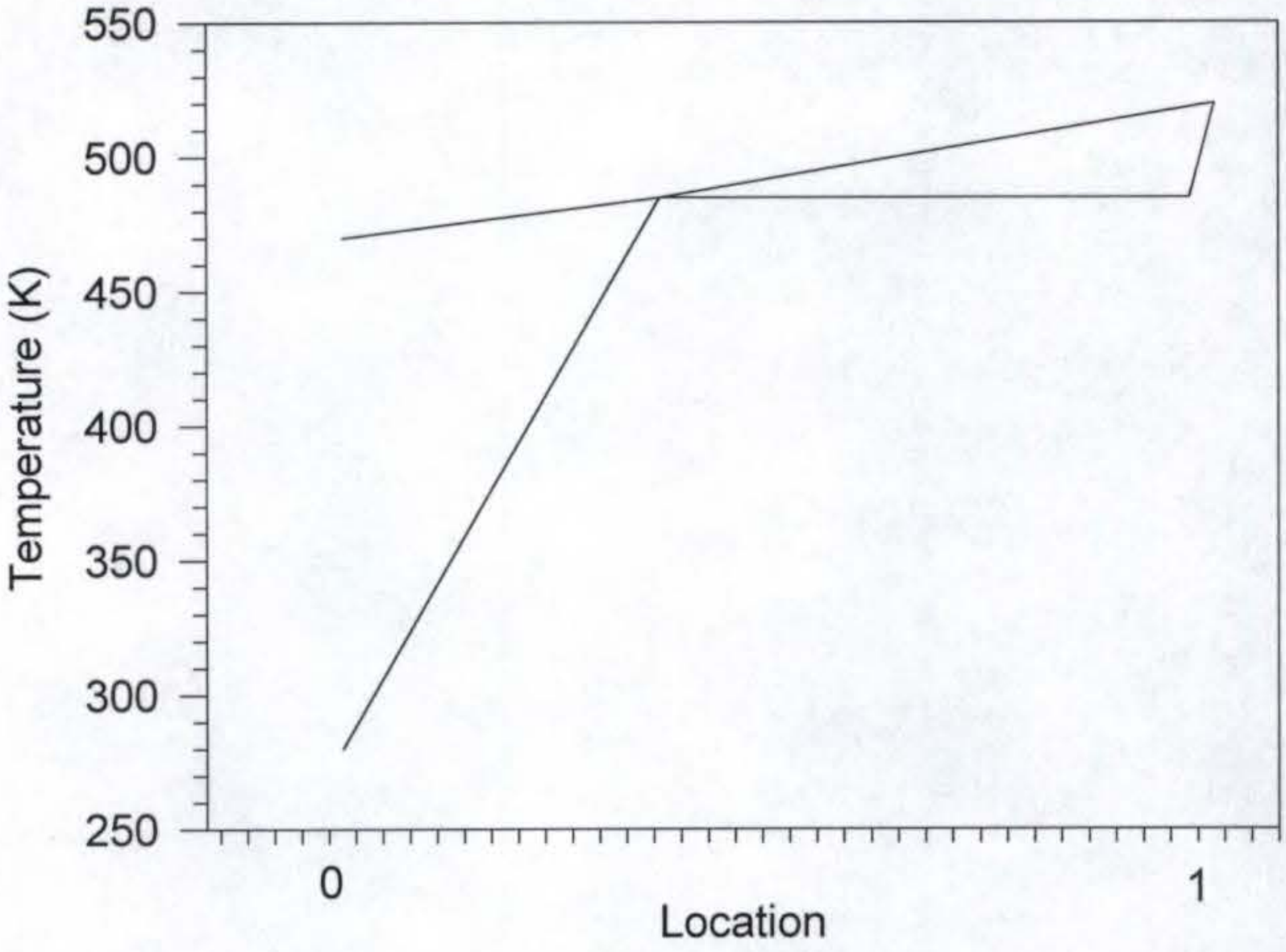

Figure 5-2 Temperature profile of a steam generator

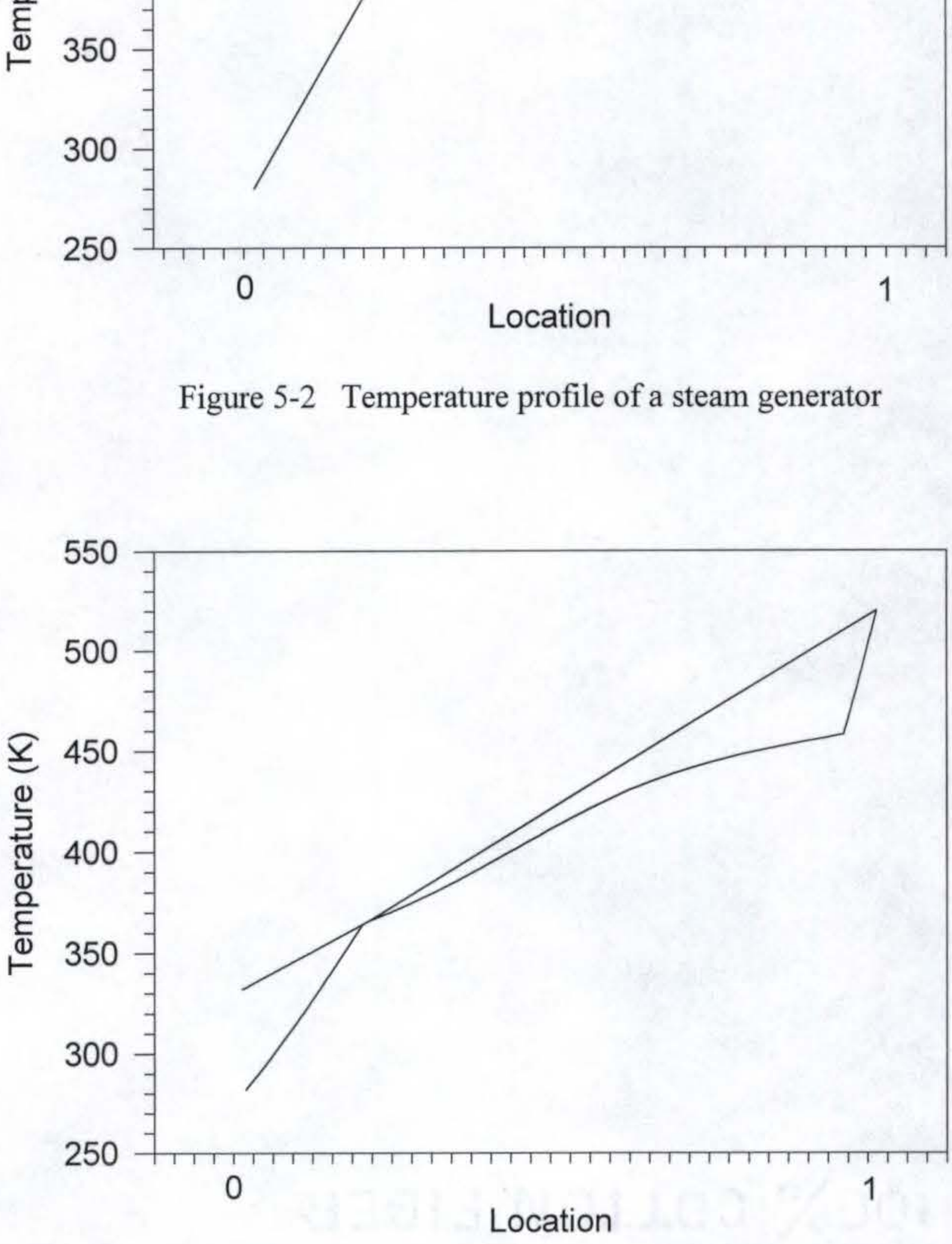

Figure 5-3 Temperature profile of a NH_3/H_2O vapor generator

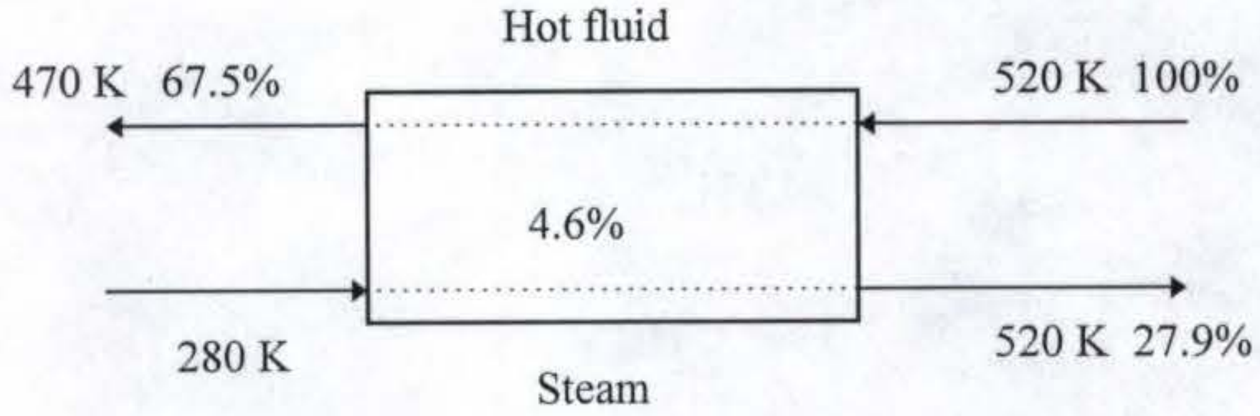

Figure 5-4 Performance of a steam generator assuming infinite heat transfer area at 20 bar

Table 5-1 Properties at state points of Figure 5-4

State points	T (K)	P (bar)	h (kJ/kg)	s (kJ/kg K)	m/m gas	e (kJ/kg)
Hot fluid inlet	520	1	247	0.6444	1	66.7
Hot fluid outlet	470	1	197	0.5433	1	45.0
Hot fluid pinch	485.3	1	212.3	0.5754	1	51.3
Water pinch	485.3	20	907.5	2.4479	0.017	3.9
Water inlet	280	20	30.5	0.1058	0.017	0.0
Steam outlet	520	20	2890	6.5263	0.017	18.6

If the pinch point and exit temperature differences are assumed zero, the leaving gas will have been cooled to 345 K and will only carry 7.8% of the original exergy. This shows significant improvement due to a better temperature match using ammonia-water mixtures. Ammonia-water working fluid will carry 84.4% of the original exergy as compared with only 27.9% by the steam as a working fluid. Figure 5-5 shows the exergy distribution in a ammonia-water vapor generator.

Since it is unrealistic to have an infinite heat transfer area in a heat exchanger, there will be a temperature difference between the hot gases and the working fluid. There also exists a temperature difference at the pinch point. Assuming a good heat exchanger and no friction loss, it is assumed that there is a 10 K temperature difference between the hot gas inlet and the working fluid exit. It is also assumed a 5 K temperature difference exists at the pinch point. By doing this, the performance of a steam generator will be miserable. Figures 5-6 and 5-7 show the exergy profile assuming a finite heat transfer area in the heat exchanger.

For a steam generator, It is possible to lower the pinch point by reducing the pressure. But it still does not compare will with an ammonia-water vapor generator. Figure 5-8 shows the improvement of a steam generator by reducing the pressure from 20 bar to 10 bar.

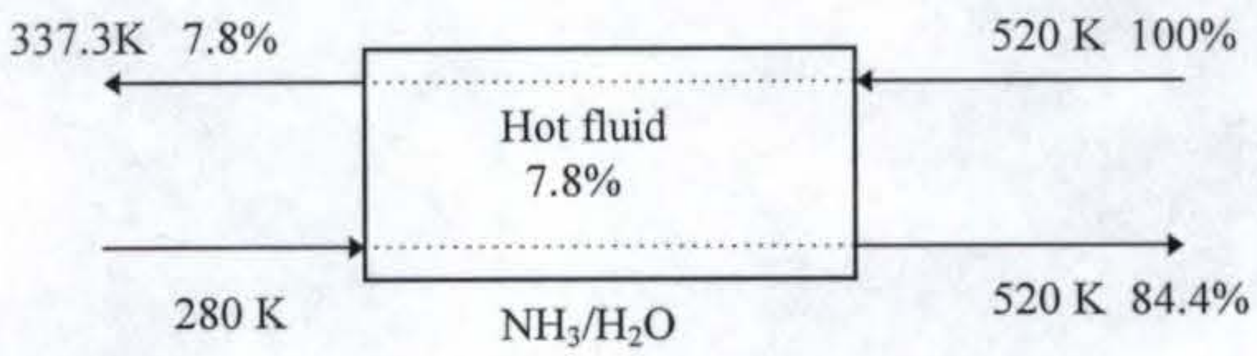

Figure 5-5 Performance of a NH_3/H_2O vapor generator assuming infinite heat transfer area at 20 bar

Table 5-2 Properties at state points of Figure 5-5

State points	T (K)	P (bar)	h (kJ/kg)	s (kJ/kg K)	m/m gas	e (kJ/kg)
Hot fluid inlet	520	1	247	0.6444	1	66.7
Hot fluid outlet	337.3	1	64.3	0.2116	1	5.2
Hot fluid pinch	364.8	1	91.8	0.2899	1	10.7
NH_3/H_2O pinch	364.8	20	178.8	1.1400	0.071	3.6
NH_3/H_2O inlet	280	20	-207.9	-0.0647	0.071	0.1
NH_3/H_2O outlet	520	20	2363.9	6.2900	0.071	56.4

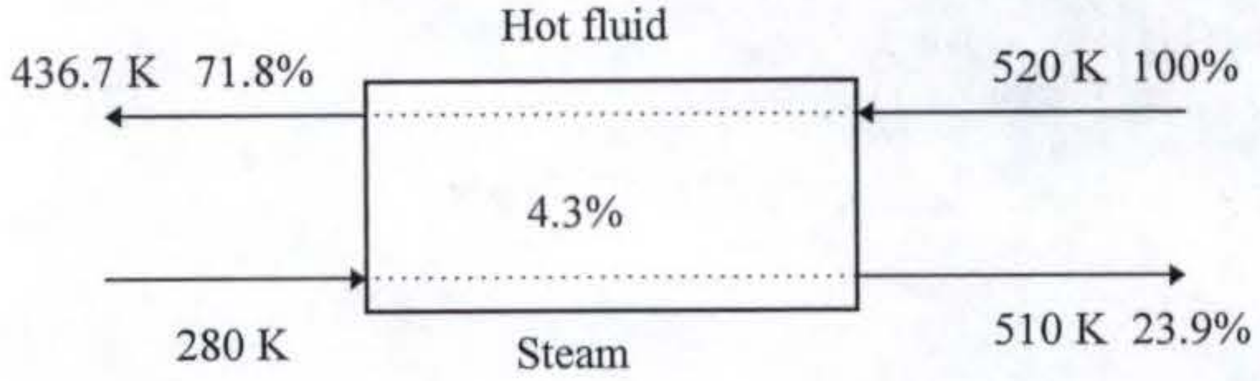

Figure 5-6 Performance of a steam generator assuming finite heat transfer area at 20 bar

Table 5-3 Properties at state points of Figure 5-6

State points	T (K)	P (bar)	h (kJ/kg)	s (kJ/kg K)	m/m gas	e (kJ/kg)
Hot fluid inlet	520	1	247	0.6444	1	66.7
Hot fluid outlet	477	1	204	0.5581	1	47.9
Hot fluid pinch	490.3	1	217.3	0.5856	1	53.4
Water pinch	485.3	20	907.5	2.4479	0.015	3.4
Water inlet	280	20	30.5	0.1058	0.015	0.0
Steam outlet	520	20	2890	6.5263	0.015	16.0

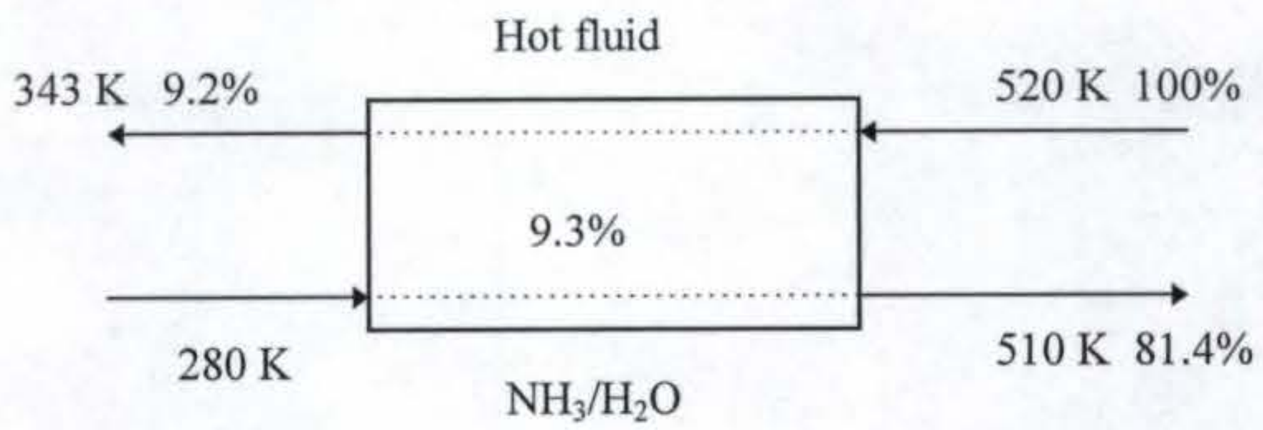

Figure 5-7 Performance of a NH_3/H_2O vapor generator assuming finite heat transfer area at 20 bar

Table 5-4 Properties at state points of Figure 5-7

State points	T (K)	P (bar)	h (kJ/kg)	s (kJ/kg K)	m/m gas	e (kJ/kg)
Hot fluid inlet	520	1	247	0.6444	1	66.7
Hot fluid outlet	342.9	1	69.9	0.2280	1	6.2
Hot fluid pinch	369.8	1	96.8	0.3035	1	11.9
NH_3/H_2O pinch	364.8	20	178.8	1.1400	0.070	3.5
NH_3/H_2O inlet	280	20	-207.9	-0.0647	0.070	0.1
NH_3/H_2O outlet	520	20	2363.9	6.2900	0.070	54.4

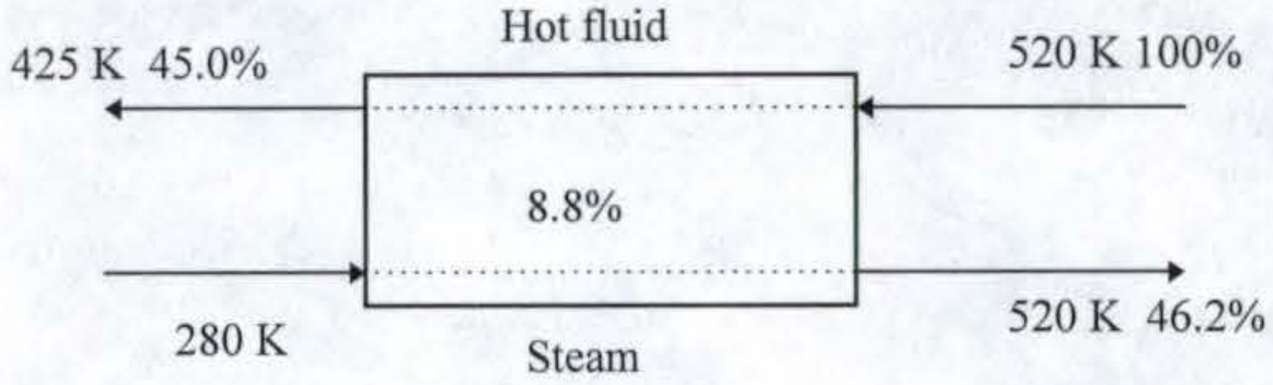

Figure 5-8 Performance of a steam generator assuming infinite heat transfer area at 10 bar

Table 5-5 Properties at state points of Figure 5-8

State points	T (K)	P (bar)	h (kJ/kg)	s (kJ/kg K)	m/m gas	e (kJ/kg)
Hot fluid inlet	520	1	247	0.6444	1	66.7
Hot fluid outlet	430.3	1	157.3	0.4550	1	30.0
Hot fluid pinch	452.9	1	179.9	0.5063	1	38.3
Water pinch	452.9	10	762.7	2.1415	0.031	5.1
Water inlet	280	10	29.5	0.1059	0.031	0.0
Steam outlet	520	10	2931.3	6.9068	0.031	30.9

5.5 Cycle Analysis

The previous section shows a superior performance of ammonia-water mixture in a finite heat capacitance heat addition process as compared with water. In this section, the performance of the boiler will be incorporated in a cycle, together with a turbine and a condenser.

For simplicity, an adiabatic efficiency of 100% is used in the calculations for both cycles. Studies show that exergy loss in a turbine due to irreversibility in expansion is about the same in both cycles, or less than 0.2%.

The selection of turbine back pressure is based on two criteria: 1. The condensation at the turbine exit should be less than 10%. 2. The working fluid can be condensed at 300K.

For hot gases at a temperature of 520 K, a 10 K temperature difference is assumed between the hot gas inlet and the working fluid exit. Also a 5 K temperature difference is assumed at the pinch point. The Rankine cycle is taken to operate between 10 bar and 0.63 bar, so that the boiler may get the high output from hot gas and 90% quality at the turbine exit. At the pressure of 0.63 bar, steam can be condensed at 360 K. The ammonia-water cycle is taken to operate between 15 bar and 2 bar. An ammonia-water mixtures with 0.5 ammonia mass fraction and a 2 bar pressure can be condensed at 300 K. That is a 5 K degree difference with the coolant inlet temperature.

Figures 5-9 and 5-10 show the performance of a Rankine cycle and an ammonia-water cycle.

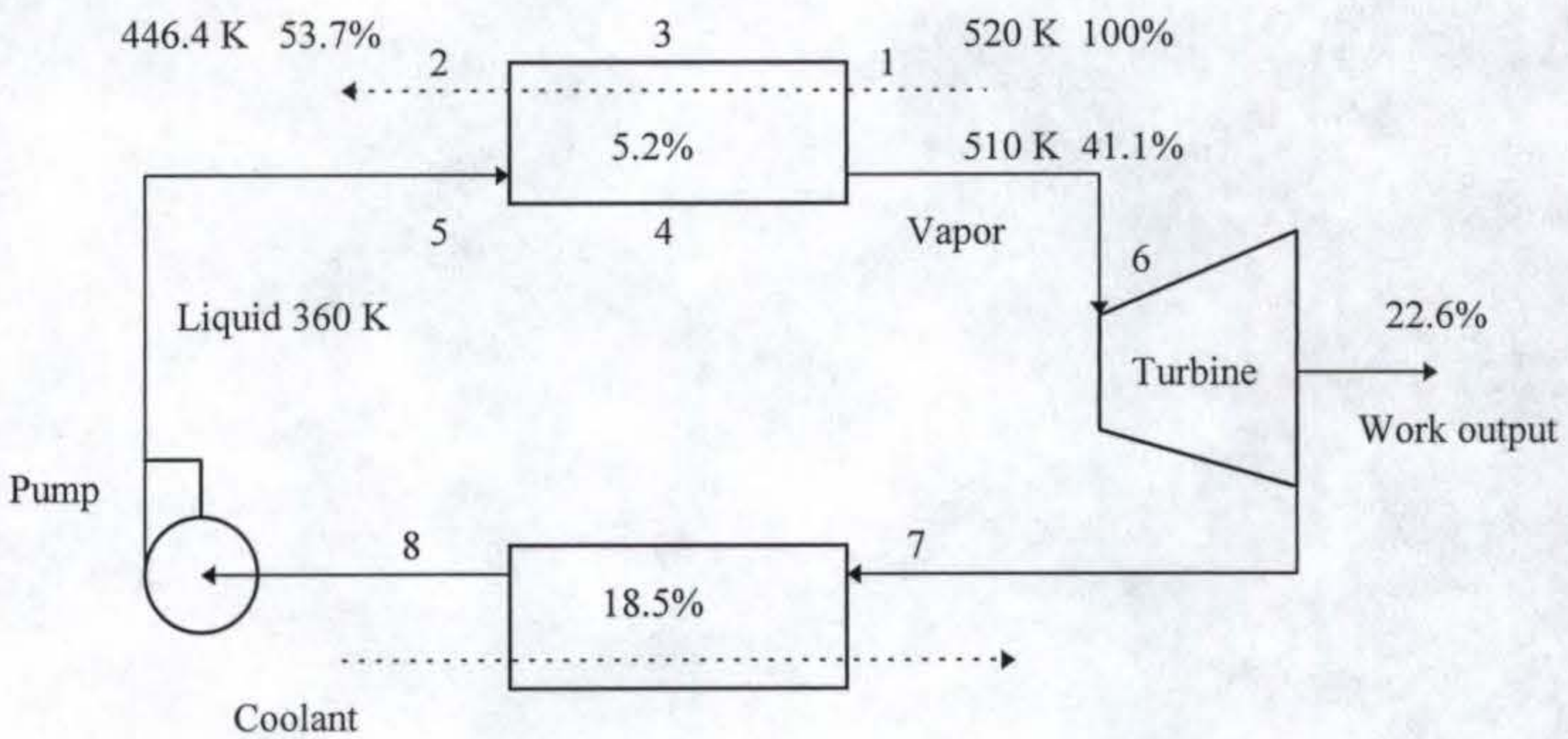

Figure 5-9 Performance of a Rankine cycle

First law efficiency of the above cycle is

$$\eta_I = \frac{W_t}{H_2 - H_1} = 19.0\%$$

and the second law efficiency is

$$\eta_{II} = 22.6\%.$$

Table 5-6 Properties at state points of Figure 5-9

State points	T (K)	P (bar)	h (kJ/kg)	s (kJ/kg K)	kg/kg gas	e (kJ/kg gas)
1	520	1	247	0.6444	1	66.7
2	446.4	1	173.4	0.4918	1	35.8
3 pinch point	457.9	1	184.9	0.5173	1	40.2
4 pinch point	452.9	10	762.7	2.1415	0.029	4.7
5	360	10	364.7	1.1591	0.029	1.2
6	510	10	2909.0	6.8635	0.029	28.6
7	360	0.63	2426	6.8635	0.029	14.6
8	360	0.63	364.3	1.1576	0.029	1.2

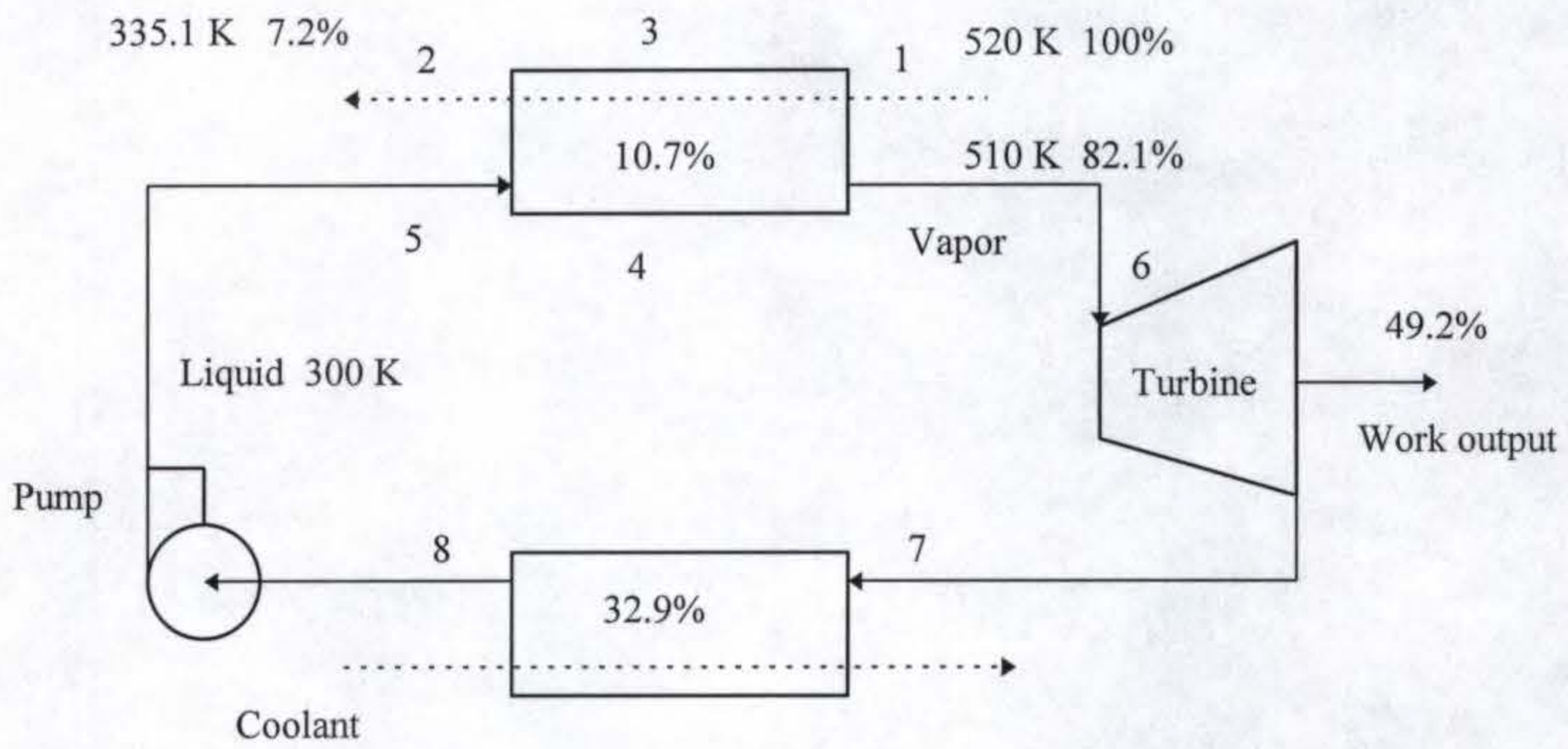

Figure 5-10 Performance of a ammonia-water cycle

First law efficiency of the above is

$$\eta_I = \frac{W_t}{H_2 - H_1} = 17.2\%$$

and the second law efficiency is

$$\eta_{II} = 49.2\%.$$

Table 5-7 Properties of state points of Figure 5-10

State points	T (K)	P (bar)	h (kJ/kg)	s (kJ/kg K)	kg/kg gas	e (kJ/kg gas)
1	520	1	247	0.6444	1	66.7
2	335.1	1	62.1	0.2049	1	4.8
3 pinch point	357.3	1	84.3	0.2691	1	9.0
4 pinch point	352.3	15	119.4	0.9763	0.073	2.7
5	285	15	-185.8	0.0155	0.073	0.1
6	510	15	2352.3	6.3977	0.073	54.8
7	370.7	2	1915.5	6.3979	0.073	23.7
8	285	2	-187.1	0.0164	0.073	0.0

5.6 Conclusion

Chapter 3 has qualitatively shown that ammonia-water mixture has favorable heat transfer characteristics. In this Chapter, we have demonstrated quantitatively that ammonia-water mixture has a big advantage over steam in a bottoming cycle.

An interesting point shown here is that the first law analysis is misleading. In figure 9, a Rankine cycle has a first law efficiency of 19.0% while from figure 5-10, an ammonia-water cycle has a first law efficiency of 17.2% under identical source and sink conditions. But ammonia-water cycle has a 49.2% second law efficiency as compared with only 22.6% for the Rankine cycle. In Rankine cycle, most of the available heat in the source is wasted and only a small amount of heat is input into the cycle. The first law thermodynamic efficiency is based on only the amount of heat input and the work output The second law analysis shows how well the available energy is used. An ammonia-water cycle certainly makes a good use of the available energy as shown in this chapter. If the heat transfer effectiveness from the heat source is not considered, an ammonia-water cycle may seem less favorable than a Rankine cycle. Most heat sources available to the bottoming cycles are sensible-heat sources, so the temperature of the source varies during the heat transfer process. A constant boiling temperature of a Rankine cycle mismatches the heat transfer process which generates irreversibility.

CHAPTER 6
SYSTEM SIMULATION AND PARAMETRIC ANALYSIS

6.1 Introduction

The novel ammonia based power/cooling cycle was simulated as descried in chapter 3 figure 3-4. This chapter describes the results of computer simulation of the cycle. The results are presented as a parametric analysis to conduct a systematic study of the effect of turbine inlet vapor temperature, turbine pressure ratio, boiler and condenser temperature and absorber temperature.

6.2 Thermodynamic Analysis of the Proposed Cycle

This section gives a thermodynamic analysis of this novel cycle with assumed thermal boundary conditions as

1. Boiler temperature: 400 K - 450 K
2. Turbine inlet temperature: 400 K - 500 K
3. Turbine inlet pressure: 18 bar - 32 bar
4. Ammonia concentration in basic solution: 0.20 - 0.55 by mass

The thermodynamic state conditions of the proposed combined cycle were evaluated assuming an idealized cycle (that is , irreversibilities associated with real apparatus were neglected.) The idealized cycle does provide the analytical maximum limits for the real cycle and is necessary in determining the efficiency limits of a real system.

A computer program for ammonia-water mixture thermodynamic properties has been developed for the cycle analysis. The program uses Gibbs free energy method and has shown good agreement of thermodynamic properties with published literature data.

Following are the assumptions for the cycle analysis.

1. At point 1, the working fluid is saturated liquid at low pressure. Temperature is set at 280 K to keep fluid at liquid state at a 2 bar pressure.

2. At point 2, saturated liquid is pumped to a high pressure at 20-30 bar.

3. Mixture passes through a preheat heat exchanger and the temperature is raised to about 350 K, assuming that the boiler temperature is 400 K.

4. Basic solution of ammonia-water mixture enters the boiler where it is heated to 400 K. NH_3/H_2O mixtures will evaporate with a higher concentration of NH_3. So at point 4, ammonia mass concentration is expected to be over 0.90. At point 10, weak aqua returns to the absorber via a heat exchanger.

5. Because we need high concentration mixture(pure ammonia is ideal but it is impossible), part of the moisture is condensed in the condenser. The condenser temperature is set at about 360 K.

6. After the condenser, the ammonia concentration in the mixture can be as high as 0.99.

7. The mixture is superheated before it enters the turbine. Superheater temperature is set at 410 K.
8. The mixture with high pressure, temperature and ammonia concentration expands in the turbine and transfers output work to a generator. We can expand the mixture to a very low temperature and still maintain a vapor state. A very small amount of moisture may condense after the turbine. Based on the operating experience of steam turbines in the literature, it is assumed that less than 10% moisture after the turbine exit won't affect turbine's performance.

6.3 Basic Equations

Boiler heat transfer:

$$q_{boiler} = m_4h_4 + m_{10}h_{10} - m_3h_3 - m_5h_5$$

Condenser heat transfer:

$$q_{cond} = m_5h_5 + m_6h_6 + m_{3'}h_{3'} - m_4h_4 - m_3h_2$$

Superheat input:

$$q_{superheater} = m_6(h_7 - h_6)$$

Absorber heat rejection:

$$q_{absorber} = m_1h_1 - m_{12}h_{12} - m_9h_9$$

Cooling capacity:

$$q_{cool} = m_8(h_9 - h_8)$$

Turbine work output and pump work input:

$$w_t = m_7(h_7 - h_8)$$

$$w_p = m_1(h_2 - h_1)$$

$$w_{net} = w_t - w_p$$

The thermal efficiency is:

$$\eta = \frac{w_{net} + q_{cool}}{q_{superherter} + q_{boiler}}$$

6.4 Results and Discussion

1. Effect of turbine inlet pressure

With boiler temperature at 400 K and condenser temperature at 360 K, figure 6-1 shows thermal efficiency changes with turbine inlet pressure and ammonia mass fraction. The turbine exit pressure is maintained at 2 bar.

Figure 6-2 shows that vapor production goes linearly down as the turbine inlet pressure increases. Figure 6-3 shows that turbine power output goes almost linearly down as the pressure increases, this figure matches figure 6-2. It is known that the enthalpy drop across the turbine is increased as the pressure ratio increases. But the enthalpy gains from high pressure ratio do not make up the vapor flow rate drops, so the turbine work output decreases. Cooling capacity increases first as the pressure goes up. Then due to the low vapor flow rate, the cooling capacity goes down at a pressure of about 28

bar. Figure 6-4 shows this trend. The maximum point of cooling capacity changes with the basic solution ammonia mass fraction. It occurs at a higher turbine inlet pressure for a higher ammonia mass fraction.

Although turbine work output decreases as the pressure increases, the thermal efficiency goes up first to a maximum and then decreases. This result is shown in figure 6-1. This figure is similar to figure 6-4 showing the cycle cooling capacity, however the maximum point of thermal efficiency does not coincide with the maximum cycle cooling capacity. The maximum thermal efficiency increases as the ammonia mass fraction increases. There is a limit to the increase in ammonia composition at a given absorber pressure and temperature. In a later section, the limitation of the absorber condition on the cycle performance will be discussed.

2. Effect of boiler temperature

The effect of boiler temperature is shown in figures 6-5 to 6-8 at a turbine pressure ratio of 12.5, a condenser temperature of 360 K and a superheater temperature of 410 K. Since the turbine pressure ratio and inlet temperature are fixed, the enthalpy drop will remain the same regardless of the boiler temperature. What is affected by the boiler temperature is the vapor flow rate. Figure 6-6 shows that the vapor flow rate goes up almost linearly as boiler temperature goes up. It is easy to explain this result since the higher the boiler temperature, the more vapor will be generated. Consequently, turbine work output and cooling capacity follow the vapor flow rate changes. Curves of turbine

work output in figure 6-7 and cooling capacity in figure 6-8 show trends similar to the curves of vapor flow rate in figure 6-6.

The heat input increases rapidly as the boiler temperature increases. So the thermal efficiency will reach a limit even though the turbine power output and cooling capacity increase. To change this limit, the condenser temperature has to increase as the boiler temperature goes up so that more vapor will remain available to the turbine.

3. Effect of condenser temperature

The condenser temperature controls the vapor ammonia concentration. Low condenser temperature will condense more moisture from the vapor thereby increasing the ammonia concentration vapor and vice versa. The advantage of low condenser temperature is that the system will produce ammonia vapor with very small amount of moisture so that the vapor can be allowed to drop to low temperature in turbine. The disadvantage is that the vapor flow rate will also drop.

Figure 6-9 shows that the cooling capacity drops as the condenser temperature increases. There is no cooling available when the condenser temperature is greater than 390 K. Figures 6-10 and 6-11 show that the vapor flow rate and turbine work output increase as the condenser temperature goes up. Figure 6-12 shows the change in thermal efficiency with the condenser temperature, which is due to the combined effect of the results shown in figures 6-9 to 6-11. In figure 6-12, the thermal efficiency drops first as the condenser temperature increases, but the efficiency increases when condenser temperature is greater than 390 K where no cooling capacity is available. When the

condenser temperature is less than 390 K the cooling capacity drops faster than the turbine work output increases, so the thermal efficiency decreases while the turbine work output increases. When condenser temperature is greater than 390 K no cooling capacity is available, the thermal efficiency increases as the turbine work output increases.

4. Effect of superheater temperature

Figure 6-13 shows that thermal efficiency drops first and then goes up as the superheat temperature increases. Vapor flow rate is not affected by the superheat temperature, as can be seen from figure 6-14. From figure 6-15, it is expected that turbine work output would increase with higher superheat temperature. The cooling capacity drops as the superheat temperature increases as shown in figure 6-16. There is no cooling capacity available when the superheat temperature is greater than 470 K. The reason is that the turbine inlet vapor entropy is higher at a higher inlet temperature, with the same pressure ratio, therefore the turbine exit temperature is higher also.

In a conventional Rankine cycle, the thermal efficiency increases as the superheat temperature increases since most of the superheat is converted to work output. In the novel cycle, cooling capacity is a factor in thermal efficiency. With an increase in superheat temperature, the cooling capacity drops steeper than the increase in turbine work output. That is why the thermal efficiency drops steadily against the superheat temperature. However, the thermal efficiency increases when the superheat temperature is greater that 470 K where the cycle stops providing cooling capacity.

5. Effect of absorber temperature

The absorber in the proposed cycle acts as a condenser in a conventional Rankine cycle. The absorber temperature is decided by the cooling media. The lower the absorber temperature, the higher the thermal efficiency will be. In the proposed cycle with the same ammonia concentration, the turbine exit pressure has to be increased as the absorber temperature increases in order to condense the solution.

Figures 6-17 to 6-20 show the effect of absorber temperature for an ammonia mass fraction of 0.5. When the absorber temperature is 320 K, there is no cooling effect. At 300 K, no cooling effect is observed when the turbine inlet pressure is less than 25 bar.

6. Other considerations

From figure 6-17, the thermal efficiency drops substantially when the absorber temperature increases at 0.50 ammonia mass fraction. At a high absorber temperature, absorber pressure has to be maintained at a high level in order to condense the ammonia-water mixture, this requires a higher turbine exit pressure which brings the thermal efficiency down.

In order to operate at a low turbine exit pressure and consequently a low turbine exit temperature, the ammonia mass concentration of the basic solution must be low also. A lower ammonia concentration solution has a higher boiling temperature.

Figure 6-21 shows the effect of turbine inlet pressure on the thermal efficiency for ammonia concentrations of 0.20, 0.25, 0.30 and the corresponding turbine exit pressure that would allow condensation in the absorber. Basic solutions with 0.25 and 0.30 ammonia mass fraction are able to maintain 16%-18% thermal efficiency, while a basic

solution with 0.20 ammonia mass fraction performs poorly. Figures 6-22 and 6-23 show the vapor flow rate and turbine work output respectively at the conditions of figure 6-21.

Figure 6-21 may not reflect the best performance range for each ammonia mass fraction in the basic solution. In fact, the basic solution with lower ammonia mass fraction performs well in a lower pressure range. In figure 6-21, it can be told that which ammonia mass fraction in the basic solution is before, right at and after its best operation range. The order in this case is 0.3, 0.25 and 0.2 of ammonia mass fraction in the basic solution.

6.5 Conclusion

A combined power/cooling cycle using ammonia-water mixtures as a working fluid is proposed. The cycle is a combination of the Rankine and absorption refrigeration cycles. It will not only produce power but also provide certain amount of cooling.

Initial simulation results show that the power output is limited by cycle pressure and temperature. This cycle certainly has flexibility for various applications. We can have a multi-stage turbine system for high pressure and temperature applications. For multi-stage expansion system, we can discard condenser and let the ammonia-water mixture go through the expansion directly. Because of high pressure and temperature, ammonia-water mixture will still be in a vapor state after the first stage turbine or we can condense some of the moisture at each stage. That will allow us to expand the working fluid to very low temperature while maintaining condensation at less than 10% level in each turbine stage.

$T_{absorber} = 280$ K, $T_{superheat} = 410$ K, $T_{boiler} = 400$ K
$T_{condenser} = 360$ K, $p_{low} = 2$ bar

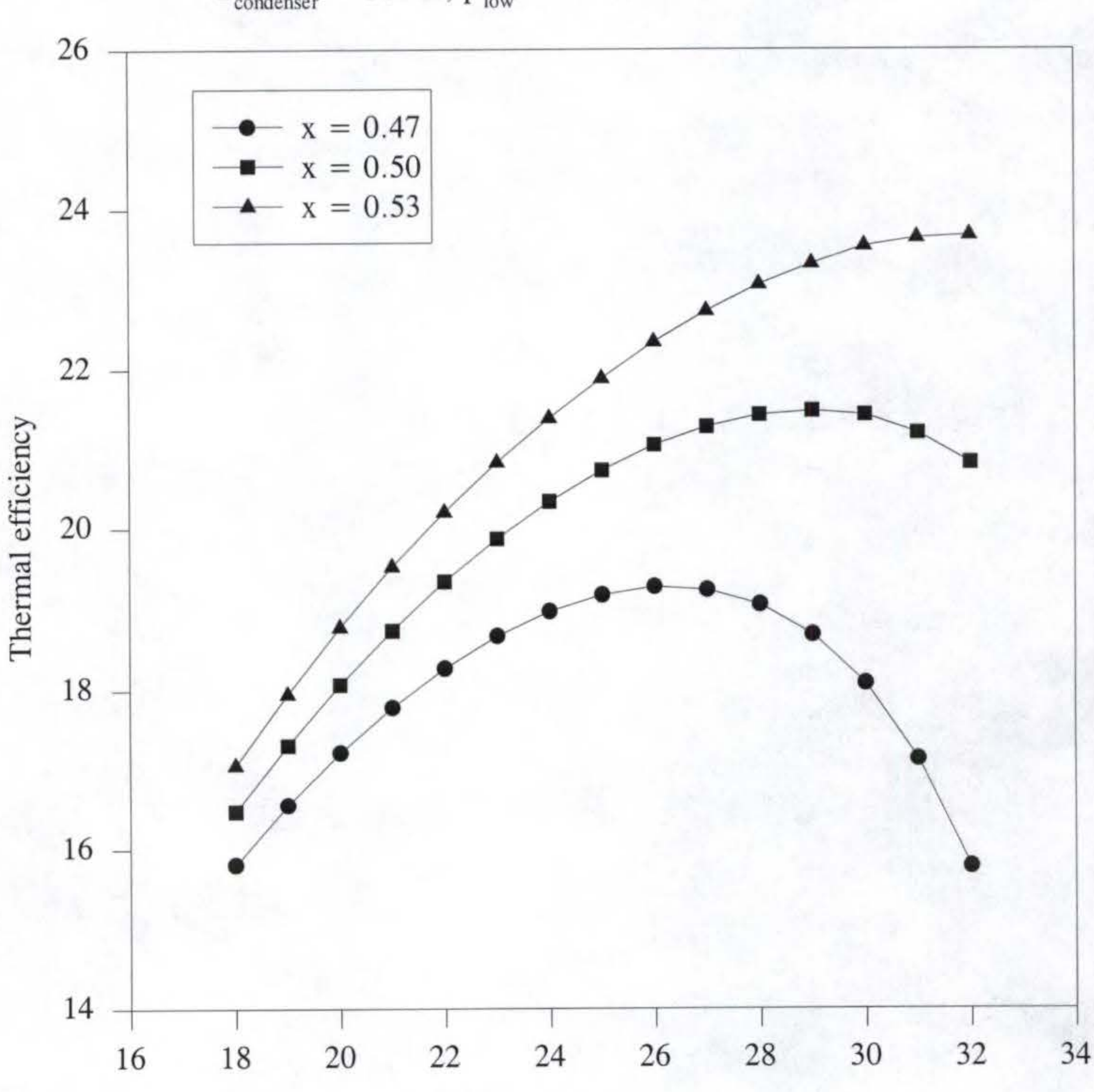

Figure 6-1 Effect of turbine inlet pressure on thermal efficiency

$T_{absorber} = 280$ K, $T_{superheat} = 410$ K, $T_{boiler} = 400$ K
$T_{condenser} = 360$ K, $p_{low} = 2$ bar

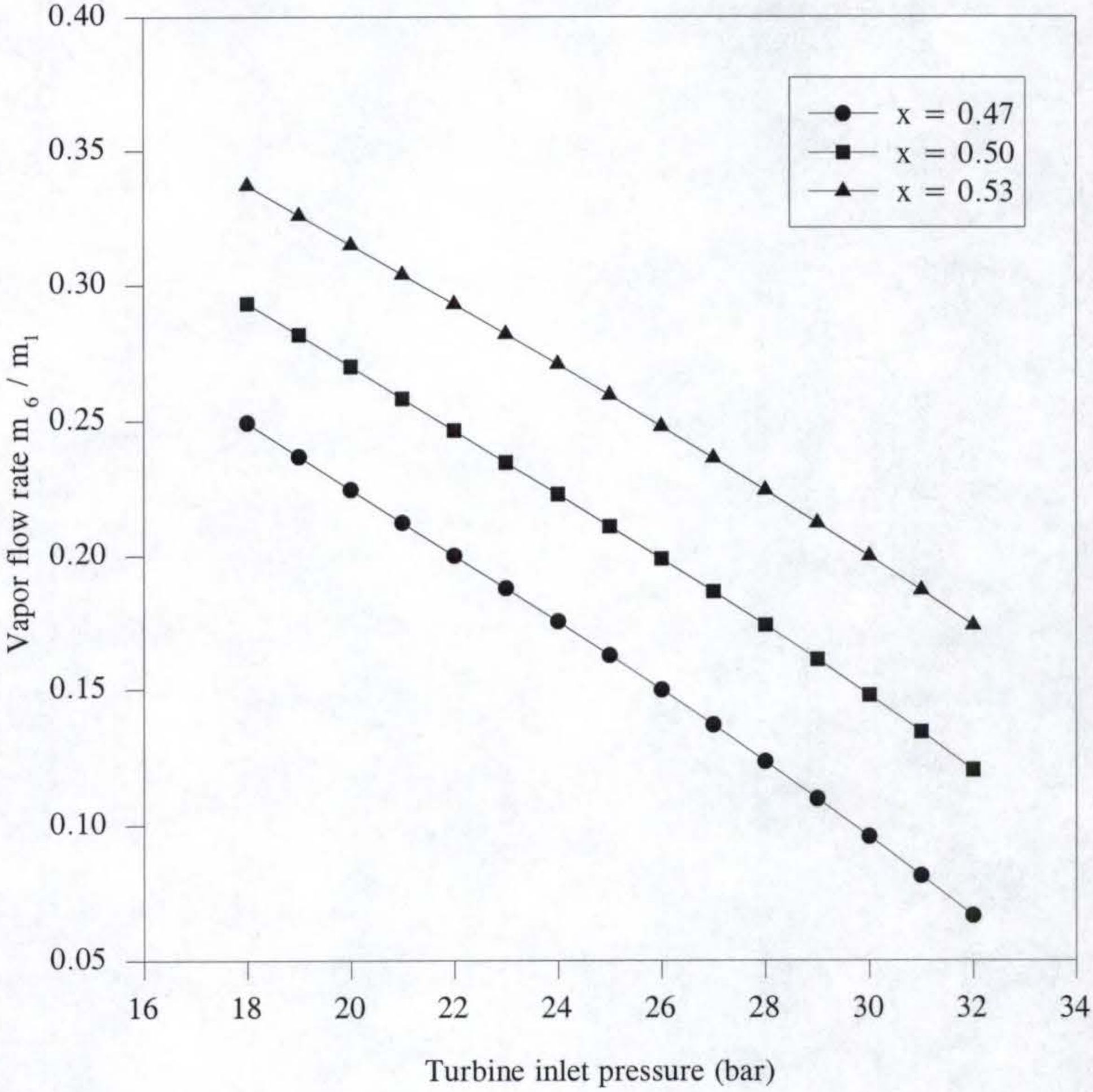

Figure 6-2 Effect of turbine inlet pressure on vapor flow rate

$T_{absorber} = 280$ K, $T_{superheat} = 410$ K, $T_{boiler} = 400$ K
$T_{condenser} = 360$ K, $p_{low} = 2$ bar

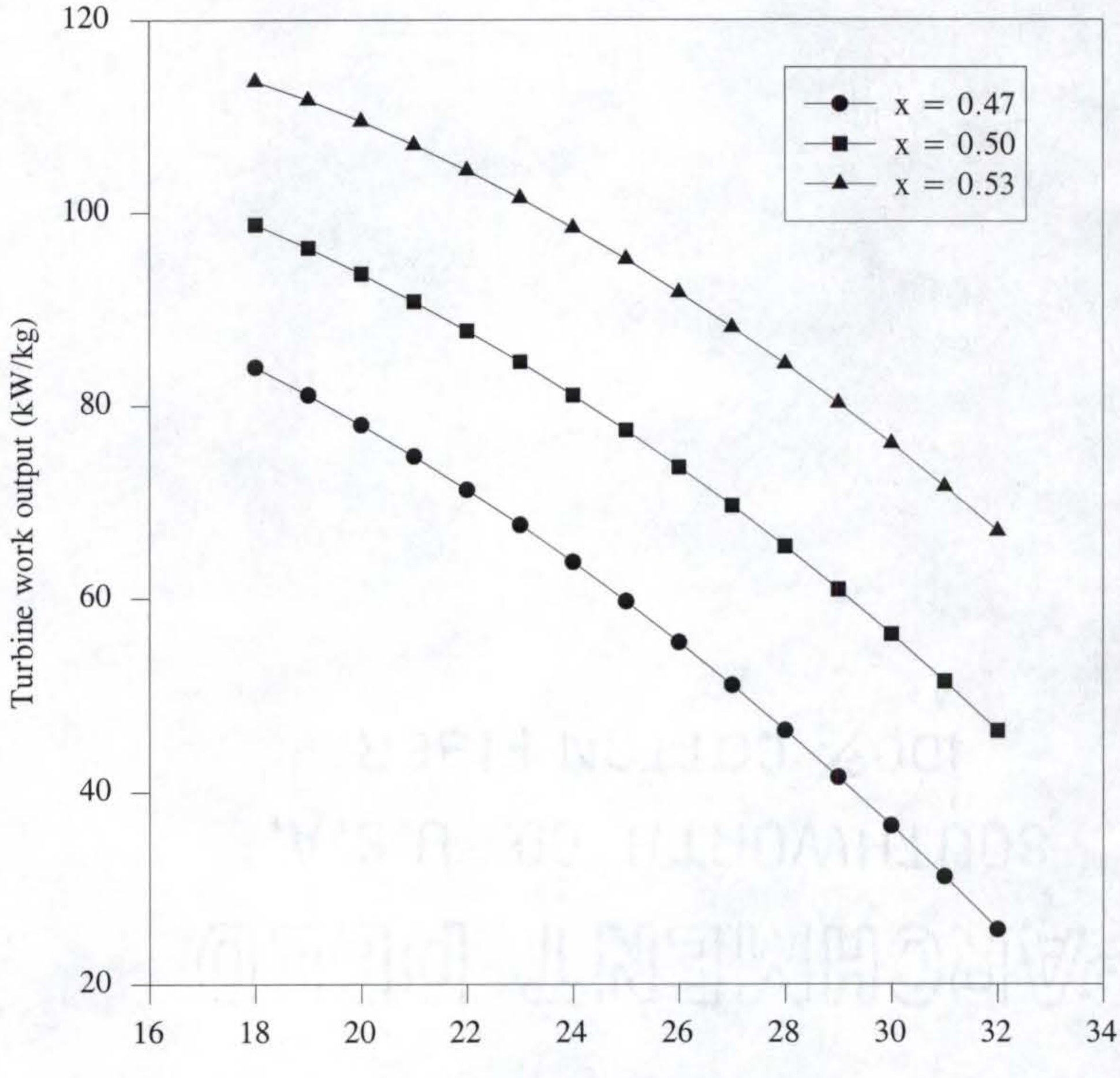

Figure 6-3 Effect of turbine inlet pressure on turbine work output

$T_{absorber} = 280$ K, $T_{superheat} = 410$ K, $T_{boiler} = 400$ K
$T_{condenser} = 360$ K, $p_{low} = 2$ bar

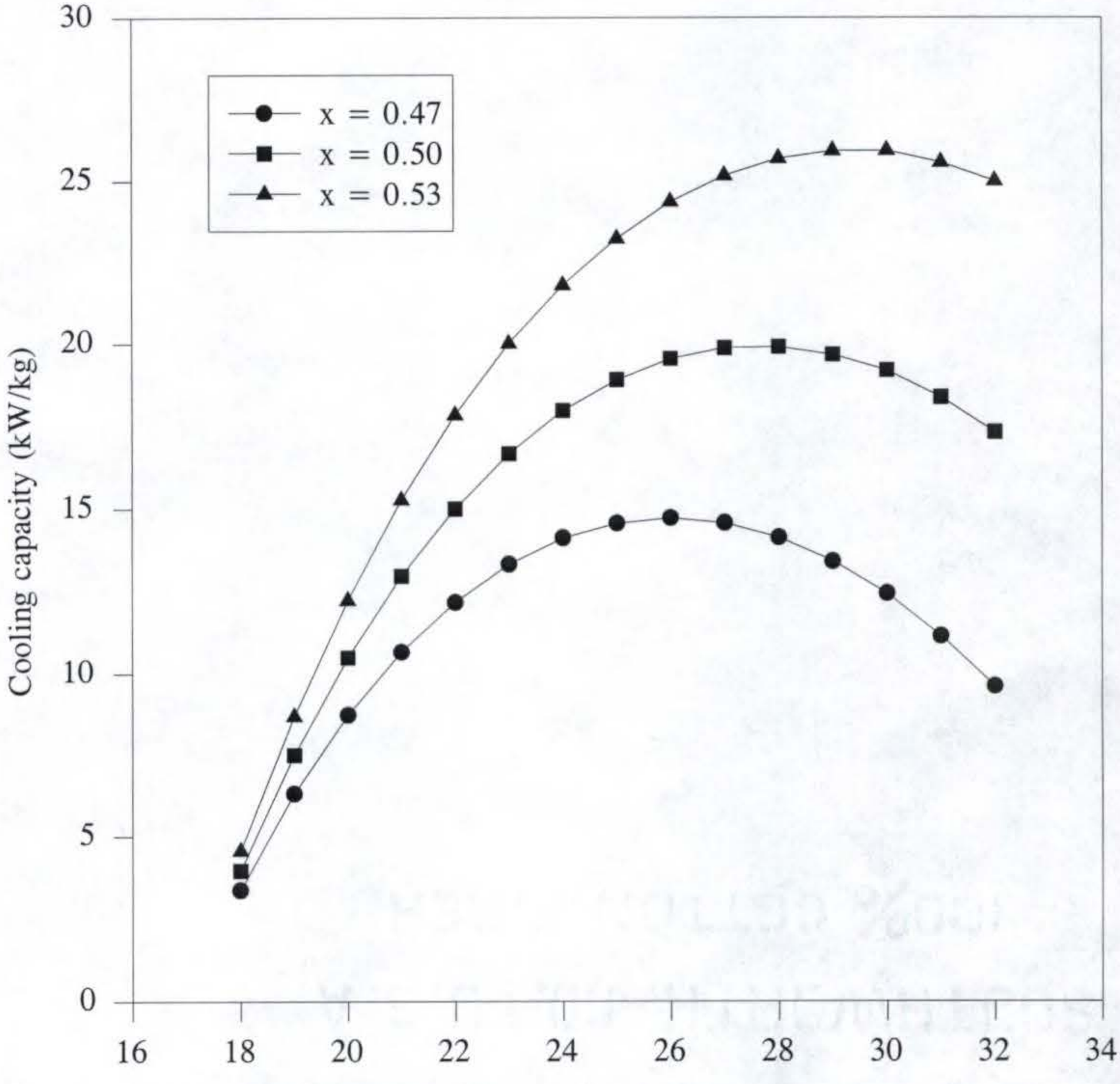

Figure 6-4 Effect of turbine inlet pressure on cooling capacity

$T_{absorber} = 280$ K, $T_{superheat} = 410$ K, $T_{condenser} = 360$ K
$p_{high} = 25$ bar, $p_{low} = 2$ bar

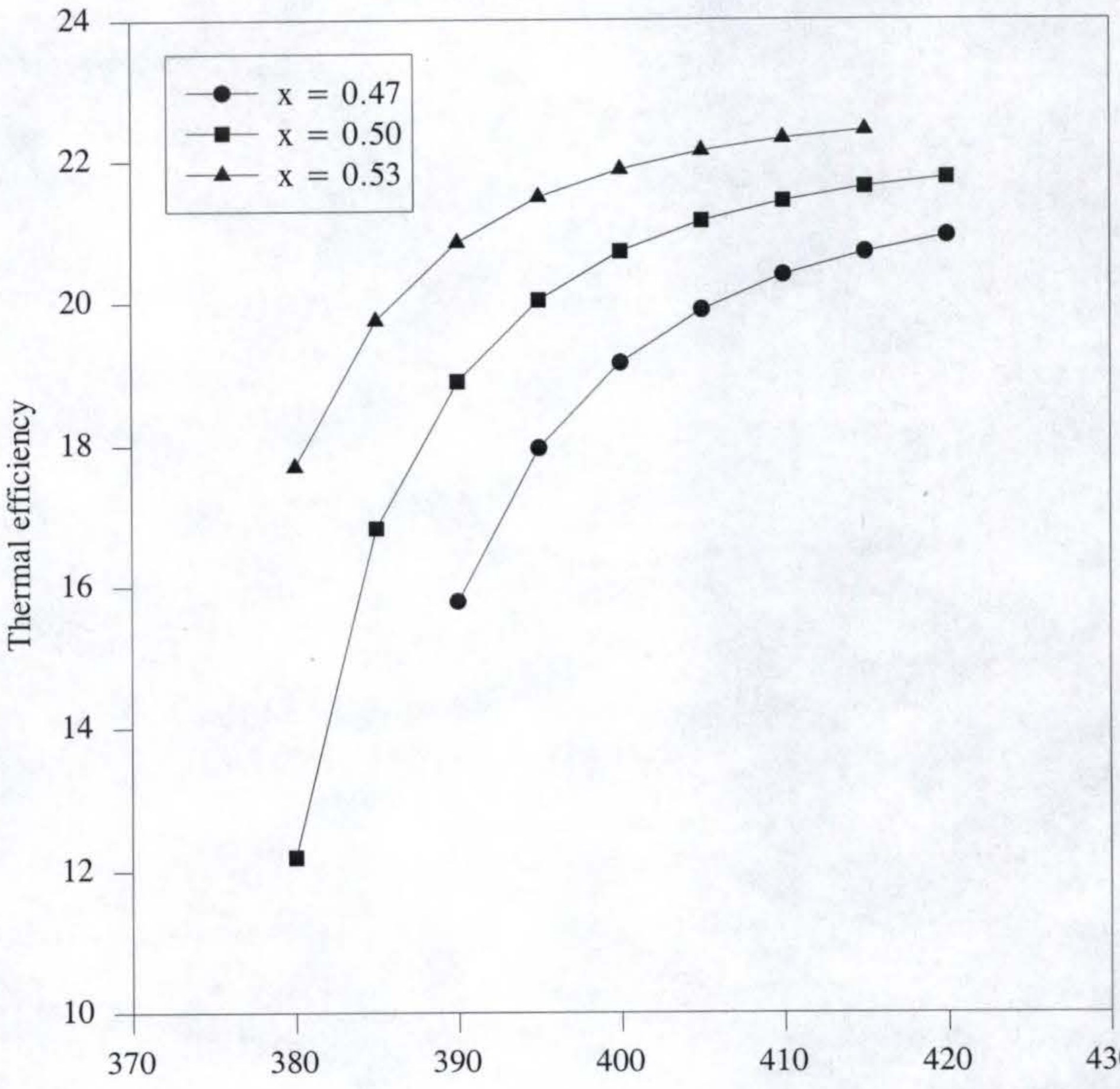

Figure 6-5 Effect of boiler temperature on thermal efficiency

$T_{absorber} = 280$ K, $T_{superheat} = 410$ K, $T_{condenser} = 360$ K

$p_{high} = 25$ bar, $p_{low} = 2$ bar

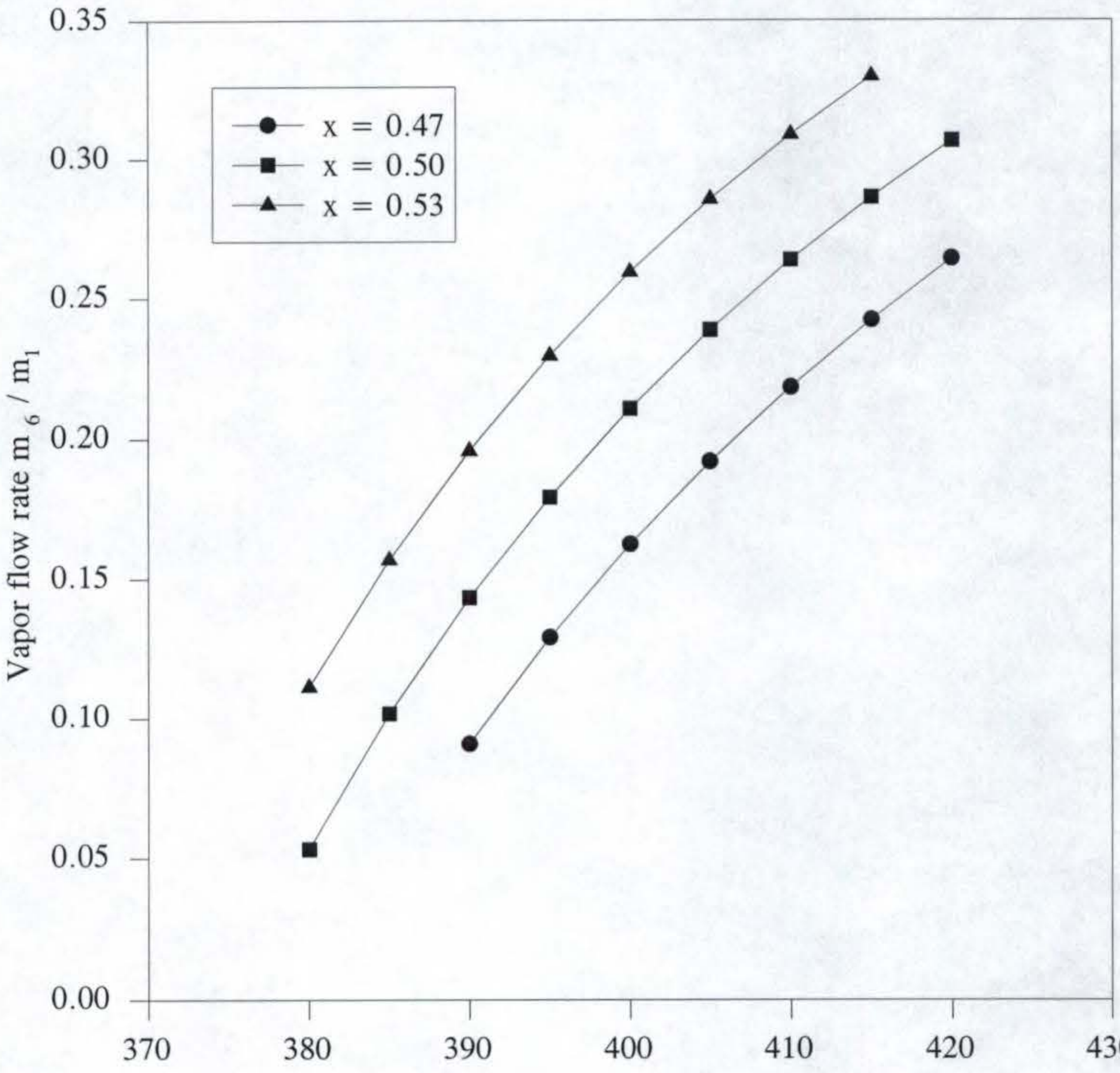

Figure 6-6 Effect of boiler temperature on vapor flow rate

$T_{absorber} = 280$ K, $T_{superheat} = 410$ K, $T_{condenser} = 360$ K
$p_{high} = 25$ bar, $p_{low} = 2$ bar

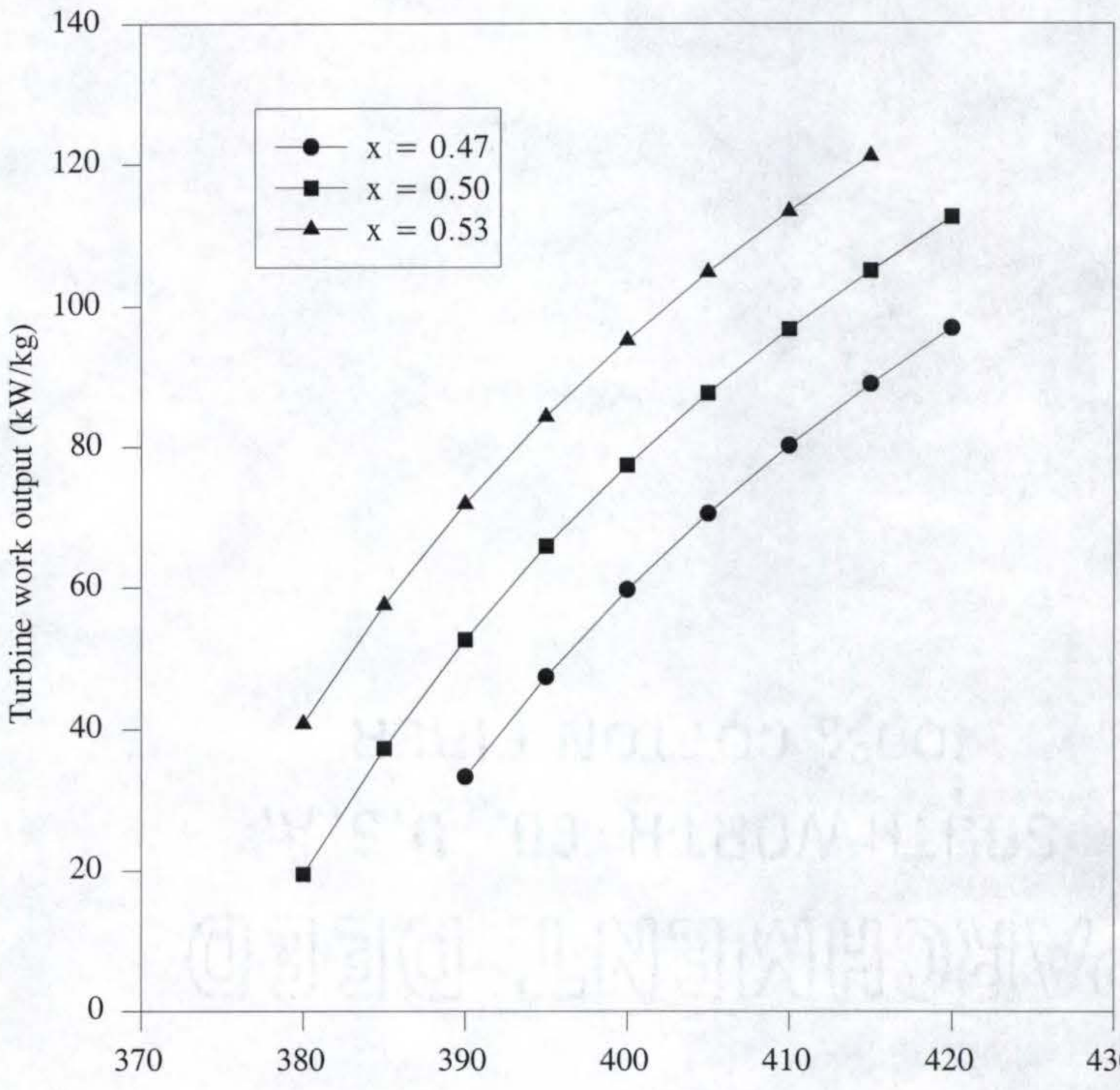

Figure 6-7 Effect of boiler temperature on turbine work output

$T_{absorber} = 280$ K, $T_{superheat} = 410$ K, $T_{condenser} = 360$ K
$p_{high} = 25$ bar, $p_{low} = 2$ bar

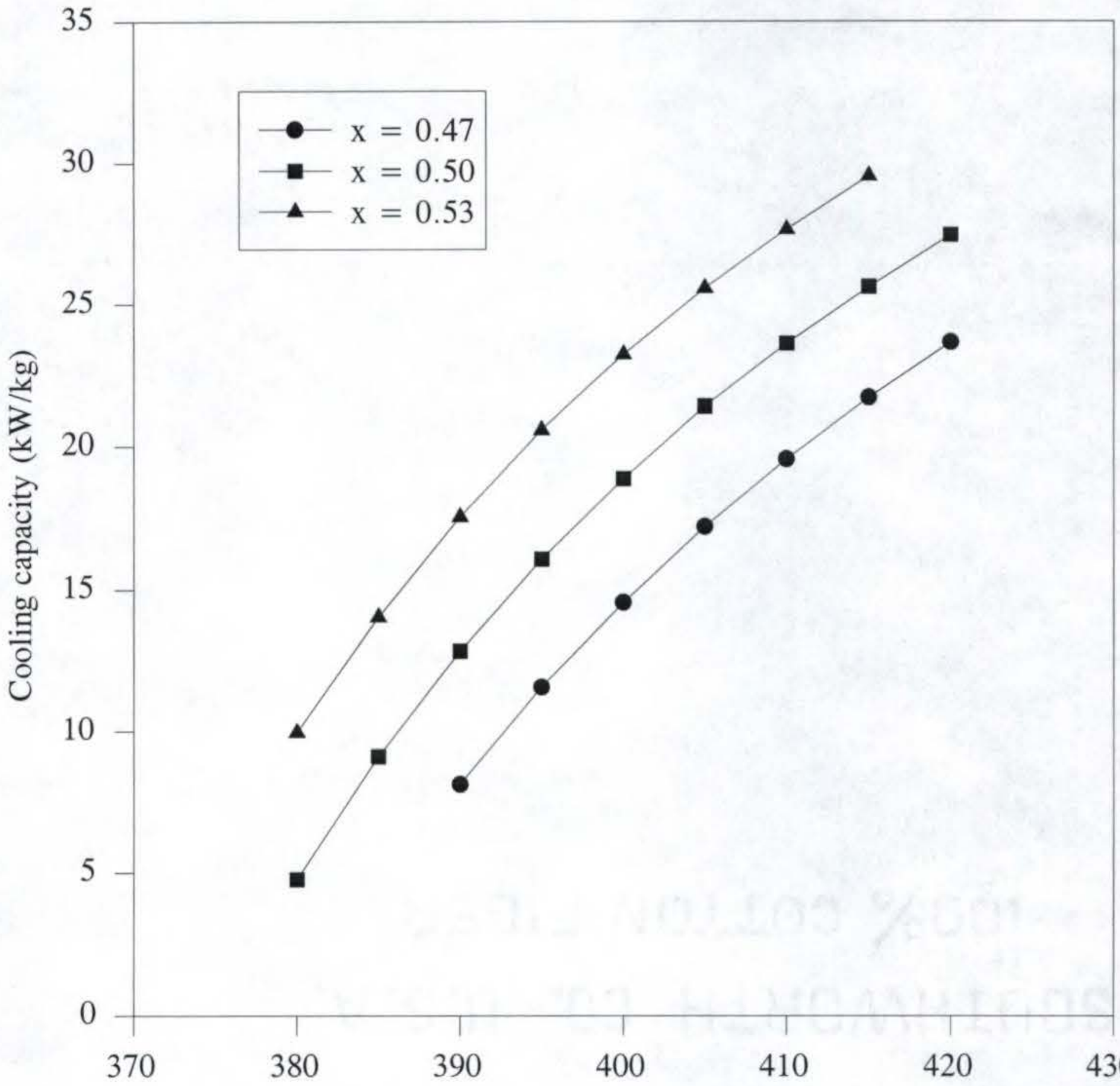

Figure 6-8 Effect of boiler temperature on cooling capacity

$T_{absorber}$ = 280 K, $T_{superheat}$ = 410 K, T_{boiler} = 400 K
p_{high} = 25 bar, p_{low} = 2 bar

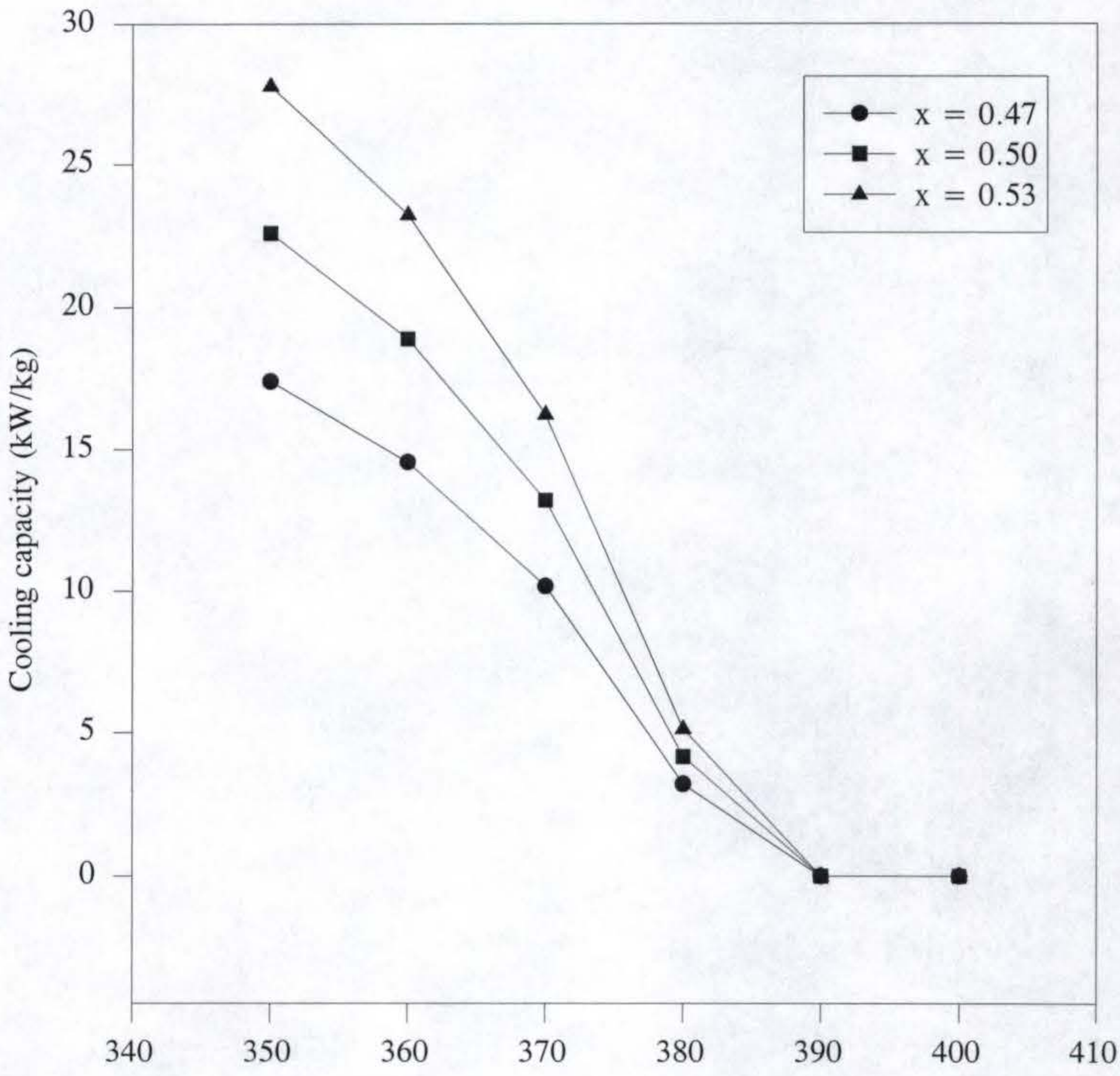

Figure 6-9 Effect of condenser temperature on cooling capacity

$T_{absorber}$ = 280 K, $T_{superheat}$ = 410 K, T_{boiler} = 400 K
p_{high} = 25 bar, p_{low} = 2 bar

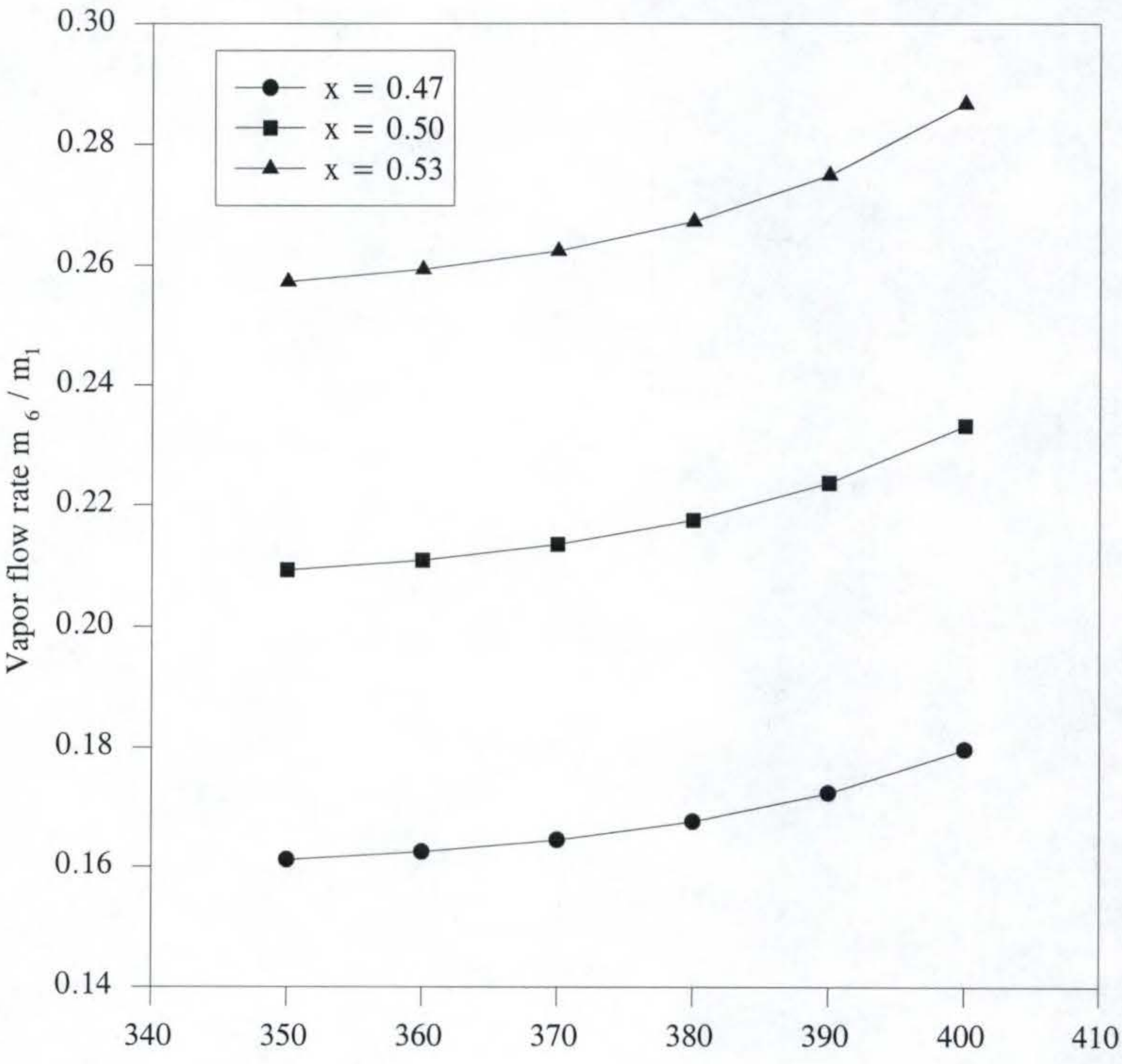

Figure 6-10 Effect of condenser temperature on vapor flow rate

$T_{absorber} = 280$ K, $T_{superheat} = 410$ K, $T_{boiler} = 400$ K
$p_{high} = 25$ bar, $p_{low} = 2$ bar

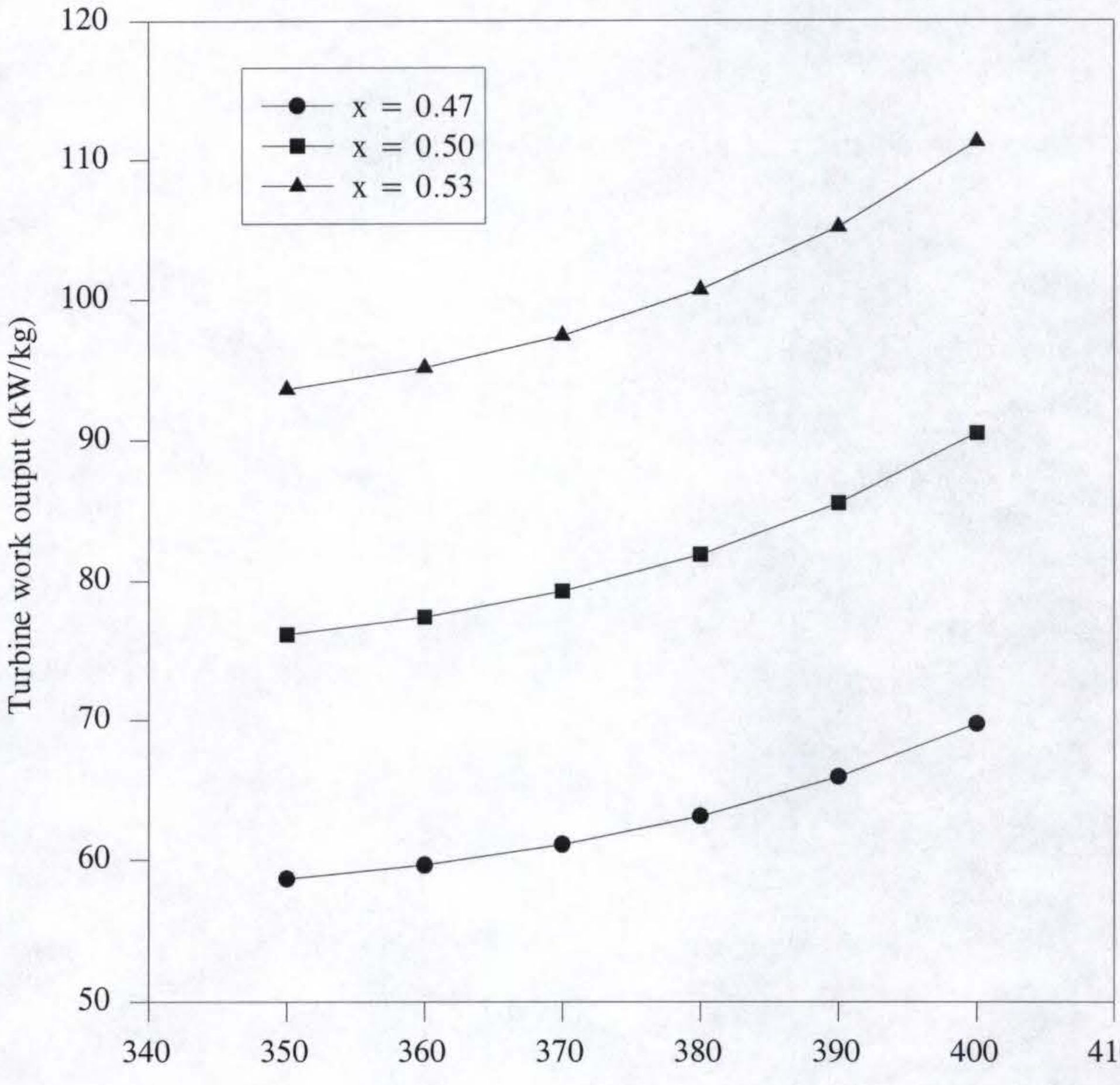

Figure 6-11 Effect of condenser temperature on turbine work output

$T_{absorber}$ = 280 K, $T_{superheat}$ = 410 K, T_{boiler} = 400 K
p_{high} = 25 bar, p_{low} = 2 bar

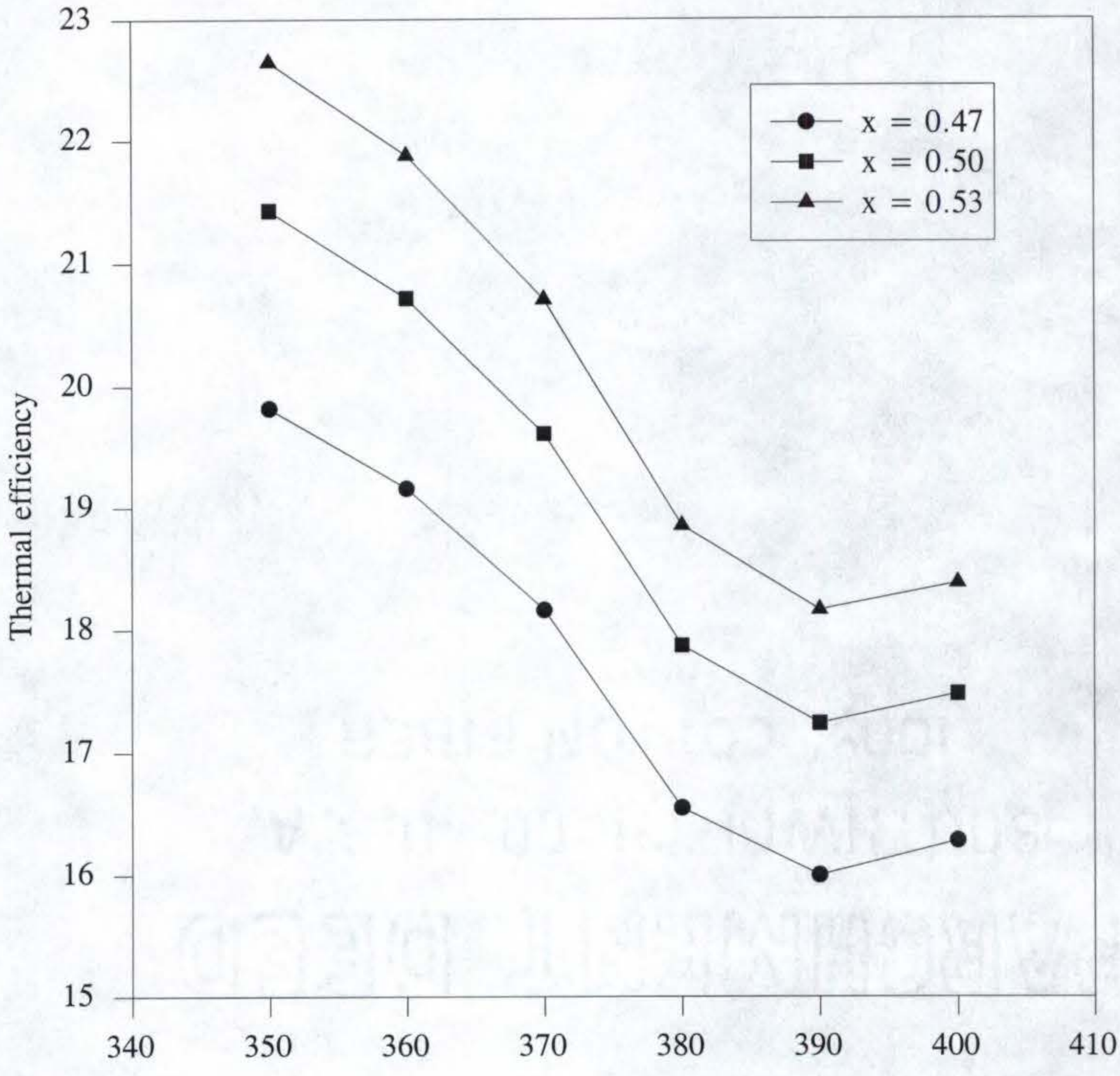

Figure 6-12 Effect of condenser temperature on thermal efficiency

$T_{absorber} = 280$ K, $T_{boiler} = 400$ K, $T_{condenser} = 360$ K
$P_{high} = 25$ bar, $P_{low} = 2$ bar

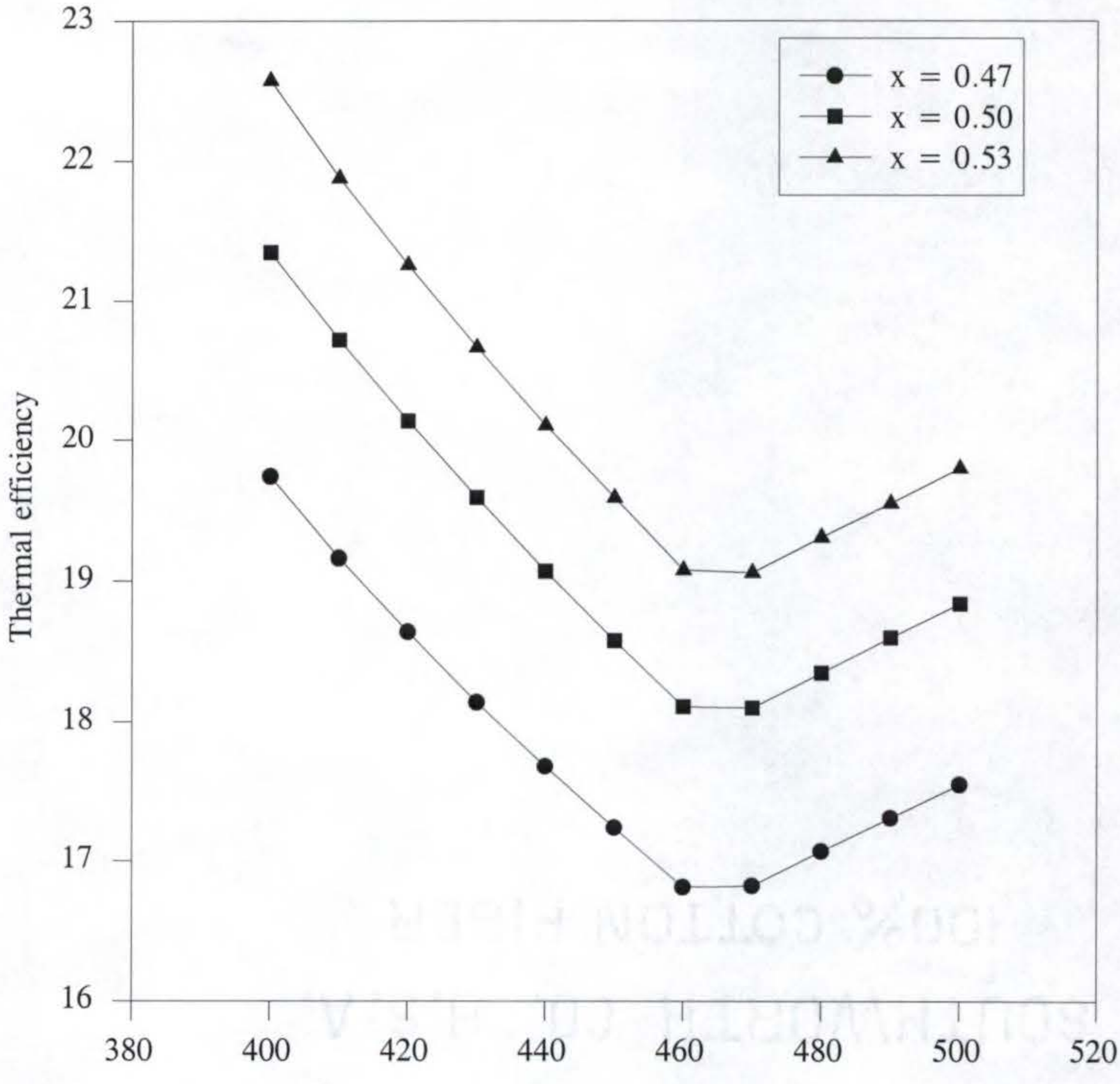

Figure 6-13 Effect of superheat temperature on thermal efficiency

$T_{absorber} = 280$ K, $T_{boiler} = 400$ K, $T_{condenser} = 360$ K
$P_{high} = 25$ bar, $P_{low} = 2$ bar

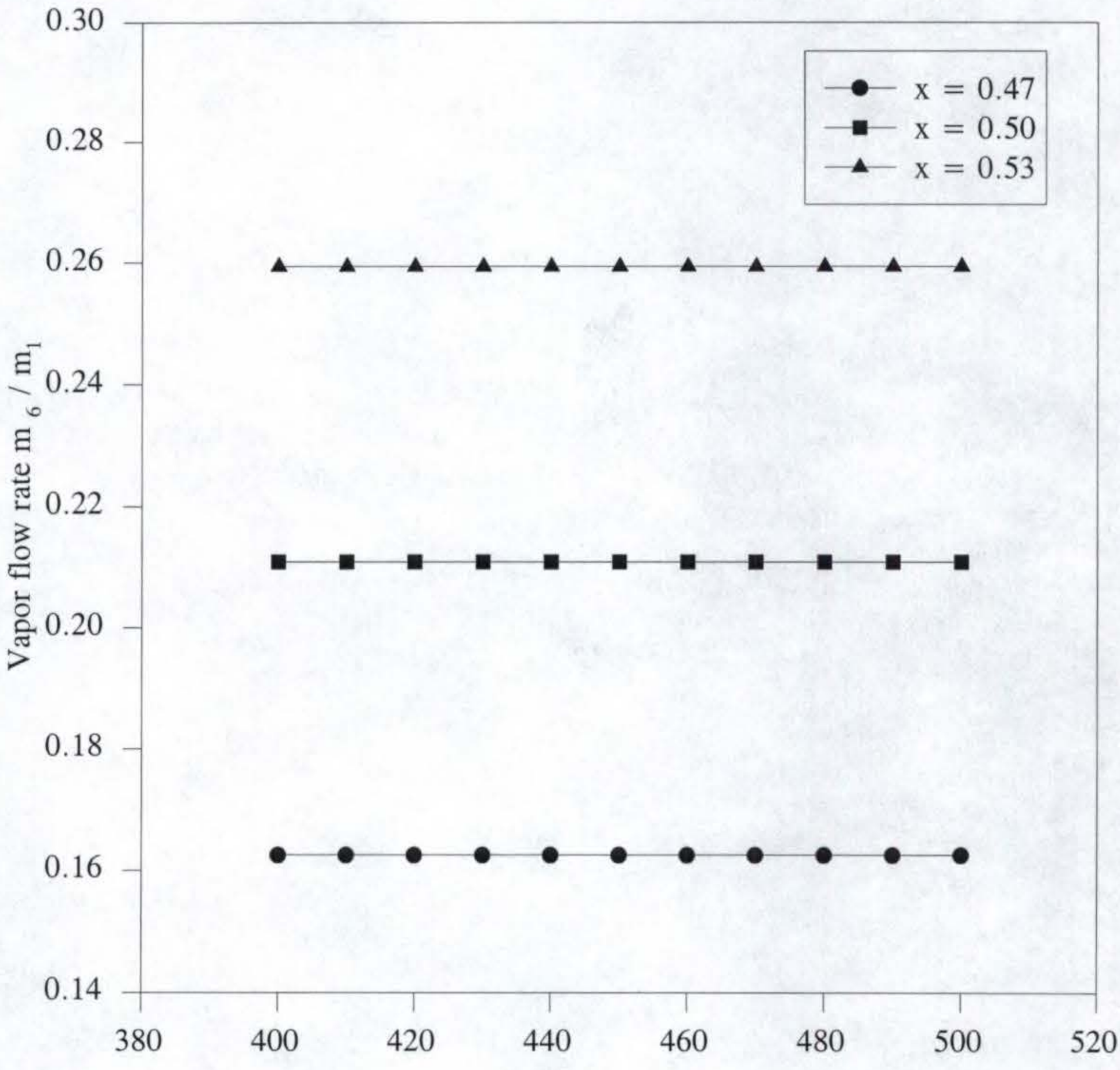

Figure 6-14 Effect of superheat temperature on vapor flow rate

$T_{absorber} = 280$ K, $T_{boiler} = 400$ K, $T_{condenser} = 360$ K
$P_{high} = 25$ bar, $P_{low} = 2$ bar

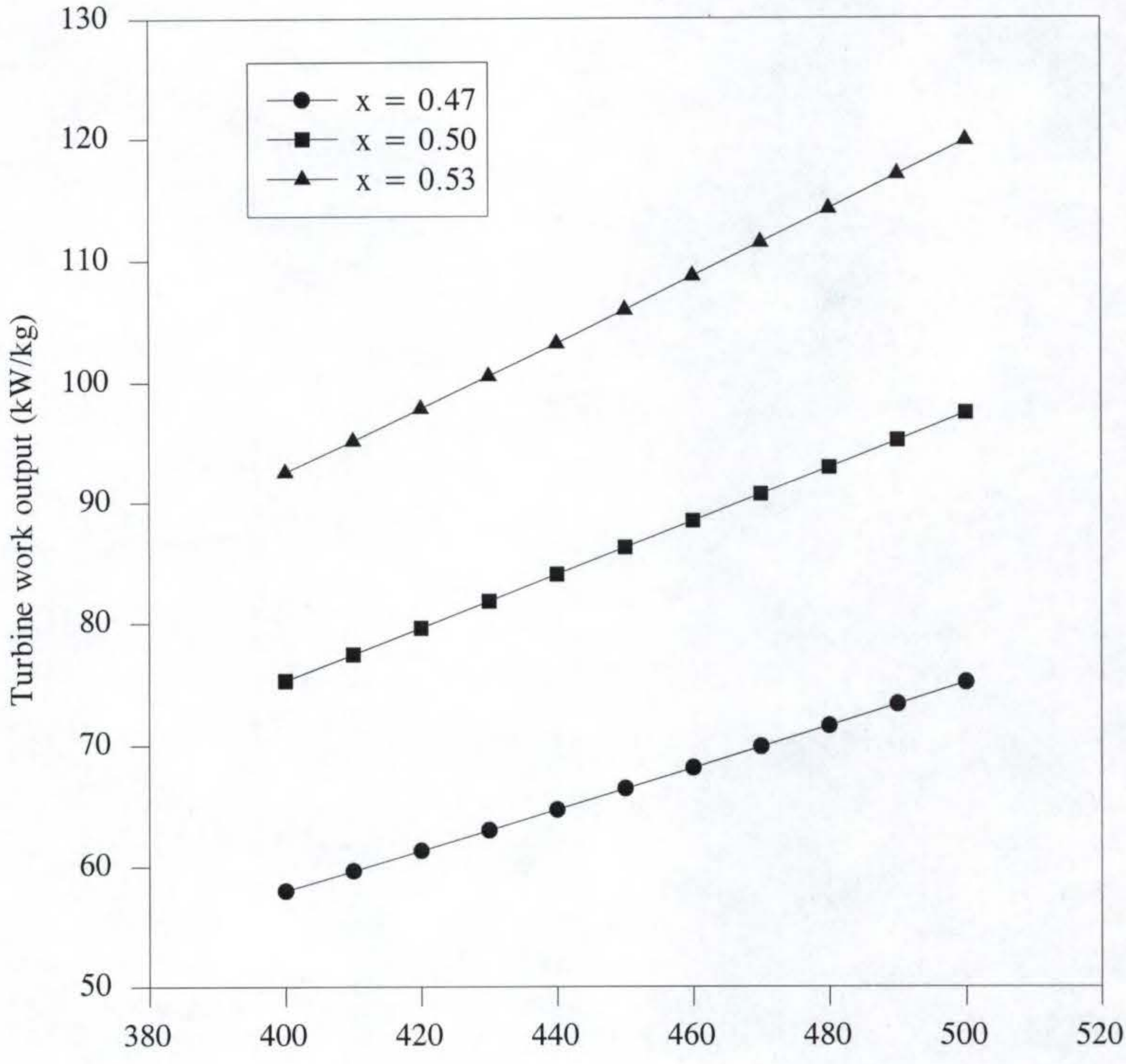

Figure 6-15 Effect of superheat temperature on turbine work output

$T_{absorber} = 280$ K, $T_{boiler} = 400$ K, $T_{condenser} = 360$ K
$P_{high} = 25$ bar, $P_{low} = 2$ bar

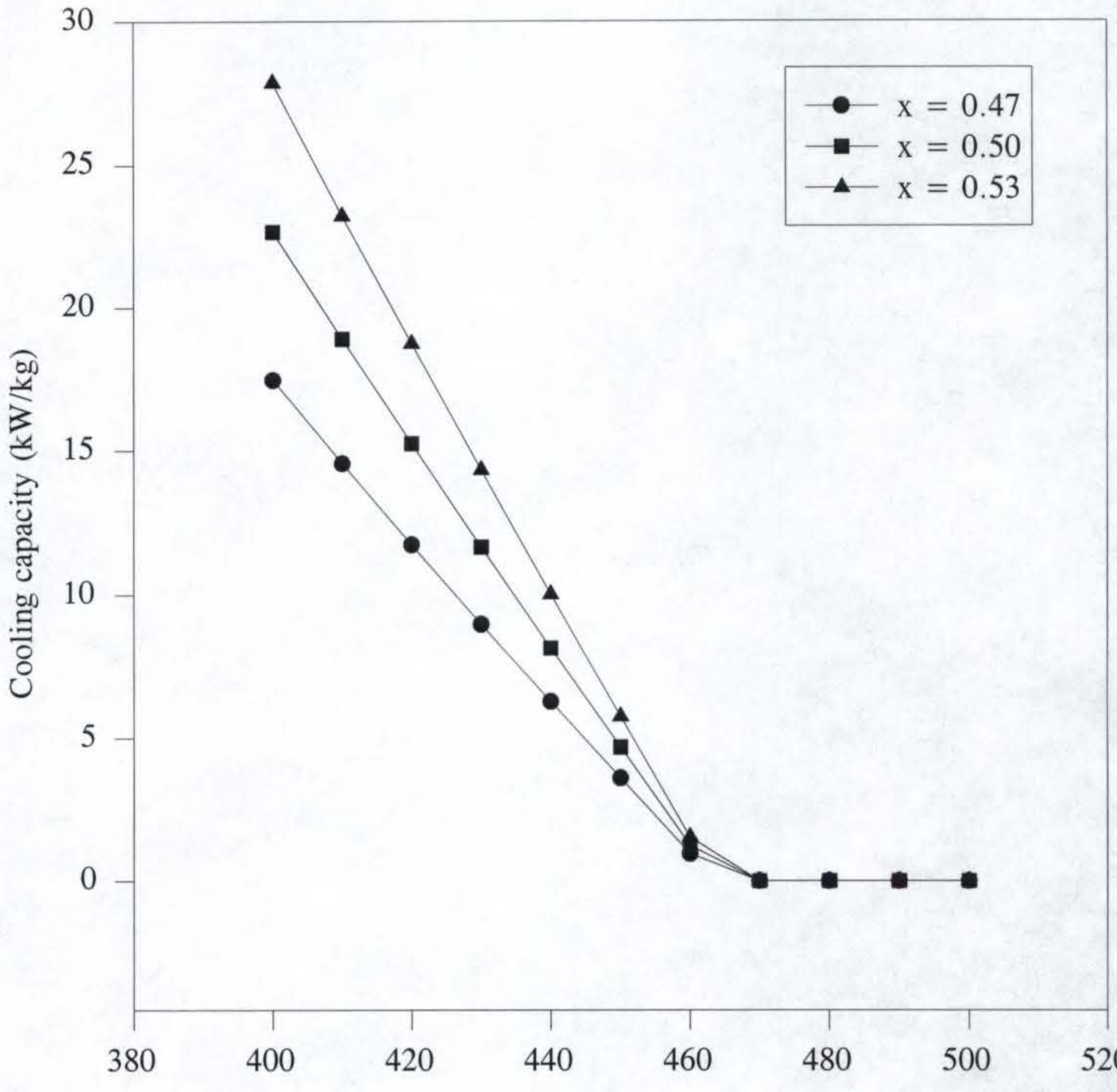

Figure 6-16 Effect of superheat temperature on cooling capacity

$T_{superheat}$ = 410 K, T_{boiler} = 400 K, $T_{condenser}$ = 360 K
p_{low} = 2 bar, x = 0.50

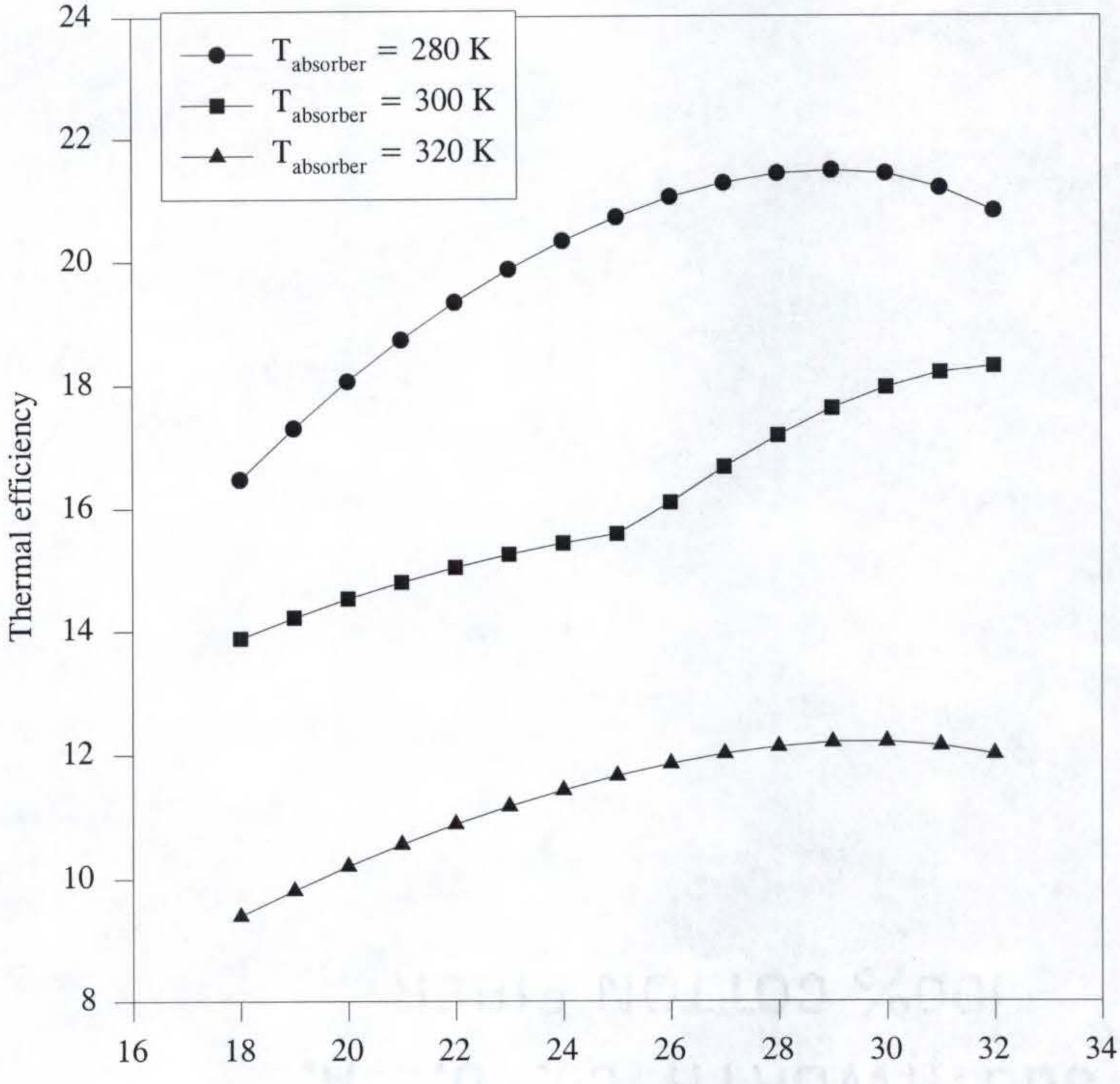

Figure 6-17 Effect of absorber temperature on thermal efficiency

$T_{superheat}$ = 410 K, T_{boiler} = 400 K, $T_{condenser}$ = 360 K
p_{low} = 2 bar, x = 0.50

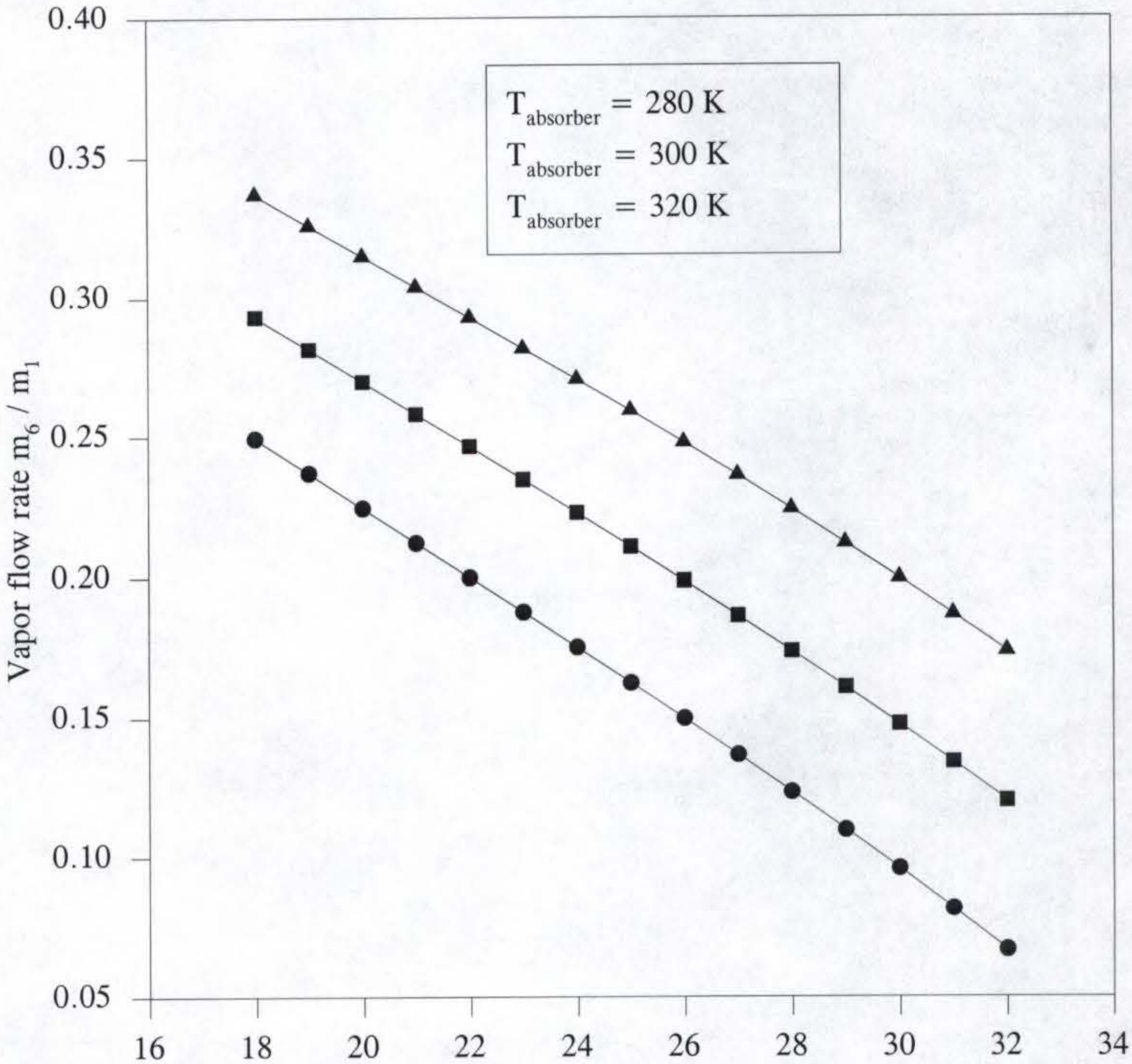

Figure 6-18 Effect of absorber temperature on vapor flow rate

$T_{superheat}$ = 410 K, T_{boiler} = 400 K, $T_{condenser}$ = 360 K
p_{low} = 2 bar, x = 0.50

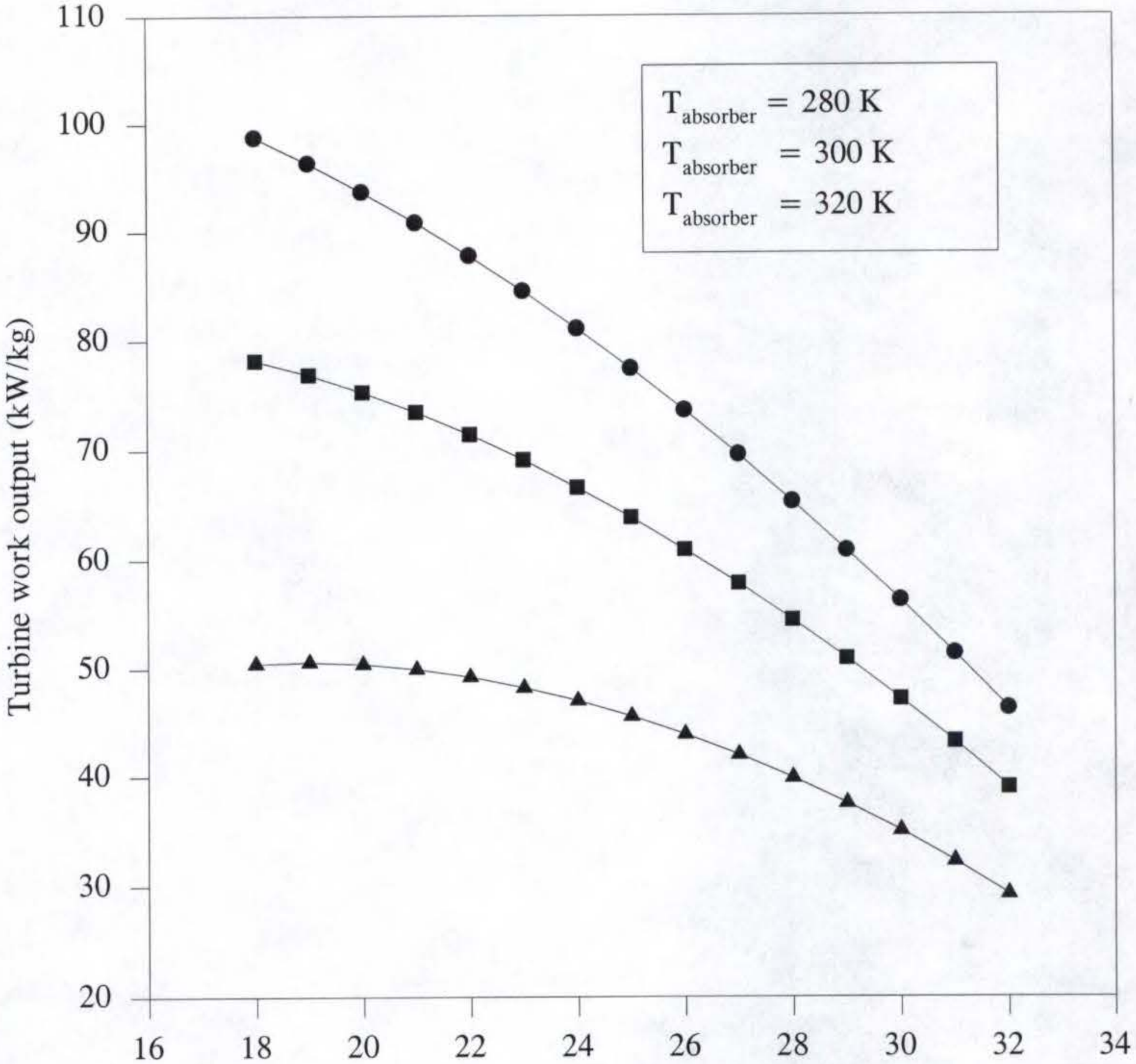

Figure 6-19 Effect of absorber temperature on turbine work output

$T_{superheat} = 410$ K, $T_{boiler} = 400$ K, $T_{condenser} = 360$ K
$p_{low} = 2$ bar, $x = 0.50$

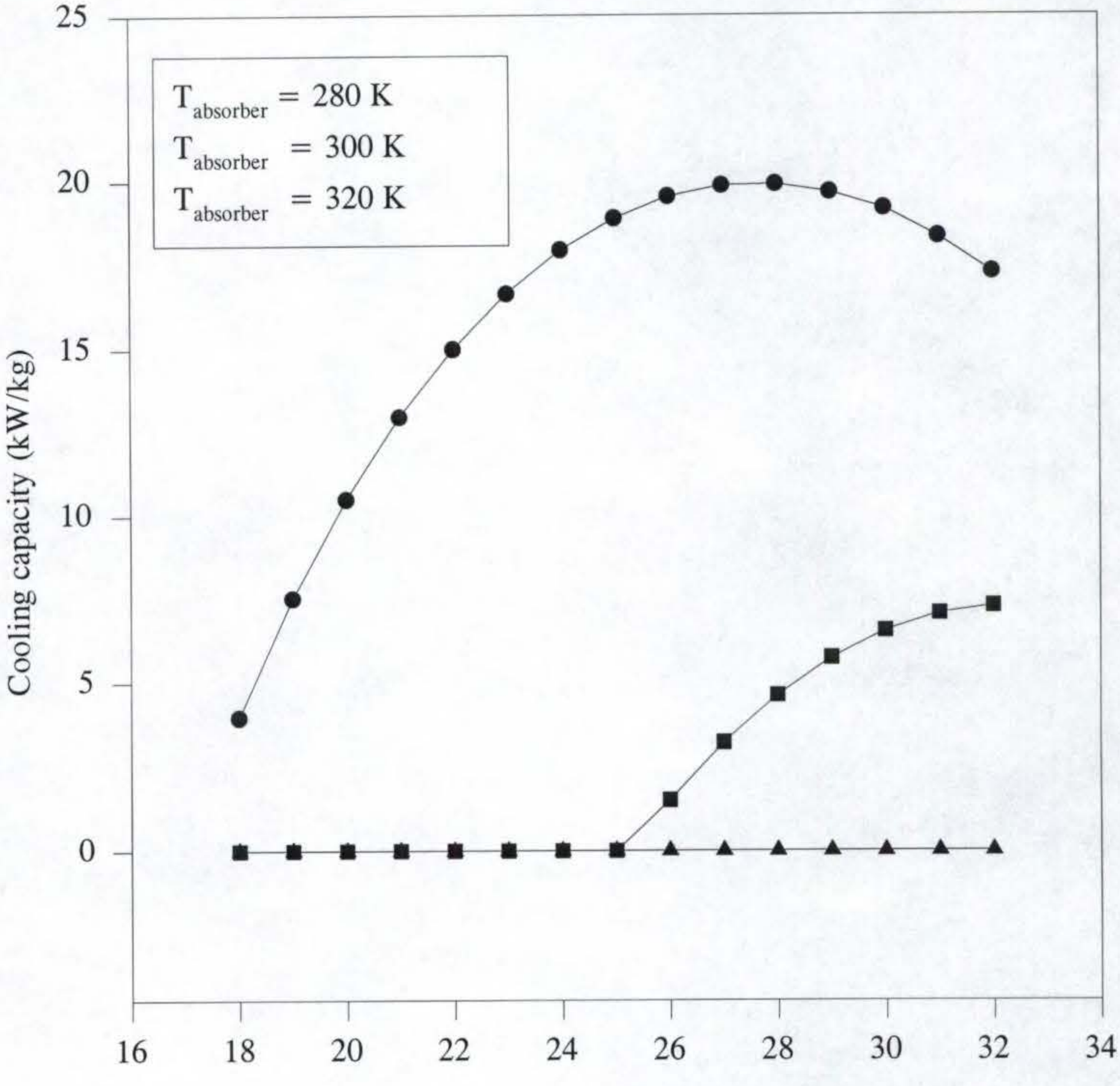

Figure 6-20 Effect of absorber temperature on cooling capacity

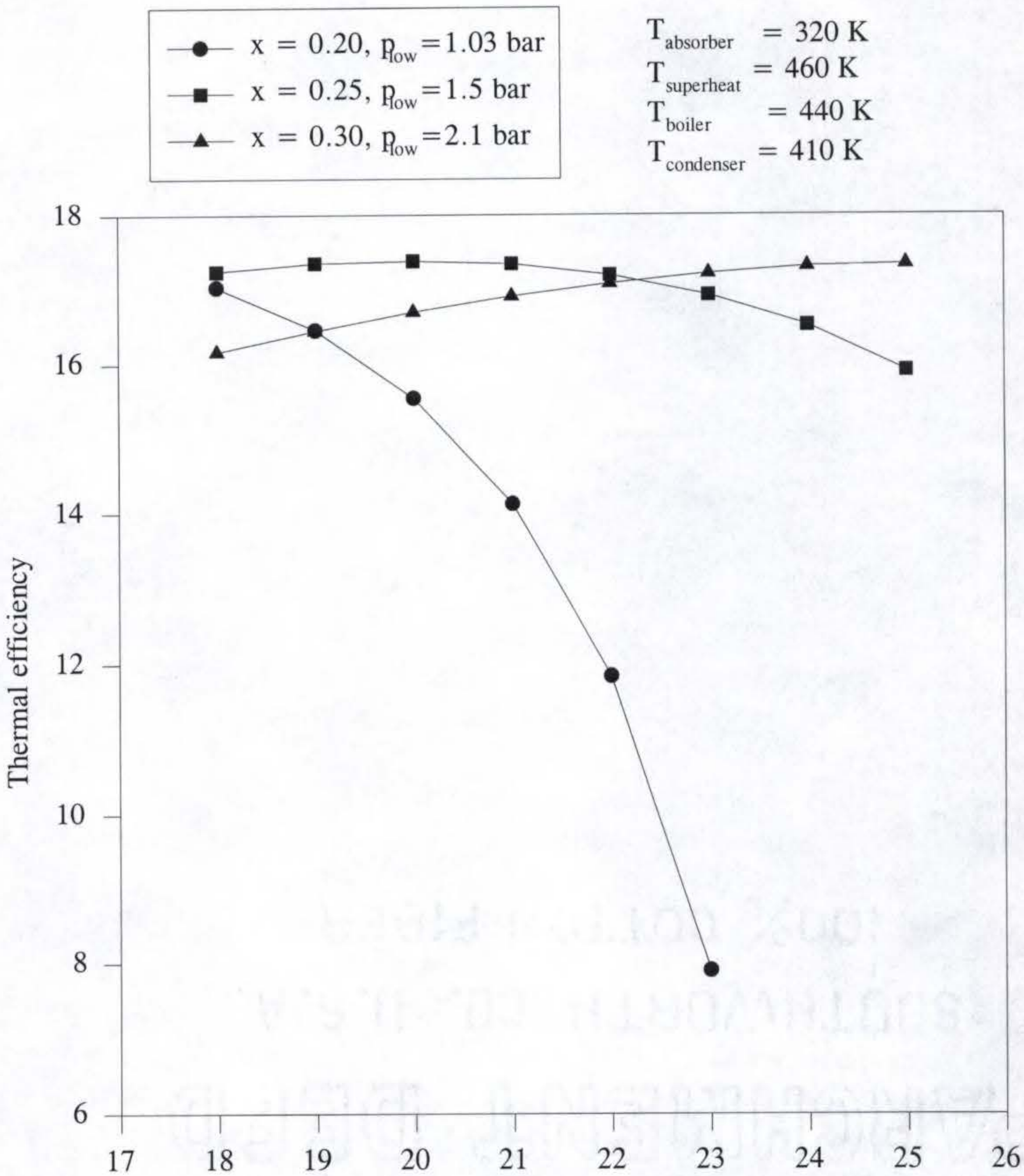

Figure 6-21 Effect of turbine inlet pressure on thermal efficiency for different turbine exit pressure

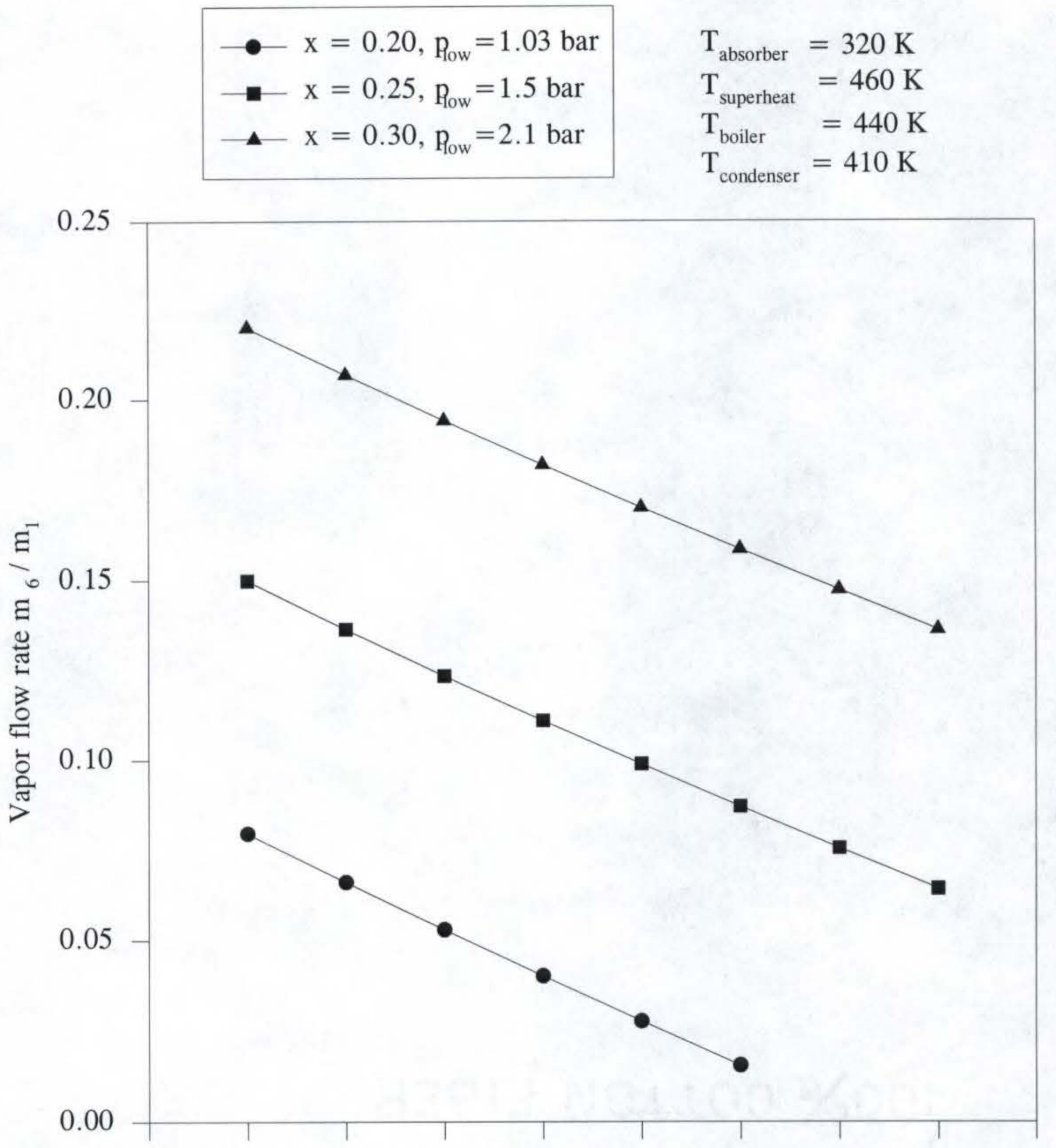

Figure 6-22 Effect of turbine inlet pressure on vapor flow rate for different turbine exit pressure

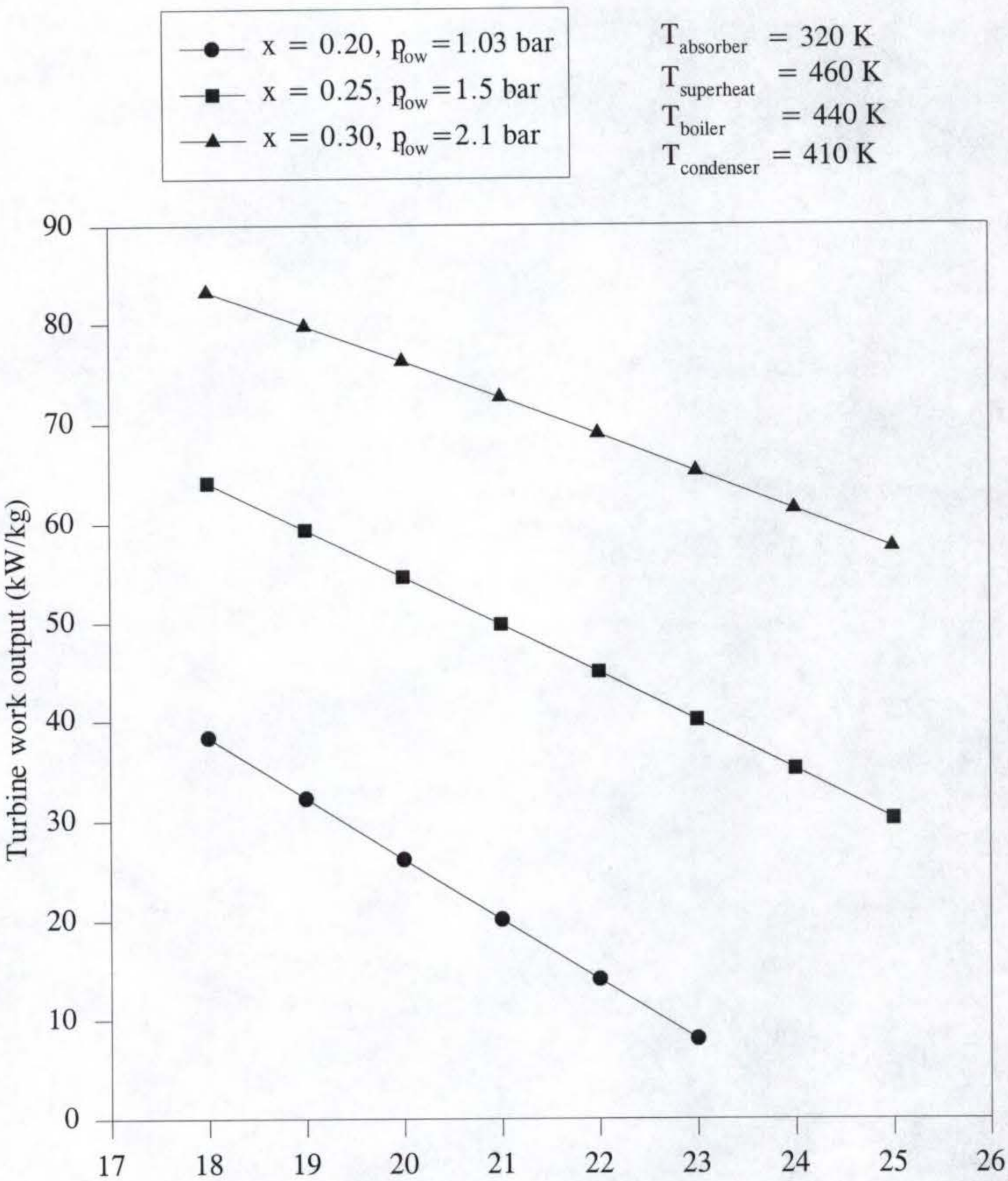

Figure 6-23 Effect of turbine outlet pressure on turbine work output for different turbine exit pressure

CHAPTER 7
CONCLUSIONS AND FUTURE WORK

This thesis consists of two different but strongly related topics: thermodynamic properties of ammonia-water mixtures and a study of a novel cycle with multicomponent working fluid integrated with absorption refrigeration cycle. The thermodynamic analysis entails the thermodynamic properties of ammonia-water mixtures, which are the working fluids of our proposed power system.

The thermodynamic properties of ammonia-water mixtures are of fundamental importance for the proposed power cycle analysis. A few models for the thermodynamic properties of these mixtures have been proposed. The criteria for a successful computer program for predicting the thermodynamic properties is accuracy, a wide range of conditions, reliability and computing time. Therefore the previous works have been critically reviewed and a new approach is developed using Gibbs free energy method. This method is based on extensive experimental data, avoiding some suspect assumptions. However, because of the nature of the experiments and the data from different sources, it is necessary to further investigate the coefficients of the computing equation. Theoretical approach should be investigated in order to validate the experimental data. This sounds odd. The reason for doing this is that the reported

experimental data were taken by different individuals at different times and with different equipment resulting in lack of consistency.

A generalized equation of state method by Park and Sonntag (1990b) is so far the most complete theoretical approach to calculate the thermodynamic properties of ammonia-water mixtures. Although they claim that this method provides a consistent way without combining or mosaicking equilibrium data and without discontinuities or gaps, some researchers have expressed (Ibrahim and Klein, 1993)their doubts about this method in the high pressure range because of lack of experimental data.

The thermodynamic properties of ammonia-water mixture based on the model used in this study were compared with most recent experiment data. The results agree with the experimental data very well. This model was based on Macriss et al. (1964) data developed by Schulz (1971). Zieger and Trepp (1984) extended Schulz's correlations to a higher temperature and pressure range. Using Gillespie et al. (1987) VLE data, Ibrahim and Klein (1993) generated correlations for the liquid mixtures. In the 90s, several researchers in Germany have conducted measurement on ammonia-water mixtures. They are Harms-Watzenberg (1995), Pruβ and Wagner (1995), Kurz (1994), Peters (1994) and Zimmermann (1991). Using these recent data, it is possible to develop new correlations to extend the ammonia-water mixtures properties data to a higher temperature and pressure range.

The second part of this thesis is an investigation of a new power cycle proposed by Goswami (1995, 1996). It is a new concept of a power cycle. Kalina cycle which uses ammonia-water mixture as a working fluid is somewhat similar to this cycle. But there is

a major difference. The heat rejection of our cycle is a part of absorption refrigeration cycle, and the working fluid for the power generation(i.e. fluid flowing through the turbine) is pure ammonia. Kalina cycle tends to apply to a higher temperature source (above 700 K), while the proposed cycle focuses on low temperature application (about 500 K) producing both power and refrigeration.

A second law analysis method has been developed for a binary system. Most studies in the literature neglect the effect of the composition of a binary mixture in the second law analysis. The method used in this study incorporates the effect of ammonia mass fraction on exergy calculations.

The proposed cycle has been compared with Rankine cycle quantitatively and qualitatively. The results show that ammonia-water cycle has a 15%-20% advantage over a Rankine cycle. An ammonia-water cycle may not be favorable over a Rankine cycle if the type of heat source is not considered. A Rankine cycle is excellent with a constant temperature heat source. Unfortunately, most heat sources have a variable temperature.

A simulation program has been used for the analysis of the proposed system. Simulation of the boiling and condensation processes taking place in the boiler/rectifier and absorber, and the associated heat transfer processes has been also conducted. Results from the simulation study have been presented in Chapter 6. The effects of mass concentration of ammonia in the strong and weak ammonia-water mixtures, the temperatures and pressures in the turbine, absorber, and the boiler on the cycle performance have been studied.

The first part of this thesis in which the thermodynamic properties of ammonia-water mixtures are investigated lay down a solid foundation for the second part of this thesis. Accurate property data of the mixtures is the key for the system simulation analysis.

An experimental study of the proposed system is needed for future study. The experimental study will be conducted on a system based on a single stage turbine. Since the turbine design, the boiler size and the absorber design will limit the operational conditions, the data obtained will be limited. However, even a limited amount of data will be helpful in validating the results obtained from the simulation program.

LIST OF REFERENCES

Alefeld, G., 1989 "Second Law Analysis for an Absorption Chiller," Newsletter of the IEA Heat Pump Center, Vol. 7, No. 2, pp. 54-57.

Amrane, K. and Radermacher, R., 1994 "Second-Law Analysis of Vapor Compression Heat Pumps with Solution Circuit," J. Eng. for Gas Turbines and Power, Vol. 116, pp. 453-461.

Anand, D. K., Lindler, K. W., Schweitzer, S. and Kennish, W. J., 1984 "Second Law Analysis of Solar Powered Absorption Cooling Cycles and Systems," J. of Solar Energy Eng., Vol. 106, pp. 291-298.

Anderson J. H., 1989 "The Anderson Power Cycle," Pollution Engineering, Vol. 21, pp. 94-97.

Aphornratana, S. and Eames, I. W., 1995 "Thermodynamic Analysis of Absorption Refrigeration Cycles using the Second Law of Thermodynamics Method," Int. J. Refrig., Vol. 18, No.4, pp. 244-252.

Avery, K. A., 1980 "An Evaluation of the Use of the Binary Mixture 'Ammonia-Water' as the Heat Exchange Medium for Power Generation in the Ocean Thermal Energy Conversion Power Plant," Master Thesis, University of Rhode Island.

Babcock & Wilcox, 1978 "Steam/Its Generation and Use," 39th edition. New York, Babcock & Wilcock.

Bannister R. L. and Silvestri G. J. Jr., 1989 "The Evolution of Central Station Turbines," Mechanical Engineering, Vol. 111, pp. 70-78.

Bejan A., 1988 "Advanced Engineering Thermodynamics," New York, John Wiley and Sons.

Best, R., Islas, J. and Martinez, M., 1993 "Exergy Efficiency of an Ammonia-Water Absorption System for Ice Production," Applied Energy, Vol. 45, pp. 241-256.

Bosnjakovic, F., Knoche, K. F. and Stehmeier, D., 1986 "Exergetic Analysis of Ammonia/Water Absorption Heat Pumps," Computer-Aided Engineering of Energy Systems, AES-Vol. 3, pp. 93-104.

Duffy J. W., 1964 "Power, Prime Mover of Technology," Bloomington, IL, McKnight & McKnight.

Egrican, N., 1988 "The Second Law Analysis of Absorption Cooling Cycles," Heat Recovery Systems & CHP, Vol. 8, No. 6, pp. 549-558.

El-Sayed Y. M. and Tribus M. 1985a, "Thermodynamic Properties of Water-Ammonia Mixtures: Theoertical Implementation for Use in Power Cycle Analysis," ASME Special Publication, AES-Vol. 1, pp. 89-95.

El-Sayed Y. M. and Tribus M., 1985 b "A Theoretical Comparison of the Rankine and Kalina Cycles," ASME Special Publication, AES-Vol. 1, pp. 97-102.

Foster-Pegg R. W., 1978 "Steam Bottoming Plants for Combined Cycles," J Eng. for Power, Vol. 100, pp. 124-130.

Gaffert G. A., 1946 "Steam Power Stations," New York, McGraw-Hill.

Gillespie, P. C., Wilding W. V. and Wilson G. M. 1987 "Vapor-Liquid Equilibrium Measurements on the Ammonia-Water System from 313K to 589K," AICHE Symposium Series, Vol. 83, No. 256, pp. 97-127.

Goswami, D. Y. 1995 "Solar Thermal Power-Status and Future Directions," Proceedings of the 2nd ASME-ISHMT Heat and Mass Transfer Conference, Mangalore, India, Dec 1995.

Goswami, D. Y. 1996 Plenary Lecture at the ENERGEX'96, Beijing, China, June 1996. To appear in Energy Sources Journal.

Harms-Watzenberg, F., 1995 "Messung und Korrelation der thermodynamischen Eigenschaften von Wasser-Ammoniak-Gemischen" Fortschr.-Ber. VDI-Verlag, Düsseldorf, VDI 3, No. 380.

Haar, L. and Gallagher, J. S., 1978 "Thermodynamic Properties of Ammonia," Journal of Physical and Chemical Reference Data, Vol. 7, pp. 635-792.

Herold K. E., Han K. and Moran M. J. 1988, "AMMWAT: A Computer Program for Calculating the Thermodynamic Properties of Ammonia and Water Mixtures Using a Gibbs Free Energy Formulation," ASME Proceedings Vol. 4, pp. 65-75.

Herold, K. E. and Moran, M. J., 1987 "Recent Advances in the Thermodynamic Analysis of Absorption Heat Pumps," The Fourth International Symposium on Second Law Analysis of Thermal Systems, Rome, Italy, May, 1987, pp. 97-103.

Ibrahim O. M. and Klein S. A., 1993 "Thermodynamic Properties of Ammonia-Water Mixtures," ASHRAE Transactions Vol. 99, pp.1495-1502.

Ibrahim M. B. and Kovach R. M., 1993 "A Kalina Cycle Application for Power Gereration," Energy, Vol. 18, No. 9, pp. 961-969.

Kalina A. I., 1983 "Combined Cycle and Waste-Heat Recovery Power Systems Based on a Novel Thermodynamic Energy Cycle Utilizing Low-Temperature Heat for Power Generation," ASME Paper 83-JPGC-GT-3.

Kalina A. I., 1984 "Combined Cycle System with Novel Bottoming Cycle," ASME J. Eng. Gas Turbines and Power, Vol. 106, pp. 737-742.

Kalina A. I. and Tribus M., 1990 "Advances in Kalina Cycle Technology(1980-1991): Part I Development of a Practical Cycle," Energy for the Transition Age, Proceedings of the Florence World Energy Research Symposium, Firenze, Italy, pp. 97-110.

Kalina A. I. and Tribus M., 1990 "Advances in Kalina Cycle Technology(1980-1991): Part II Iterative Improvements," Energy for the Transition Age, Proceedings of the Florence World Energy Research Symposium, Firenze, Italy, pp. 111-124.

Kalina A. I., Tribus M. and El-Sayed Y. M., 1986 "A Theoretical Approach to the Thermophysical Properties of Two-Miscible-Component Mixtures for the Purpose of Power-Cycle Analysis," ASME Paper 86-WA/HT-54.

Koehler, W. J., Ibele, W. E., Soltes, J. and Winter, E. R., 1988 "Availability Simulation of a Lithium Bromide Absorption Heat Pump," Heat Recovery Systems & CHP, Vol. 8, No. 2, pp. 157-171.

Koremenos, D. A., Rogdakis, E. D. and Antonopoulos K. A., 1994 "Cogeneration with Combined Gas and Aqua-Ammonia Absorption Cycles," In Thermodynamics and The Design Analysis, and Improvement of Energy Systems, (Ed.) R.J. Krane, AES-Vol. 33 New York, ASME, pp. 231-238.

Krakow, K. I., 1991 "Exergy Analysis: Dead-State Definition," ASHRAE Transactions, Vol. 97, pp. 328-336.

Kurz, F., 1994 "Untersuchungen zur simultanen Lösung von Ammoniak und Kohlendioxid in Wasser und salzhaltigen wäβrigen Lösungen" Dissertation Universität Kaiserslautern.

Lorenz, V. H., 1894 "Die Ausnützung der Brennstoffe in den Kühlmaschinen," Zeitschrift für die gesammte Kälte-Industrie, Vol. 1, pp. 10-15.

Macriss, R. A., Eakine, B. E., Ellington, R. T. and Huebler, J. 1964, "Physical and Thermodynamic Properties of Ammonia-Water Mixtures," Chicago Institute of Gas Technology, Research Bulletin No. 34.

Maloney, J. D. and Robertson, R. C., 1953 "Thermodynamic Study of Ammonia-Water Heat Power Cycles," ORNL Report CF-53-8-43, Oak Ridge, TN.

Marston C. H., 1990 "Parametric Analysis of the Kalina Cycle," J. Eng. for Gas Turbines and Power, Vol. 112, pp. 107-116.

Marston C. H., 1990 "A Family of Ammonia-Water Adjustable Proportion Fluid Mixture Cycles," Proceedings of the 25th Intersociety Energy Conversion Engineering Conference, Vol. 2, pp. 160-165.

Milora S. T. and Tester J. W., 1976 "Geothermal Energy as a Source of Electric Power Thermodynamic and Economic Design Criteria," Cambridge, The MIT Press.

Moran, M. J. and Sciubba, E., 1994 "Exergy Analysis: Principles and Practice," J. Eng. for Gas Turbines and Power, Vol. 116, pp. 285-290.

Mumah, S. N., Adefila, S. S. and Arinze, E. A., 1994 "Properties Generation Procedures for First and Second Law Analyses of Ammonia-Water Heat Pump System," Energy Convers. Mgmt. Vol. 35, No. 8, pp. 727-736.

Park Y. M. and Sonntag R. E., 1990a "A Preliminary Study of the Kalina Power Cycle in Connection with a Combined Cycle System," Int. J. of Energy Res., Vol. 14, pp. 153-162.

Park Y. M. and Sonntag R. E., 1990b "Thermodynamic Properties of Ammonia-Water Mixtures: A Generalized Equation-of-State Approach," ASHRAE Transactions, Vol. 96, pp. 150-159.

Peng D. Y. and Robinson D. B., 1976 "A New Two-Constant Equation of State," Fundementals of Industrial Engineering Chemistry, Vol. 15, No. 1, pp. 59-64.

Perman, E. P., 1901 "Vapour Pressure of Aqueous Ammonia Solution," Part I, J. Chem. Soc., Vol. 79, pp. 718-725;

Peters, R., 1994 "Dampf-Flüssgkeits-Phasengleichgewichte im Stoffsystem Ammoniak-Wasser-Lthiumbromid," PhD thesis, Universität Siegen.

Reid R. C., Prausnitz J. M. and Poling B. E., 1987 "The Properties of Gases and Liquids," 4th ed. New York, McGraw-Hill.

Rogdakis, E. D. and Antonopoulos, K. A., 1991 "A High Efficiency NH_3/H_2O Absorption Power Cycle," Heat Recovery Systems, Vol. II, pp. 263-275.

Scatchard G., Epstein L. F., Warburton J. and Cody P. J., 1947 "Thermodynamic Properties of Saturated Liquid and Vapour of Ammonia-Water Mixtures," Refrigerating Engineering, Vol. 53, pp. 413-452.

Schulz S. C. G. 1972, "Equations of State for the System Ammonia-Water for Use with Computers," Proceedings of the XII th International Congress of Refrigeration. Vol. 2, pp. 431-436.

Stecco S. S., 1989 "A Thermodynamic Analysis of the Kalina Cycles: Comparisons, Problems and Perspectives," ASME Paper 89-GT-149.

Szargut J., Morris D. R. and Steward F. R. 1988 "Exergy Analysis of Thermal, Chemical, and Metallurgical Processes," New York, Hemisphere Publishing Corporation.

Tyagi, K. P., 1986 "Second Law Analysis of NH_3-NaSCN Absorption Refrigeration Cycle," Heat Recovery Systems, Vol. 6, No. 1, pp. 73-82.

Waked, A. M., 1991 "Second Law Analysis of a Cogeneration Power-Absorption Cooling Plant," Heat Recovery System & CHP, Vol. 11, No. 2/3, pp. 113-120.

Walas S. M., 1985 "Phase Equilibria in Chemical Engineering.," Stoneham, MD, Butterworth Publishers.

Wucherer, J., 1932 "Measurements of Pressure, Temperature and Composition of Liquids and Vaporous Phase of Ammonia-Water Mixtures at Saturation Point," Z. Gesamt. Kalte-Ind. Vol. 39, pp. 97-104, 136-140.

Zerban A. H. and Nye E. P., 1957 "Power Plants," Scranton, International Textbook.

Ziegler B. and Trepp C., 1984 "Equation of State for Ammonia-Water Mixtures," International Journal of Refrigeration, Vol. 7, No. 2, pp. 101-106.

Zimmermann, A. 1991 "Experimentelle Untersuchung der Dampf- Flüssgkeit-gewichte im Stoffsystem Ammoniak-Wasser-Lithiumbromid" PhD thesis, Universität Siegen.

Zinner, K., 1934 "The Heat Content of Mixtures of Ammonia and Water Dependent on the Composition and Temperature," Z. Gesamt. Kalte-Ind., Vol. 41, pp. 21-29.

Zubair, S. M., 1994 "Thermodynamics of a Vapor-Compression Refrigeration Cycle with Mechanical Subcooling," Energy, Vol. 19, No. 6, pp. 707-715.

BIOGRAPHICAL SKETCH

Feng Xu was born on June 11, 1967 in Quanzhou city, P. R. China. He completed his bachelor's degree in flying vehicle design and applied mechanics in July 1988 and master's degree in low temperature engineering and refrigeration technology in January 1991 from Beijing University of Aeronautics and Astronautics, Beijing, P.R. China, where he met his wife.

Feng Xu enrolled in the Department of Mechanical Engineering, University of Florida in Spring of 1994 working for his Ph.D. degree. His wife also got her Ph.D. degree from the Department of Aerospace Engineering, Mechanics and Engineering Science, University of Florida. During their stay at UF, they had their first child, Tom.

I certify that I have read this study and that in my opinion it conforms to acceptable standards of scholarly presentation and is fully adequate, in scope and quality, as a dissertation for the degree of Doctor of Philosophy.

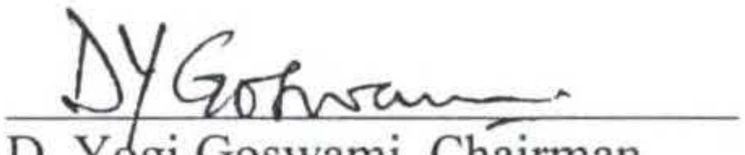

D. Yogi Goswami, Chairman
Professor of Mechanical Engineering

I certify that I have read this study and that in my opinion it conforms to acceptable standards of scholarly presentation and is fully adequate, in scope and quality, as a dissertation for the degree of Doctor of Philosophy.

C. K. Hsieh
Professor of Mechanical Engineering

I certify that I have read this study and that in my opinion it conforms to acceptable standards of scholarly presentation and is fully adequate, in scope and quality, as a dissertation for the degree of Doctor of Philosophy.

Jill E. Peterson
Associate Professor of Mechanical Engineering

I certify that I have read this study and that in my opinion it conforms to acceptable standards of scholarly presentation and is fully adequate, in scope and quality, as a dissertation for the degree of Doctor of Philosophy.

Sherif A. Sherif
Associate Professor of
Mechanical Engineering

I certify that I have read this study and that in my opinion it conforms to acceptable standards of scholarly presentation and is fully adequate, in scope and quality, as a dissertation for the degree of Doctor of Philosophy.

Barney L. Capehart
Professor of Industrial and Systems
Engineering

This dissertation was submitted to the Graduate Faculty of the College of Engineering and to the Graduate School and was accepted as partial fulfillment of the requirements for the degree of Doctor of Philosophy.

August, 1997

Winfred M. Phillips
Dean, College of Engineering

Karen A. Holbrook
Dean, Graduate School